

UC Riverside

UC Riverside Electronic Theses and Dissertations

Title

Stated Skein Theory and Double Affine Hecke Algebra Representations

Permalink

<https://escholarship.org/uc/item/9j5281f2>

Author

Matson, Raymond

Publication Date

2024

Copyright Information

This work is made available under the terms of a Creative Commons Attribution License, available at <https://creativecommons.org/licenses/by/4.0/>

Peer reviewed|Thesis/dissertation

UNIVERSITY OF CALIFORNIA
RIVERSIDE

Stated Skein Theory and Double Affine Hecke Algebra Representations

A Dissertation submitted in partial satisfaction
of the requirements for the degree of

Doctor of Philosophy

in

Mathematics

by

Raymond Alexander Dzintars Matson

September 2024

Dissertation Committee:

Dr. Peter Samuelson, Chairperson

Dr. Jacob Greenstein

Dr. Wee Liang Gan

Copyright by
Raymond Alexander Dzintars Matson
2024

The Dissertation of Raymond Alexander Dzintars Matson is approved:

Committee Chairperson

University of California, Riverside

Acknowledgments

First and foremost, I would like to express my deepest gratitude to my advisor, Peter Samuelson, for his immense kindness, remarkable guidance, and continuous patience throughout my doctoral journey. Thank you for being a wonderful mentor, a phenomenal mathematician, and most importantly, a great friend. I have no doubt that your future students will look up to you the way I do.

I would especially like to thank Jacob Greenstein, Chris Grossack, Melody Molander, Shane Rankin, Alex Space, Elliott Vest, and Stefano Vidussi for their incredibly helpful conversations and constructive comments over the years. I am also deeply thankful to Neima Ghandian, Will Hoffer, and Rahul Rajkumar for always engaging with my relentless algebra nonsense and their consistently helpful feedback.

I owe a tremendous thank you to my WeierstrHouse roommates for all of the unforgettable adventures and lifelong memories we created together. My time in Riverside was made so much better by your companionship, and I could not have asked for better friends.

A major thank you to Margarita Roman for her instrumental role in keeping our department running smoothly and for all the unwavering support she provides us. We all love and deeply appreciate all that you do for us. I would also like to thank all of the UCR math graduate students that I had the privilege to meet during my time here. I'll never forget the frustration, laughter, passion, tears, and growth we all experienced together. Know that I appreciate each and every one of you!

ABSTRACT OF THE DISSERTATION

Stated Skein Theory and Double Affine Hecke Algebra Representations

by

Raymond Alexander Dzintars Matson

Doctor of Philosophy, Graduate Program in Mathematics

University of California, Riverside, September 2024

Dr. Peter Samuelson, Chairperson

In this thesis, we explore the representation theory of double affine Hecke algebras (DAHAs) through the lens of stated skein theory. Over the past decade, there have been several works establishing robust connections between skein algebras and DAHAs. Particularly, Samuelson proved that a spherical subalgebra of the type A_1 DAHA can be realized as a quotient of the Kauffman bracket skein algebra of the torus with boundary, $K_q(T^2 \setminus D^2)$. Since the A_1 double affine Hecke algebra is Morita equivalent to its spherical subalgebra, discovering modules for $K_q(T^2 \setminus D^2)$ immediately provides us with modules for the A_1 DAHA.

Stated skein theory enhances traditional Kauffman bracket skein theory by incorporating the boundary components of manifolds, thereby offering additional properties such as excision that enrich the algebraic structure. Furthermore, Kauffman bracket skein algebras embed into their stated counterparts, showing that stated skein algebras are extensions of Kauffman bracket skein algebras. We use this extended framework to further develop the representation theory of the A_1 DAHA.

After identifying generators for the stated skein algebra of $T^2 \setminus D^2$, we embed this algebra into a quantum 6-torus and leverage the nice representation-theoretic properties of quantum tori to construct a module of Laurent polynomials. Additionally, as T^2 is the boundary of any knot complement, we discuss how to construct a more topologically-defined module from various knots and provide an explicit example for the unknot. This approach builds upon the ideas of Berest and Samuelson, who showed that there exists a natural DAHA action on the Kauffman bracket skein module of knot complements.

Contents

List of Figures	ix
1 Introduction	1
2 Background	6
2.1 Categorical Framework	6
2.2 Quantum Groups	14
2.3 Ribbon Hopf Algebras	19
2.4 Skein Modules	24
2.5 Kauffman Bracket Skein Algebras	36
2.6 Stated Skein Algebras	39
2.7 The Conventional Model	43
2.8 Spherical Double Affine Hecke Algebra	50
3 The Stated Skein Algebra of the Torus with Boundary	54
3.1 $\mathcal{S}(T^2 \setminus D^2)$ Notation	55
3.2 Half-Twists Around the Boundary	58
3.3 Generators of $\mathcal{S}(T^2 \setminus D^2)$	60
3.4 Relation to Factorization Homology	71
3.5 Towards a PBW Basis	74
4 Representations from Quantum Tori	77
4.1 Embedding Into Quantum Tori	77
4.2 The Quantum 6-Torus	80
4.3 A Module of Laurent Polynomials	84
5 Topologically Defined Representations	88
5.1 Knot Invariants	88
5.2 Knot Complements as $\mathcal{S}(T^2 \setminus D^2)$ -Modules	94
5.3 The Unknot Module	98
5.4 A Note on the Genus Two Surface	100
Bibliography	107

A	Diagrammatic Calculations	111
A.1	Commuting Relation for $X_{1,0}(-, -)$ and $X_{2,0}(+, +)$	112
A.2	Image of $\varphi_{\mathcal{E}}$	113
A.2.1	Longitude	113
A.2.2	(1, 1)-Curve	114
A.2.3	(1, -1)-Tangle	116
A.2.4	$X_{1, \frac{1}{2}}(+, +)$	116
A.2.5	$X_{3, \frac{1}{2}}(+, +)$	118
A.2.6	$X_{1, 1}(+, +)$	119
A.2.7	$X_{1, -\frac{1}{2}}$	121
A.2.8	Boundary Curve	122
A.3	Parallel Tangle	122
B	Python Code	127
B.1	Quantum Commuting Relations	127
B.2	Quantum 6-Torus Operators	132

List of Figures

2.1	The zigzag identities for rigid categories	8
2.2	A graphical interpretation of the hexagonal identities	10
2.3	Symmetric braidings	11
2.4	A graphical interpretation of a twist	11
2.5	Equivalent identities for categorical twists	12
2.6	A blackboard framing of a tangle	25
2.7	An example of a \mathcal{C} -colored ribbon graph embedded into a cylinder	26
2.8	Example of multiplication in $TL_5(\delta)$	33
2.9	An σ -ordered diagram on a punctured bordered surface	46
2.10	Example of consistent boundary orientations	47
3.1	Expressing Y_1 as stated $\partial(T^2 \setminus D^2)$ -tangles	57
3.2	Strict inclusion of simple elements of fundamental groups	59
3.3	Constructing geodesic paths, γ_i	62
3.4	Examples of $f_A(p, q, r)$	64
3.5	Turning a tangle into a closed curve on the torus	65
3.6	Constructing geodesic paths, γ_i	66
3.7	Diagram of transmutation multiplication	73
4.1	A quasitriangulation of $T^2 \setminus D^2$	80
5.1	Extending stated endpoints in a knot complement	97
5.2	Properly creating $T^2 \setminus D^2$ for knot complements	98

Chapter 1

Introduction

The inception of double affine Hecke algebras (DAHAs) is credited to Ivan Cherednik [14], who used certain properties of DAHAs to solve the Macdonald conjectures. Macdonald polynomials, which are intrinsically related to quantum physics, have led to DAHAs finding applications across numerous fields, including string theory, operator theory, homological algebra, Harish-Chandra theory, gauge theory, Fourier analysis, mirror symmetry, quantum topology, and even the Langlands program.

In 1962, Freeman Dyson conjectured that the constant term of a certain Laurent polynomial in n variables is given by

$$\text{CT} \left(\prod_{i \neq j} (1 - x_i x_j^{-1})^k \right) = \frac{(nk)!}{(k!)^n}$$

for $k \in \mathbb{Z}_{\geq 0}$ (Conjecture B in [20]). Here, “CT” refers to the function that extracts the constant term of the Laurent polynomial.

Ian Macdonald later generalized this conjecture in 1982 [43] to a root system generalization. Specifically, let \mathfrak{g} be a finite-dimensional (real or complex) reductive Lie

algebra, $\mathfrak{h} \subset \mathfrak{g}$ its Cartan subalgebra, and $R \subset \mathfrak{h}^*$ a corresponding reduced root system.

Macdonald conjectured that

$$\text{CT} \left(\prod_{\alpha \in R_+} \prod_{i=1}^k (1 - q^{i-1} e^{-\alpha}) (1 - q^i e^{\alpha}) \right) = \prod_{i=1}^l \begin{bmatrix} kd_i \\ k \end{bmatrix},$$

where $l = \dim(\mathfrak{h})$, e^α is the formal exponential corresponding to $\alpha \in R$, $\{d_1, d_2, \dots, d_l\}$ are the fundamental degrees of R (by this we mean the fundamental invariants of W , the Weyl group of R), and $\begin{bmatrix} n \\ k \end{bmatrix}$ are the Gaussian binomial coefficients (see Section 2.2 for the definition of Gaussian binomial coefficients).

Furthermore, Macdonald extended this conjecture to affine root systems by introducing an additional parameter $t \in \mathbb{C}^*$, leading to his famous Constant Term (q, t) -Conjecture:

$$\frac{1}{|W|} \text{CT} \left(\prod_{n \geq 0} \prod_{\alpha \in R} \frac{1 - q^n e^\alpha}{1 - q^n t e^\alpha} \right) = \prod_{n \geq 0} \prod_{i=1}^l \frac{(1 - q^n t) (1 - q^{n+1} t^{d_i-1})}{(1 - q^{n+1}) (1 - q^n t^{d_i})}.$$

This was proved in 1995 by Ivan Cherednik [13], using the representation theory of double affine Hecke algebras.

Since then, extensive work has been done to better understand double affine Hecke algebras from various perspectives. However, much remains to be explored regarding the representation theory of DAHAs. This thesis approaches DAHAs through the lens of quantum topology, particularly further exploring the connections between the representation theory of DAHAs and the representation theory of skein algebras of tori. When viewed appropriately, the Kauffman bracket skein algebra of a torus with boundary (or simply a punctured torus) is Morita equivalent to the A_1 double affine Hecke algebra.

In the 1980s, Vaughan Jones discovered what is now known as the Jones polynomial, a knot invariant derived from von Neumann algebras, which was further simplified by

Louis Kauffman's introduction of the Kauffman bracket. This polynomial invariant for links in 3-dimensional space paved the way for the development of skein modules, first introduced by Józef Przytycki in 1987 [50] and independently by Vladimir Turaev in 1988 [59]. These modules serve as 3-manifold invariants, capturing information about the manifold based on the kind of knot theory and algebraic structures that manifold admits. For example, the Kauffman bracket skein algebra uses links and crossing relations to forge a comprehensive algebraic framework. These algebras have become a cornerstone in quantum topology, connecting knot theory with quantum gravity and furthering our understanding of quantum field theories. For a far better explanation of the history and development of skein theory than I could ever give, see [49].

In recent years, Thang T. Q. Lê and others have laid substantial groundwork for a particular generalization of Kauffman bracket skein algebras, known as stated skein algebras. These algebras coincide with Kauffman bracket skein algebras when the corresponding manifold lacks a boundary. One of the main benefits this generalization offers is an excision property that enables gluing and splitting by leveraging the boundary components. Stated skein algebras encompass their corresponding Kauffman bracket skein algebras and are, in general, significantly larger objects to work with. The primary question explored in this thesis is whether we can extract more interesting representations of DAHAs through the framework of stated skein algebras.

Chapter 2 of this thesis provides a thorough background of the setting, including a discussion on the origin of diagrammatically-defined modules, their utility, and the representation-theoretic data they offer. We also define the A_1 double affine Hecke algebra

along with its spherical subalgebra, and examine its relationship with the Kauffman bracket skein algebra of $T^2 \setminus D^2$, as well as the corresponding stated skein algebra. While our definition of stated skein algebras differs slightly from the conventional definition found in the literature, we demonstrate that both models are naturally isomorphic.

Given that stated skein algebras are larger than Kauffman bracket skein algebras, we review common algebraic techniques to convert modules over the stated skein algebra into modules over the spherical A_1 DAHA. In Chapter 3, we first get our hands dirty and classify all simple closed curves based at the boundary of $T^2 \setminus D^2$. Using this classification, we then explicitly compute the generators for the main algebra we care about, the stated skein algebra of the torus with boundary and one marking. Once the generators for this algebra have been established, we then proceed to define modules over it.

Chapter 4 briefly explains and employs an embedding technique introduced by Lê and Yu in [42], where we map our stated skein algebra into a quantum 6-torus. Since the representation theory of quantum tori is well-known and behaves quite nicely, this approach allows us to compute representations for our algebra and, consequently, our double affine Hecke algebra. Notably, we uncover how our algebra acts non-trivially on the vector space of complex Laurent polynomials in four variables.

Chapter 5 expands upon a well-known module structure for Kauffman bracket skein algebras. For a 3-manifold M with boundary ∂M , the Kauffman bracket skein module of M naturally becomes a module over the Kauffman bracket skein algebra of ∂M . The module action is defined by gluing $\partial M \times [0, 1]$ into the boundary and “pushing” any curves in $\partial M \times [0, 1]$ into M . We begin by exploring a more geometrically-centered understanding

of skein algebras, particularly in relation to knot theory and quantizations of character varieties, and discuss how knot complements induce modules over the Kauffman bracket skein algebra of the torus. We then define and explore how these structures can be upgraded to stated skein algebras and stated skein modules.

Chapter 2

Background

2.1 Categorical Framework

We begin by discussing the categorical setting for our categories of interest. We will introduce a more concrete example of these definitions in section 2.3. However, it will be beneficial to introduce the proper language of these objects first.

Definition 2.1.1. A *monoidal category*, \mathcal{C} , is a \mathbb{K} -linear category equipped with

1. a bifunctor $\otimes : \mathcal{C} \times \mathcal{C} \rightarrow \mathcal{C}$ written as $(a, b) \mapsto a \otimes b$ called the monoidal product or tensor product,
2. an object $1 \in \mathcal{C}$ called the monoidal unit,
3. a natural isomorphism $\alpha : (- \otimes -) \otimes - \rightarrow - \otimes (- \otimes -)$ called the associator, with components $\alpha_{A,B,C} : (A \otimes B) \otimes C \rightarrow A \otimes (B \otimes C)$,
4. natural isomorphisms $\lambda : 1 \otimes - \rightarrow -$ and $\rho : - \otimes 1 \rightarrow -$ called the left unitor and right unitor, with respective components $\lambda_A : 1 \otimes A \rightarrow A$ and $\rho_A : A \otimes 1 \rightarrow A$

such that for all $A, B, C, D \in \mathcal{C}$, the following diagrams commute.

$$\begin{array}{ccc}
 & A \otimes (B \otimes (C \otimes D)) & \\
 \text{id}_A \otimes \alpha_{B,C,D} \swarrow & & \searrow \alpha_{A,B,C \otimes D} \\
 A \otimes ((B \otimes C) \otimes D) & & (A \otimes B) \otimes (C \otimes D) \\
 \alpha_{A,B \otimes C,D} \searrow & & \swarrow \alpha_{A \otimes B,C,D} \\
 (A \otimes (B \otimes C)) \otimes D & \xrightarrow{\alpha_{A,B,C} \otimes \text{id}_D} & ((A \otimes B) \otimes C) \otimes D
 \end{array}$$

$$\begin{array}{ccc}
 (A \otimes 1) \otimes B & \xrightarrow{\alpha_{A,1,B}} & A \otimes (1 \otimes B) \\
 \text{id}_A \otimes \lambda_B \searrow & & \downarrow \rho_A \otimes \text{id}_B \\
 & & A \otimes B
 \end{array}$$

If the α , λ , and ρ are all identity maps, then we say that \mathcal{C} is *strict*.

If \mathcal{D} is a category enriched over the monoidal category \mathcal{C} , then we require that \otimes be a \mathcal{C} -enriched functor, and α and λ be \mathcal{C} -enriched natural transformations. When this happens we say the monoidal structure is *compatible* with the enrichment.

An effective way of to think about the following categorical definitions is by using a diagrammatic interpretation, which will be discussed in greater detail later in section 2.4. This interpretation is typically reserved for strict categories, however, it's a useful tool to better understand the properties trying to be expressed in these definitions. For now, just imagine these morphisms as (oriented) strings connecting their corresponding sources and targets. If we want to consider a map between monoidal product of objects, we can instead consider multiple strings next to each other, possibly being weaved together in some way, and composition is attaching strings on top of each other. For example, a map $A \otimes B \rightarrow C \otimes D$ might look something like

$$\begin{array}{c}
 C \otimes D \\
 \uparrow \quad \uparrow \\
 \text{ } \\
 \downarrow \quad \downarrow \\
 A \otimes B
 \end{array}$$

I will incorporate pictures of the diagrammatic interpretations throughout this section and use the convention that morphisms move upwards.

Definition 2.1.2. An object X^* in \mathcal{C} is said to be a *left dual* of X if there exist morphisms $\text{ev}_X : X^* \otimes X \rightarrow 1$ and $\text{coev}_X : 1 \rightarrow X \otimes X^*$, called the evaluation and coevaluation respectively, such that the following diagrams commute.

$$\begin{array}{ccc}
 X & \xrightarrow{\text{coev} \otimes \text{id}_X} & (X \otimes X^*) \otimes X \\
 \text{id}_X \downarrow & & \downarrow \alpha_{X, X^*, X} \\
 X & \xleftarrow{\text{id}_X \otimes \text{ev}} & X \otimes (X^* \otimes X)
 \end{array}
 \qquad
 \begin{array}{ccc}
 X^* & \xrightarrow{\text{id}_{X^*} \otimes \text{coev}} & X^* \otimes (X \otimes X^*) \\
 \text{id}_{X^*} \downarrow & & \downarrow \alpha_{X^*, X, X^*}^{-1} \\
 X^* & \xleftarrow{\text{ev} \otimes \text{id}_{X^*}} & (X^* \otimes X) \otimes X^*
 \end{array}$$

Definition 2.1.3. Similarly, an object X^* in \mathcal{C} is said to be a *right dual* of X if there exist morphisms $\text{ev}_X : X \otimes X^* \rightarrow 1$ and $\text{coev}_X : 1 \rightarrow X^* \otimes X$ such that the following diagrams commute.

$$\begin{array}{ccc}
 X & \xrightarrow{\text{id}_X \otimes \text{coev}} & X \otimes (X^* \otimes X) \\
 \text{id}_X \downarrow & & \downarrow \alpha_{X, X^*, X}^{-1} \\
 X & \xleftarrow{\text{ev} \otimes \text{id}_X} & (X \otimes X^*) \otimes X
 \end{array}
 \qquad
 \begin{array}{ccc}
 X^* & \xrightarrow{\text{coev} \otimes \text{id}_{X^*}} & (X^* \otimes X) \otimes X^* \\
 \text{id}_{X^*} \downarrow & & \downarrow \alpha_{X^*, X, X^*} \\
 X^* & \xleftarrow{\text{id}_{X^*} \otimes \text{ev}} & X^* \otimes (X \otimes X^*)
 \end{array}$$

These commuting diagrams are often called the “zigzag identities”.

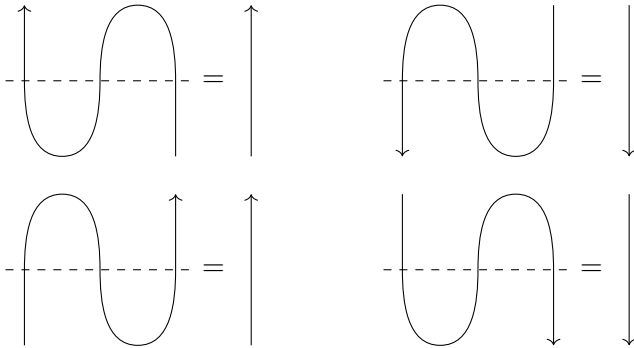


Figure 2.1: The zigzag identities can be understood as curved strings being straightened out.

When an object has a dual, evaluation and coevaluation maps can be pictorially represented using cups and caps, as the notion of duals corresponds to reversing the

orientation of our strings. In figure 2.1, the top left picture corresponds to the identity $(\text{id}_X \otimes \text{ev}) \circ \alpha_{X, X^*, X} \circ (\text{coev} \otimes \text{id}_X) = \text{id}_X$ for left duals, while the bottom right corresponds to $(\text{id}_{X^*} \otimes \text{ev}) \circ \alpha_{X^*, X, X} \circ (\text{coev} \otimes \text{id}_{X^*}) = \text{id}_{X^*}$ for right duals.

Remark 2.1.4. It's hopefully clear that if X^* is a left dual of an object X , then X is a right dual of X^* and in any monoidal category, 1 is equal to its left and right duals. Moreover, left and right duals are unique up to a unique isomorphism.

Remark 2.1.5. Changing the order of tensor products, when possible, switches left duals and right duals. Therefore, for any statement concerning right duals there corresponds a symmetric statement about left duals.

Remark 2.1.6. Some texts use the notation *X for right duals to distinguish between the two. However, we won't need to worry about this distinction too much in this thesis and so we will not use this notation.

Definition 2.1.7. An object in a monoidal category is called *rigid* if it has left and right duals. A monoidal category \mathcal{C} is called *rigid* if every object of \mathcal{C} is rigid.

For those that have never seen the definition of a rigid category before, you should think of this as merely saying each object has a well-defined dual that acts exactly as we expect it to. A quick example is the category of finite dimensional complex vector spaces $\text{FdVect}_{\mathbb{C}}$, where $V^* := \text{Hom}_{\mathbb{C}}(V, \mathbb{C})$ and

$$\begin{aligned} \text{ev} : V \otimes V^* &\rightarrow \mathbb{C} & \text{coev} : \mathbb{C} &\rightarrow V^* \otimes V \\ (v, \varphi) &\mapsto \varphi(v) & k &\mapsto k \cdot \sum_{i \in I} \varphi_i \otimes v_i \end{aligned}$$

where $\{v_i\}_{i \in I}$ is a basis for V and $\{\varphi_i\}_{i \in I}$ is the dual basis such that $\varphi_i(v_j) = \delta_{i,j}$ (the usual evaluation map that we all know and love).

Definition 2.1.8. A monoidal category, \mathcal{C} , is *braided* if for every pair of objects $X, Y \in \mathcal{C}$, there is a natural isomorphism $B_{X,Y} : X \otimes Y \rightarrow Y \otimes X$ such that for all $X, Y, Z \in \mathcal{C}$, the following hexagonal diagrams commute.

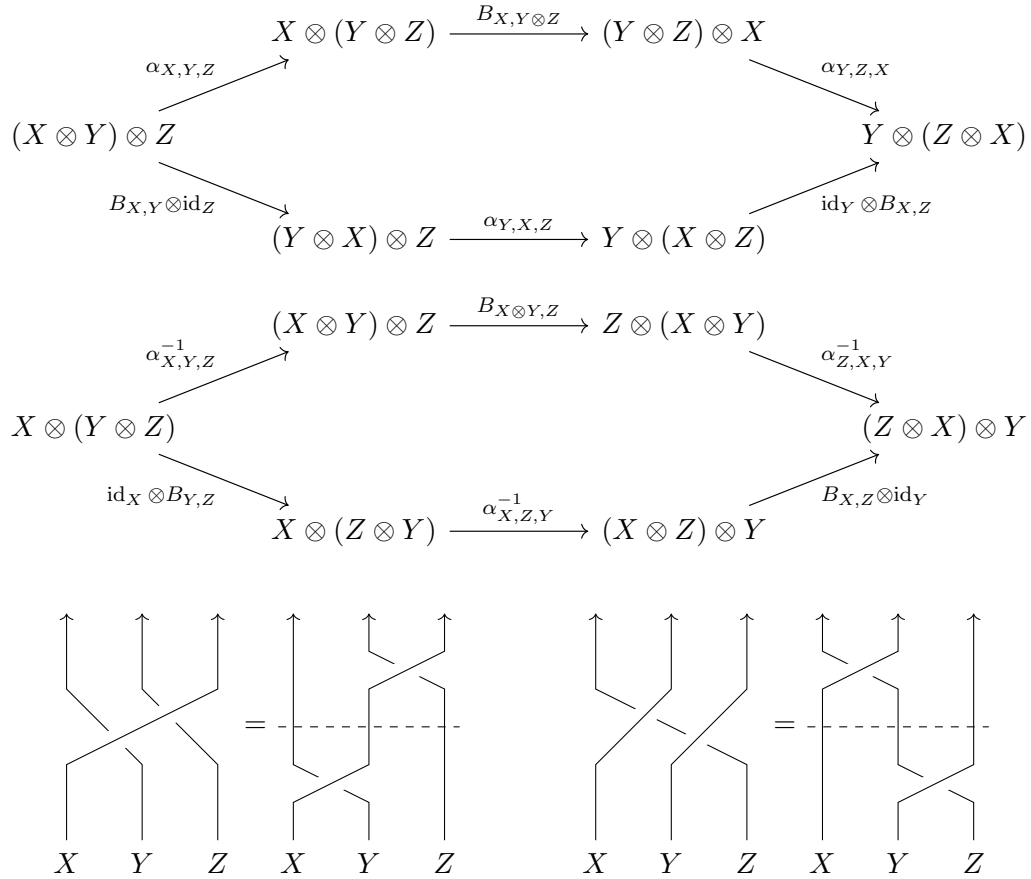


Figure 2.2: A graphical interpretation of the hexagonal identities.

These isomorphisms are called *braidings* and should be thought of as a commutativity constraint. When $B_{Y,X} \circ B_{X,Y} = \text{id}_{X \otimes Y}$ for every $X, Y \in \mathcal{C}$, we call \mathcal{C} a *symmetric monoidal category*. When understanding a symmetric monoidal category diagrammatically, we often

drop the “depth” to the braidings as $B_{X,Y}$ and $B_{Y,X}$ are inverse to each other.

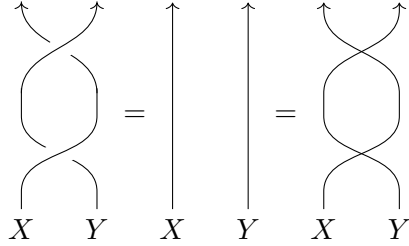


Figure 2.3: A graphical interpretation of a symmetric braiding.

As the setting of this work revolves around quantum groups, you can reasonably expect our braidings to lack symmetric properties.

Definition 2.1.9. A *twist* on a rigid braided monoidal category is a natural isomorphism from the identity functor to itself, with components $\theta_X : X \rightarrow X$ such that for all $X, Y \in \mathcal{C}$ the following identities hold.

$$\theta_{X \otimes Y} = (\theta_X \otimes \theta_Y) \circ B_{Y,X} \circ B_{X,Y} \tag{2.1}$$

$$\theta_{X^*} = (\theta_X)^*$$

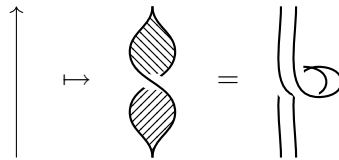


Figure 2.4: A graphical interpretation of a twist.

The graphical interpretation of a twist involves thickening up the string and creating a full twist in the now “ribbon”, distinguishing it from the identity map. This is graphically equivalent to creating a loop instead.¹

¹You can verify this for yourself by grabbing the ends of a belt, giving it a full twist, slowly bringing the ends together, and watching your prop unravel into a loop.

Remark 2.1.10. Given any two objects $X, Y \in \mathcal{C}$, we also have the alternative equality

$$\theta_{X \otimes Y} = B_{Y,X} \circ B_{X,Y} \circ (\theta_X \otimes \theta_Y).$$

Figure 2.5 sketches a diagrammatic proof of how these identities are equivalent. These equalities follow from the naturality of the braidings and of the twists. For clarity, note that the first two pictures correspond to the compositions $B_{Y,X} \circ B_{X,Y} \circ (\theta_X \otimes \theta_Y)$ and $B_{Y,X} \circ (\text{id}_Y \otimes \theta_X) \circ B_{X,Y} \circ (\text{id}_X \otimes \theta_Y)$, respectively. The last picture corresponds to the right hand side of equation 2.1. For more details see section 14.3.1 in [34].

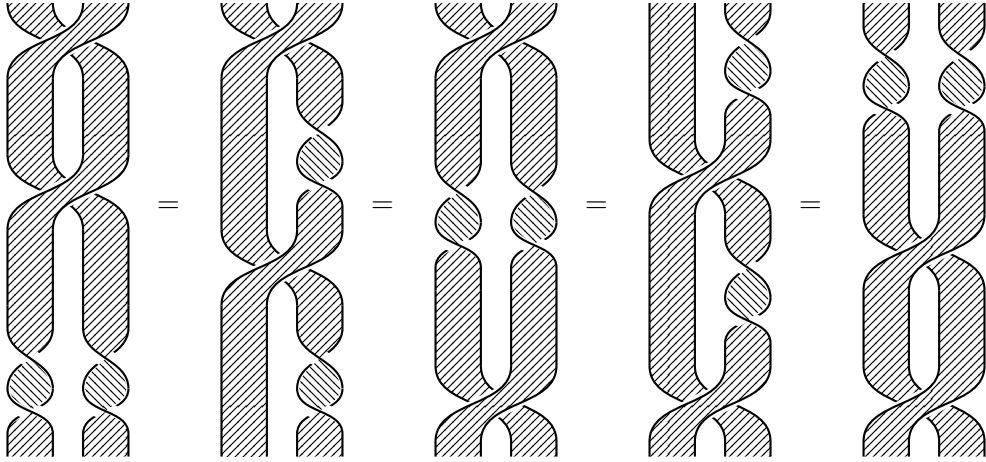


Figure 2.5: Equivalent identities for categorical twists.

We can now provide the definition of a ribbon category.

Definition 2.1.11. A *ribbon category*, \mathcal{C} , is a rigid braided monoidal category equipped with a twist such that for all $X \in \mathcal{C}$,

$$(\theta_X \otimes \text{Id}_{X^*}) \circ \text{coev} = (\text{Id}_X \otimes \theta_{X^*}) \circ \text{coev}.$$

You can read more about these kinds of categories in detail in [11, 21, 34, 44].

Lastly, we descend from the level of categories to the level of algebras in order to provide a few other useful definitions.

Definition 2.1.12. A *bialgebra* over a field \mathbb{K} is a tuple $(A, \mu, \iota, \Delta, \varepsilon)$ such that (A, μ, ι) is an algebra over \mathbb{K} , (A, Δ, ε) is a coalgebra over \mathbb{K} , and the following diagrams commute.

$$\begin{array}{ccccc}
 A \otimes A & \xrightarrow{\varepsilon \otimes \varepsilon} & \mathbb{K} \otimes \mathbb{K} & \xrightarrow{\iota \otimes \iota} & A \otimes A \\
 \downarrow \mu & & \downarrow \wr & & \uparrow \Delta \\
 A & \xrightarrow{\varepsilon} & \mathbb{K} & \xrightarrow{\iota} & A
 \end{array}$$

$$\begin{array}{ccc}
 A \otimes A & \xrightarrow{\Delta \otimes \Delta} & A \otimes A \otimes A \otimes A \\
 \downarrow \Delta \circ \mu & & \downarrow \text{id} \otimes \tau \otimes \text{id} \\
 A \otimes A & \xleftarrow{\mu \otimes \mu} & A \otimes A \otimes A \otimes A
 \end{array}$$

$$\begin{array}{ccc}
 \mathbb{K} & & A \\
 \downarrow \text{id} & \searrow \iota & \\
 \mathbb{K} & & \swarrow \varepsilon
 \end{array}$$

Definition 2.1.13. A coalgebra is said to be *cocommutative* if $\tau \circ \Delta = \Delta$, where τ is the transposition map $\tau : a \otimes b \mapsto b \otimes a$.

Incorporating specific additional structure upgrades a bialgebra to a Hopf algebra, which is a primary object of interest throughout this work.

Definition 2.1.14. A *Hopf algebra*, A , is a bialgebra equipped with a \mathbb{K} -linear map, $S : A \rightarrow A$, called the antipode map, such that the following diagrams commute.

$$\begin{array}{ccc}
 A & \xrightarrow{\Delta} & A \otimes A \\
 \downarrow \iota \circ \varepsilon & & \downarrow \text{id} \otimes S \\
 A & \xleftarrow{\mu} & A \otimes A
 \end{array}
 \qquad
 \begin{array}{ccc}
 A & \xrightarrow{\Delta} & A \otimes A \\
 \downarrow \iota \circ \varepsilon & & \downarrow S \otimes \text{id} \\
 A & \xleftarrow{\mu} & A \otimes A
 \end{array}$$

Although not every bialgebra is a Hopf algebra, it's a simple and quick exercise to show that these commuting diagrams force S to be unique, when it does exist.

Definition 2.1.15. Let A be a Hopf algebra. We define $A\text{-Rep}$ to be the category whose objects are finite dimensional A -modules and morphisms are A -module homomorphisms.

2.2 Quantum Groups

When we first start learning about multiplication in mathematics, everything we concerned ourselves with would always commute. For example $7 \cdot 3$ is the same as $3 \cdot 7$. As we progress in our mathematical journeys, we eventually learn about certain objects that don't commute at all, like matrices or free groups. When attempting to multiply matrices of different dimensions, AB may not even be well-defined where as BA might be. Quantum commuting lies somewhere in-between. Roughly speaking, we say A and B q -commute if $AB = qBA$ for some $q \in \mathbb{C}^\times$. The idea is as we limit $q \rightarrow 1$, we get back full commutivity.

Using this notion, we can take an algebra and throw in some q 's to try to give it a *quantum deformation*. For example, take the free algebra in two variables $\mathbb{C}\langle X, Y \rangle$. If we want X and Y to commute in this algebra, we need to additionally quotient out by the ideal generated by $XY - YX$. We often refer to this algebra as a *torus* to indicate that both X and Y are commutative and invertible. In order to “deform” or “quantize” this object, we slightly change this quotient to be $XY - qYX$ for some $q \in \mathbb{C}^\times$ instead and can now say that X and Y q -commute.

Unfortunately, there is no universally accepted definition for the term *quantum group*. However, there are some generally agreed upon properties that that these objects should contain. In particular, quantum groups should include deformations of particular objects that relate to algebraic groups. The main examples most mathematicians tend to care about are quantum Lie groups.

Unless specified otherwise, this thesis will exclusively use \mathbb{C} as the underlying ring and $q \in \mathbb{C}^\times$. However, it should be noted that much of this story can be adapted for any

Noetherian domain, \mathcal{R} , and using the ring $\mathcal{R}[q^{\pm 1}]$ or a localization of it over polynomials in q .

A *quantum Lie group* is a non-commutative, non-cocommutative Hopf algebra, $U_q(\mathfrak{g})$, which is a deformation of the universal enveloping algebra, $U(\mathfrak{g})$. We will primarily be working with the Lie algebra $\mathfrak{g} = \mathfrak{sl}_2(\mathbb{C})$ in this thesis. Fix an element $q \in \mathbb{C}^\times$ and suppose it's not a root of unity.² The corresponding quantized enveloping algebra is defined as

$$U_q(\mathfrak{sl}_2) = \frac{\mathbb{C}[E, F, K^{\pm 1}]}{\left(\begin{array}{l} KEK^{-1} = q^2 E \\ KFK^{-1} = q^{-2} F \\ [E, F] = \frac{K - K^{-1}}{q - q^{-1}} \end{array} \right)}$$

The set of monomials $\{F^s K^n E^r\}$ with $r, s \in \mathbb{N}$ and $n \in \mathbb{Z}$ forms a PBW basis for $U_q(\mathfrak{sl}_2)$ (see Theorem 1.5 in [32] for details). As we can grade a free algebra using arbitrary degrees for each generator, we typically consider $\deg(E) = 1$, $\deg(F) = -1$, and $\deg(K) = \deg(K^{-1}) = 0$, giving this algebra a \mathbb{Z} -grading. In particular, a monomial $F^s K^n E^r$ would have degree $r - s$.

In the theory of quantized enveloping algebras, there are many parallels to formulas found in the theory of universal enveloping algebras. In particular, we often replace the traditional binomial coefficients with their quantum counterparts, known as Gaussian

²Many of the results throughout this work fail when q is a root of unity. Although many people study these kinds of problems at roots of unity, we will not consider this case as it is quite a different beast to work with.

binomial coefficients. For any $m \in \mathbb{N}$, we first define

$$[m] = \frac{q^m - q^{-m}}{q - q^{-1}} \quad \text{and} \quad [m]! = [1][2] \cdots [m]$$

with $[0]! = 1$. The *Gaussian binomial coefficients* are then defined as:

$$\begin{bmatrix} m \\ k \end{bmatrix} = \frac{[m]!}{[k]![m-k]}.$$

This notation will be used throughout the remainder of this section.

As is the general trend for \mathfrak{sl}_2 -modules, we can think of F and E as raising and lowering operators, while K can be thought of, in some sense, as a diagonalizable operator since it's invertible. It turns out that when M is a finite dimensional $U_q(\mathfrak{sl}_2)$ -module, E and F must act as raising and lowering operators and so M must be fully torsion. Thus, when M is finite dimensional, there are always integers $r, s > 0$ such that $E^r M = F^s M = 0$. Moreover, any finite dimensional $U_q(\mathfrak{sl}_2)$ -module is a direct sum of all of its weight spaces and all the weights are of the form $\pm q^n$ for some $n \in \mathbb{Z}$. For further details, see [32].

Theorem 2.2.16 (2.6 in [32]). For every integer $n \geq 0$, there exists a simple $U_q(\mathfrak{sl}_2)$ -module, $L(n, +)$, with basis $\{m_0, \dots, m_n\}$ such that for all $0 \leq i \leq n$

$$K m_i = q^{n-2i} m_i,$$

$$F m_i = \begin{cases} m_{i+1}, & \text{if } i < n \\ 0, & \text{if } i = n \end{cases}$$

$$E m_i = \begin{cases} [i][n+1-i] m_{i-1}, & \text{if } i > 0 \\ 0, & \text{if } i = 0 \end{cases}$$

as well as a simple $U_q(\mathfrak{sl}_2)$ -module, $L(n, -)$, with basis $\{m'_0, \dots, m'_n\}$ such that

$$\begin{aligned}
 Km'_i &= -q^{n-2i}m'_i, \\
 Fm'_i &= \begin{cases} m'_{i+1}, & \text{if } i < n \\ 0, & \text{if } i = n \end{cases} \\
 Em'_i &= \begin{cases} -[i][n+1-i]m'_{i-1}, & \text{if } i > 0 \\ 0, & \text{if } i = 0 \end{cases}
 \end{aligned}$$

Every simple $U_q(\mathfrak{sl}_2)$ -module of dimension $n+1$ is isomorphic to either $L(n, +)$ or $L(n, -)$, giving us a full classification of $U_q(\mathfrak{sl}_2)$ -Rep (see [11, 32]). These two modules are isomorphic if and only if the underlying base field has characteristic 2. Although $L(n, +)$ is not isomorphic to $L(n, -)$ in our case as we're working over \mathbb{C} , we will only consider $L(n, +)$ and just keep a note in the back untouched recesses of our minds that there are actually two of them. Furthermore, we will condense and abuse notation by using $L(n)$ in place of $L(n, +)$ throughout. $L(n)$ are analogues of highest-weight modules of \mathfrak{sl}_2 .

A quick observation shows us that the smallest module where E , F , and K don't act trivially is $L(1)$. The two dimensional module $L(1)$ is often called the *standard representation* or *fundamental representation* of $U_q(\mathfrak{sl}_2)$ as it comes from the particular two dimensional representation $\rho : U_q(\mathfrak{sl}_2) \rightarrow \text{End}(V)$ defined by

$$\rho(K) = \begin{pmatrix} q & 0 \\ 0 & q^{-1} \end{pmatrix} \quad \rho(F) = \begin{pmatrix} 0 & 0 \\ 1 & 0 \end{pmatrix} \quad \rho(E) = \begin{pmatrix} 0 & 1 \\ 0 & 0 \end{pmatrix},$$

which matches up with the module structure of $L(1)$ defined above.

$$\begin{array}{ll}
Km_0 = qm_0 & Km_1 = q^{-1}m_1 \\
Fm_0 = m_1 & Fm_1 = 0 \\
Em_0 = 0 & Em_1 = m_0
\end{array}$$

Clearly, this representation is closely related to the standard representation of $U(\mathfrak{sl}_2)$, i.e. $\mathfrak{sl}_2(\mathbb{C})$.

$$\rho(h) = \begin{pmatrix} 1 & 0 \\ 0 & -1 \end{pmatrix} \quad \rho(f) = \begin{pmatrix} 0 & 0 \\ 1 & 0 \end{pmatrix} \quad \rho(e) = \begin{pmatrix} 0 & 1 \\ 0 & 0 \end{pmatrix}$$

It follows from the fact that $U_q(\mathfrak{sl}_2)$ is a Hopf algebra that the category of finite-dimensional $U_q(\mathfrak{sl}_2)$ representations is closed under tensor products. In particular, we have that

$$L(n) \otimes L(m) \cong \bigoplus_{k=0}^{\min\{m,n\}} L(m+n-2k). \tag{2.2}$$

By equation 2.2, we get that $L(2) \subset L(2) \oplus L(0) \cong L(1) \otimes L(1)$ and $L(m+1) \subset L(m+1) \oplus L(m-1) \cong L(m) \otimes L(1)$. By induction, every finite dimensional $U_q(\mathfrak{sl}_2)$ -module can be embedded inside a sufficiently high enough tensor power of $L(1)$. Specifically, for any non-negative integer n , $L(n) \subset L(1)^{\otimes n}$. With the appropriate projector, we can always take this tensor power and project onto the corresponding component we are interested in. For this reason, $L(1)$ is called a *tensor generator* in this category. Specifically, we have particular inclusion and projection maps that intertwine the action of $U_q(\mathfrak{sl}_2)$. Recall that

$\{m_0, m_1, \dots, m_n\}$ is a basis for $L(n)$. These inclusions and projections are

$$\begin{aligned} \iota_n : L(n) &\hookrightarrow L(1)^{\otimes n} & (2.3) \\ m_k &\mapsto \binom{n}{k}^{-1} \sum_{\substack{(\varepsilon_1, \dots, \varepsilon_k) \in \{0,1\}^n, \\ \sum_{\ell=1}^n \varepsilon_\ell = k}} q^{\sum_{i < j} \delta_{\varepsilon_i, \varepsilon_j + 1}} m_{\varepsilon_1} \otimes \dots \otimes m_{\varepsilon_n} \end{aligned}$$

$$\begin{aligned} \pi_n : L(1)^{\otimes n} &\rightarrow L(n) & (2.4) \\ (m_{\varepsilon_1} \otimes \dots \otimes m_{\varepsilon_n}) &\mapsto q^{\sum_{i < j} -\delta_{\varepsilon_i + 1, \varepsilon_j}} m_{\sum_{k=1}^n \varepsilon_k}. \end{aligned}$$

One can check that the operator $p_n = \iota_n \circ \pi_n$, which is often called the *Jones-Wenzl projector*, satisfies $p_n \circ p_n = p_n$, and so this is indeed a projector.³

2.3 Ribbon Hopf Algebras

We mentioned before that $U_q(\mathfrak{sl}_2)$ is a non-commutative non-cocommutative Hopf algebra. The algebra structure is clear and the rest of its Hopf structure is as follows:

$$\begin{aligned} \Delta(E) &= E \otimes 1 + K \otimes E & \varepsilon(E) &= 0 & S(E) &= K^{-1}E \\ \Delta(F) &= F \otimes K^{-1} + 1 \otimes F & \varepsilon(F) &= 0 & S(F) &= -FK \\ \Delta(K) &= K \otimes K & \varepsilon(K) &= 1 & S(K) &= K^{-1} \end{aligned}$$

Throughout this section, we will be using *sumless Sweedler notation*: $\Delta(u) = u_{(1)} \otimes u_{(2)}$. This also means that we may also write something like $u_{(3)}$ without further explanation as $U_q(\mathfrak{sl}_2)$ is coassociative and so $(\text{id} \otimes \Delta) \circ \Delta = (\Delta \otimes \text{id}) \circ \Delta$.

³The definitions provided here for π_n and ι_n were translated from Frenkel and Khovanov's work in [24] to better fit our notation.

Let M and N be $U_q(\mathfrak{sl}_2)$ -modules, $u \in U_q(\mathfrak{sl}_2)$, $m \in M$, and $n \in N$. $U_q(\mathfrak{sl}_2)$ has a natural action on the tensor product, $M \otimes N$, defined using the coproduct:

$$u \cdot (m \otimes n) := \Delta(u) \cdot (m \otimes n),$$

making $M \otimes N$ a $U_q(\mathfrak{sl}_2)$ -module as well. Additionally, $M^* := \text{Hom}_{\mathbb{C}}(M, \mathbb{C})$, can also be made into a (left) $U_q(\mathfrak{sl}_2)$ -module by the action

$$(u \cdot f)(m) = f(S(u) \cdot m).$$

We can look at M^* as the left and right dual of M . However, both corresponding evaluation homomorphisms can't be as simple as plugging $m \in M$ into $f \in M^*$ as $U_q(\mathfrak{sl}_2)$ is not cocommutative. In particular, the map $f \otimes m \rightarrow f(m)$ is a homomorphism of $U_q(\mathfrak{sl}_2)$ -modules, however, $m \otimes f \mapsto f(m)$ is not a homomorphism in general.

For a moment, let's suppose this is a $U_q(\mathfrak{sl}_2)$ -module homomorphism and prod the situation a bit to see what happens. When we combine these actions and consider the evaluation map corresponding to the left dual, we see that

$$\begin{aligned} u \cdot \text{ev}(f \otimes m) &= \text{ev}(u \cdot f \otimes m) \\ &= \text{ev}(u_{(1)}f \otimes u_{(2)}m) \\ &= u_{(1)}f(u_{(2)} \cdot m) \\ &= f(S(u_{(1)})u_{(2)}m) \\ &= f((\mu \circ (S \otimes \text{id}) \circ \Delta)(u) \cdot m). \end{aligned}$$

However, when we repeat this for the right dual we get

$$\begin{aligned}
u \cdot \text{ev}(m \otimes f) &= \text{ev}(u \cdot m \otimes f) \\
&= \text{ev}(u_{(1)}m \otimes u_{(2)}f) \\
&= u_{(2)}f(u_{(1)} \cdot m) \\
&= f(S(u_{(2)})u_{(1)}m) \\
&= f((\mu \circ (S \otimes \text{id}) \circ \tau \circ \Delta)(u) \cdot m).
\end{aligned}$$

Since $\tau \circ \Delta \neq \Delta$, we encounter a contradiction. Furthermore, the uniqueness of S means that the complications arising from the lack of cocommutativity in $U_q(\mathfrak{sl}_2)$ cannot be easily remedied. However, this should be viewed as a feature rather than a bug, as quantum groups were intentionally created to exhibit this defect. Moreover, if we instead define our evaluation map to be $m \otimes f \mapsto f(K^{-1}m)$, this does work as a proper evaluation map compatible with the $U_q(\mathfrak{sl}_2)$ action. Although the map $\tau : M^* \otimes M \rightarrow M \otimes M^*$ is not a proper $U_q(\mathfrak{sl}_2)$ -module homomorphism, there must exist an isomorphism when M is finite dimensional by a simple dimension counting argument. This observation indicates that $U_q(\mathfrak{sl}_2)$ -Rep must be braided but not symmetric.

Definition 2.3.17. A *quasitriangular Hopf algebra* is a pair (A, R) where A is a Hopf algebra and $R \in A \otimes A$ such that R is invertible and

$$\begin{aligned}
(\Delta \otimes \text{id})R &= R_{13}R_{23} \\
(\text{id} \otimes \Delta)R &= R_{13}R_{12} \\
(\tau \circ \Delta)(a) &= R(\Delta(a))R^{-1}
\end{aligned}$$

for all $a \in A$ where τ denotes the transposition map $\tau : a \otimes b \mapsto b \otimes a$ and R_{ij} is the tensor triple with R in the i th and j th factors and 1 in the other.

A Hopf algebra being quasitriangular corresponds to the “braiding” in the notion of a braided monoidal category. In particular, R is one of the isomorphisms that provides this braiding. While R is not unique in general, we will demonstrate how to compute a family of examples in $U_q(\mathfrak{sl}_2)$.

First define $\theta_n = (-1)^n q^{-n(n-1)/2} \frac{(q-q^{-1})^n}{[n]!} F^n \otimes E^n$, where $[n]! = \left(\frac{q^n - q^{-n}}{q - q^{-1}}\right) \cdots \left(\frac{q - q^{-1}}{q - q^{-1}}\right)$ and suppose M and N are finite dimensional $U_q(\mathfrak{sl}_2)$ -modules. Define the linear transformation $\theta : M \otimes N \rightarrow M \otimes N$ as the finite sum⁴ of operators $\theta = \sum_{n \geq 0} \theta_n$. For example, if $M = N = L(1)$, then $M \otimes N$ is 4 dimensional. Since $E^2 M = F^2 M = 0$, we get that $\theta = 1 \otimes 1 - (q - q^{-1})F \otimes E$. Furthermore, we can express θ as the following matrix with respect to the basis described in theorem 2.2.16, $\{m_0 \otimes m_0, m_0 \otimes m_1, m_1 \otimes m_0, m_1 \otimes m_1\}$.

$$\theta = \begin{bmatrix} 1 & 0 & 0 & 0 \\ 0 & 1 & 0 & 0 \\ 0 & q^{-1} - q & 1 & 0 \\ 0 & 0 & 0 & 1 \end{bmatrix}.$$

All weights of finite dimensional $U_q(\mathfrak{sl}_2)$ -modules are of the form $\pm q^n$ for $n \in \mathbb{Z}$. Therefore, all weights for all objects in $U_q(\mathfrak{sl}_2)$ -Rep lie in $\tilde{\Lambda} = \{\pm q^n \mid n \in \mathbb{Z}\}$. Define a map $f : \tilde{\Lambda} \times \tilde{\Lambda} \rightarrow \mathbb{C}^\times$ such that $f(\lambda_1, \lambda_2) = \lambda_1 f(\lambda_1, q^2 \lambda_2) = \lambda_2 f(q^2 \lambda_1, \lambda_2)$ for all $\lambda_1, \lambda_2 \in \tilde{\Lambda}$ and consider the bilinear map $\tilde{f} : M \otimes N \rightarrow M \otimes N$ defined as $\tilde{f}(m \otimes n) = f(\lambda_1, \lambda_2)m \otimes n$ where $Km = \lambda_1 m$ and $Kn = \lambda_2 n$ (see chapters 2 and 3 in [32] for more details).

⁴Although this is not technically a finite sum, we consider it as such as E and F must act nilpotently on finite dimensional modules.

Suppose $f(q, q) = q^{-1}$. Then our formulas for f imply that $f(q, q^{-1}) = qf(q, q) = 1 = f(q^{-1}, q)$ and $f(q^{-1}, q^{-1}) = q^{-1}$. Thus, $\tilde{f}(m_0 \otimes m_0) = \tilde{f}(m_1 \otimes m_1) = q^{-1}$ and $\tilde{f}(m_0 \otimes m_1) = \tilde{f}(m_1 \otimes m_0) = 1$ and so we get a matrix representation

$$\theta \circ \tilde{f} = \begin{bmatrix} q^{-1} & 0 & 0 & 0 \\ 0 & 1 & 0 & 0 \\ 0 & q^{-1} - q & 1 & 0 \\ 0 & 0 & 0 & q^{-1} \end{bmatrix}.$$

The map $R = \theta \circ \tilde{f} \circ \tau : M \otimes N \rightarrow N \otimes M$ is a nontrivial $U_q(\mathfrak{sl}_2)$ -module isomorphism.

This is called an R -matrix and is a braiding that we've been looking for, making $U_q(\mathfrak{sl}_2)$ -Rep a rigid braided monoidal category.

Definition 2.3.18. A *ribbon Hopf algebra* is a triple (A, R, v) consisting of a quasitriangular Hopf algebra (A, R) and a central invertible $v \in A$ such that

$$S(v) = v$$

$$\varepsilon(v) = 1$$

$$v^2 = \mu(S \otimes \text{id})(R_{21}) \cdot S(\mu(S \otimes \text{id})(R_{21}))$$

$$\Delta(v) = (R_{21}R_{12})^{-1}(v \otimes v)$$

We call v the *universal twist* of A . For any $X \in A\text{-Rep}$, the twist $\theta_v : X \rightarrow X$ is defined as $\theta_v(x) = v \cdot x$ and can be thought of as multiplication by v . Since a is invertible, θ_v is an isomorphism and thus is clearly compatible with $B_{Y,X} \circ B_{X,Y} : X \otimes Y \rightarrow X \otimes Y$ in the sense of equation 2.1. This brings us to the following theorem

Theorem 2.3.19 (3.2 in [60]). Let A be a ribbon Hopf algebra. Then the category of finite dimensional A -modules, $A\text{-Rep}$, is a ribbon category.

Once again using $U_q(\mathfrak{sl}_2)$ as our example, we have (partially) outlined that $U_q(\mathfrak{sl}_2)$ -Rep possesses the following properties:

- Monoidal: The tensor product of $U_q(\mathfrak{sl}_2)$ -modules is itself a $U_q(\mathfrak{sl}_2)$ -module.
- Rigid: Every object in $U_q(\mathfrak{sl}_2)$ -Rep has a left and right dual equipped with proper evaluation and coevaluation maps.
- Braided: We can construct R -matrices on these tensor products.
- Twist: There exists an element $\theta \in U_q(\mathfrak{sl}_2)$, that acts on the irreducible representation of highest weight λ as scaling by the constant $-q^{-\langle \lambda, \lambda \rangle / 2 - \langle \lambda, \rho \rangle}$ where $\rho \in \mathfrak{h}$ such that $\langle \alpha_i, \rho \rangle = (\alpha_i, \alpha_i) / 2$, where $\{\alpha_i\}$ is the usual basis for \mathfrak{h}^* .⁵

Therefore, $U_q(\mathfrak{sl}_2)$ -Rep is actually a ribbon category! For more in-depth information about quantum groups and their representations, see [32, 34, 44].

2.4 Skein Modules

Skein modules arose from the search for particular invariants in low-dimensional topology and representation theory. We construct these objects by considering embeddings of links and tangles in a manifold and imposing certain algebraic conditions on them, known as skein relations. The idea is to form a module or algebra where the basis elements are isotopy classes of knots and links inside the manifold, and the relations reflect specific topological or algebraic properties. In this way, skein modules can be thought of as a

⁵We'll eventually only care about the scaling factor $-q^{-3/2}$, which will be reparameterized to $-q^{-3}$. Computing θ becomes messy and so this computation was left out. However, it's not too much work to find this θ using SageMath.

generalization of knot polynomials. They arise naturally in the study of the representation theory of quantum groups and provide a rich, unifying framework for investigating knots, character varieties, and representations.

Before we define a skein module, we will first explain the foundations of these relations and the algebraic properties we aim to better understand.

Definition 2.4.20. A *ribbon*, or *coupon*, in a 3-manifold, M , is a smooth embedding of $[0, 1] \times [0, 1]$ into M . The image of $\{\frac{1}{2}\} \times [0, 1]$ is called the *core* of the ribbon and the images of $[0, 1] \times \{0\}$ and $[0, 1] \times \{1\}$ are the *bases* of the ribbon.

We often do not draw the “thickness” of these ribbons since it often suffices to only draw the core. We are able to avoid losing this extra information as long as there are no half-twists in the ribbon. In particular, we are able to observe and distinguish any full twists in the tangle by using loops in their place. Thus, we will equivalently say that



Figure 2.6: A blackboard framing of a tangle.

these tangles are equipped with a *framing* in these situations. A *framing* of a tangle, T , is a continuous assignment of a vector to each point of T , which is not tangent at that point. We additionally impose the condition that the framings may not include half-twists. We say a framed tangle in $\Sigma \times I$ has a *blackboard framing* if the entire framing is embedded orthogonally to Σ . Every framed link in $\Sigma \times I$ is isotopic to one with a blackboard framing

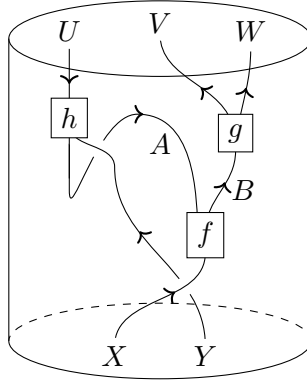


Figure 2.7: An example of a \mathcal{C} -colored ribbon graph embedded into a cylinder

(see figure 2.6). Thus, we may represent ribbons or framed links in $\Sigma \times I$ as link diagrams in Σ .

A *ribbon graph* (sometimes called *fat graph*) is a directed graph whose edges are ribbons and vertices are coupons. Given a category, \mathcal{C} , a \mathcal{C} -colored graph of a ribbon graph is an assignment of objects in \mathcal{C} to each ribbon and an assignment of morphisms in \mathcal{C} to each coupon, compatible with the assigned objects on the adjacent ribbons.⁶

Let \mathcal{C} be a \mathbb{C} -linear ribbon category and let M be the filled-in cylinder depicted in figure 2.7. Consider the oriented \mathcal{C} -colored ribbon graph, Γ , where A , B , U , V , W , X , Y are all objects in \mathcal{C} . As we introduce maps in \mathcal{C} diagrammatically, we will use the convention that everything is read as moving upwards. Note that we could have just as easily chosen downwards instead, but we need to make some choice so that we may talk about composition of Homs as stacking cylinders. Since we're using the convention of moving upwards, composition in \mathcal{C} is seen as stacking compatible cylinders vertically on top of one

⁶Technically, objects are assigned to beginning and ends of ribbons, and the identity map is assigned to (untwisted) ribbons.

another. At every introduced vertex/coupon, we have a morphism, which we've labeled as f , g , and h , that are, once again, moving upwards. The domains of these morphisms are based on the objects immediately below their vertices and codomains as objects immediately above, both read left to right (the induced orientation of the coupon's bases, $[0, 1] \times \{0\}$ and $[0, 1] \times \{1\}$). If a ribbon's orientation doesn't flow in the upwards direction, then we consider the object coloring the ribbon as the corresponding dual object instead. This is well-defined as every ribbon category is also rigid. Therefore, the morphisms in our example are defined as

$$f : X \rightarrow A^* \otimes B$$

$$g : B \rightarrow V \otimes W$$



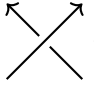
$$h : A^* \otimes Y \rightarrow U^*.$$

With this particular labeling, we are identifying our ribbon graph Γ as an element of $\text{Hom}(X \otimes Y, U^* \otimes V \otimes W)$ via the following theorem. The point of this is to allow us to use a diagrammatic approach to better understand \mathcal{C} . In particular, diagrams allow us to express some very complicated formulas in a way that can be intuitively easier to understand.

Theorem 2.4.21 (2.5 in [52]). Let $A = (A, R, v)$ be a ribbon Hopf algebra over a field of characteristic 0 and let \mathcal{E} be the corresponding category of $(A\text{-Rep})$ -colored ribbon graphs, where $A\text{-Rep}$ is the category of finite dimensional representations of A . There exists a unique covariant functor

$$RT : \mathcal{E} \rightarrow A\text{-Rep}$$

such that

1. RT transforms any decoration in \mathcal{E} into the corresponding A -module,
2. RT transforms each graph Γ into the corresponding homomorphism,
3. RT preserves tensor products, i.e. $RT(\Gamma_1 \otimes \Gamma_2) = RT(\Gamma_1) \otimes RT(\Gamma_2)$,
4. RT maps  to the homomorphism $V^* \otimes V \rightarrow \mathbb{C}$ defined by $f \otimes x \mapsto f(x)$,
5. RT maps  to the homomorphism $V \otimes V^* \rightarrow \mathbb{C}$ defined by $x \otimes f \mapsto f(v^{-1}\mu(S \otimes \text{id})(R_{21})x)$,
6. RT maps  to the R -matrix homomorphism.

See [52] for more details.

The Reshetikhin-Turaev functor, RT , was originally defined only for the case where $M = I \times I \times I$, a cylinder. However, we can attempt to use this definition on an arbitrary 3-manifold by imposing the local relations between morphisms that are in the kernel of the RT functor. Specifically, let M be any 3-manifold and consider all possible \mathcal{C} -colored ribbon graphs that can be embedded into M . By restricting to an embedded cylinder within M , we can then realize the Reshetikhin-Turaev functor as a map from the space of \mathbb{C} -spanned \mathcal{C} -colored ribbon graphs in the embedded cylinder to the appropriate Hom set. For instance, in the previous example we have

$$RT : \mathbb{C}[\Gamma] \longrightarrow \text{Hom}(X \otimes Y, U \otimes V \otimes W)$$

The fact that RT is well-defined is mostly only dependent on \mathcal{C} being a ribbon category. For any classical Lie algebra \mathfrak{g} , $U_q(\mathfrak{g})\text{-Rep}$ is a ribbon category that satisfies the above

requirements for Theorem 2.4.21. Therefore, the Reshetikhin-Turaev functor says that we can understand the category $U_q(\mathfrak{g})\text{-Rep}$ pictorially. In particular, maps in this category can be represented by (a linear combination of) ribbon graphs.

Definition 2.4.22. Given an oriented 3-manifold, M , and a Lie algebra, \mathfrak{g} , the corresponding *skein module* is

$$\text{Sk}_{\mathfrak{g},q}(M) := \mathbb{C}\langle \text{closed ribbon graphs in } M \rangle / \sim_{RT},$$

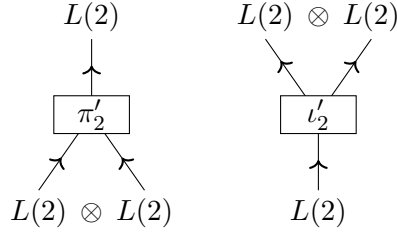
where \sim_{RT} is defined locally on every embedded $I \times I \times I$ and $q \in \mathbb{C}^\times$.

The equivalence relation, \sim_{RT} , are the relations that are picked up through the functor RT . This definition is purposefully vague, due to the fact that the relations are dependent on the category.

When mathematicians define skein modules in the literature, it is important to remember that the given relations are not arbitrary rules that happen to match with $A\text{-Rep}$. Rather, they are the consequences of the structure and properties of that category. For example, when we restrict ourselves to the case of $\mathfrak{g} = \mathfrak{sl}_2$, our graphical calculus becomes greatly simplified. Firstly, since the fundamental representation, $L(1)$, is a tensor generator of $U_q(\mathfrak{sl}_2)\text{-Rep}$, $L(1)$ is the only label we need to consider, allowing us to drop the labeling entirely. Secondly, thanks to quantum Schur-Weyl duality, we can remove any trivalent coupons, meaning we only need to consider links. Finally, the self-duality of $L(1)$ allows us to remove any edge orientations on our ribbon graphs.

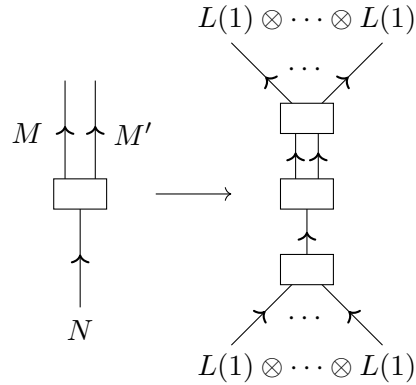
Although the first and third simplifications may be clear, the second one is a bit more complicated. It's important to understand why we don't need to consider trivalent coupons in the \mathfrak{sl}_2 case, since trivalent and other n -valent coupons are necessary in other

cases. For example, consider the subcategory of $U_q(\mathfrak{sl}_2)$ -Rep tensor generated by the adjoint representation, $L(2)$ (this ends up corresponding to PGL_2). Using 2.2, we see that $L(0) \oplus L(2) \oplus L(4) \cong L(2) \otimes L(2)$, giving us maps $\pi'_2 : L(2) \otimes L(2) \rightarrow L(2)$ and $\iota'_2 : L(2) \rightarrow L(2) \otimes L(2)$. This implies that we need to use trivalent coupons in this scenario.



So why is this not needed in the \mathfrak{sl}_2 case?

Since $U_q(\mathfrak{sl}_2)$ -Rep is tensor generated by $L(1)$, any map in this category can be understood by pre-composing and post-composing with the proper inclusion and projection maps described in (2.3) and (2.4). For example, if M , M' , and N are finite dimensional $U_q(\mathfrak{sl}_2)$ -modules, extending a map between N and $M \otimes M'$ might look something like the following picture.



In the classical case, Schur-Weyl duality says that the algebra of intertwining operators of $V^{\otimes m}$ that commute with the action of the algebra $U(\mathfrak{gl}_n)$ is generated by

the permutation of adjacent pairs in the tensor product. However, in the quantum case of $U_q(\mathfrak{sl}_2)$, maps that permute tensor products of modules, like τ , aren't necessarily module homomorphisms and so we need to upgrade to something more complex. The correct setting is to replace the S_m -action with a $\mathbf{H}(S_m)$ -action, where $\mathbf{H}(S_m)$ is the corresponding Hecke algebra.

Definition 2.4.23. The Hecke algebra, $\mathbf{H}(S_n)$, is the complex associative algebra with generators T_1, \dots, T_{n-1} and relations

$$T_i T_j = T_j T_i \quad \text{if } |i - j| > 1,$$

$$T_i T_{i+1} T_i = T_{i+1} T_i T_{i+1},$$

$$(T_i - q)(T_i + q^{-1}) = 0.$$

Remark 2.4.24. If we specialize $q = 1$, we get back the symmetric group algebra. Therefore, the Hecke algebra, $\mathbf{H}(S_n)$, is a deformation of $\mathbb{C}[S_n]$, and is why we use this notation.

Remark 2.4.25. It may seem like each generator, T_i , does not have an inverse in $\mathbf{H}(S_n)$ a priori. However, expanding the last relation provides us with a closed form of its inverse, proving its existence.

$$\begin{aligned} 1 &= T_i^2 - qT_i + q^{-1}T_i \\ \Rightarrow T_i^{-1} &= T_i - (q - q^{-1}) \end{aligned}$$

Remark 2.4.26. The last two relations of the Hecke algebra are equivalent to solutions for YBE.

Theorem 2.4.27 (12.3.10 in [11]). Suppose $m, n > 1$ and consider the module $L(n-1)^{\otimes m}$. There is a functor from $\mathbf{H}(S_m)$ -Rep to the subcategory of $U_q(\mathfrak{sl}_n)$ -Rep consisting of modules isomorphic to an irreducible component of $L(1)^{\otimes m}$ defined by

$$\mathcal{J} : M \mapsto M \otimes_{\mathbf{H}(S_m)} L(n-1)^{\otimes m}$$

where the $U_q(\mathfrak{sl}_n)$ -module structure is the natural structure induced by $L(n-1)^{\otimes m}$.

In particular, this functor is essentially surjective and thus every endomorphism in the algebra $\text{End}_{U_q(\mathfrak{sl}_n)}(L(n-1)^{\otimes m})$ can be understood using a representation of $\mathbf{H}(S_m)$. Moreover, if $m \leq n$, then \mathcal{J} is also injective, making \mathcal{J} an equivalence of categories.

One would hope that the action of the Hecke algebra has a diagrammatic interpretation nice enough to not have any n -valent coupons for $n \geq 3$. Unfortunately, the Hecke algebra does not have to play nicely and the lack of n -valent coupons is not true in general. However, a particular algebra that is diagrammatic very nice and has all of the properties that we could ask for is the *Temperley-Lieb algebra*.

Definition 2.4.28. The Temperley-Lieb algebra, $TL_n(\delta)$, where $\delta \in \mathbb{C}^\times$, is a unital associative algebra over \mathbb{C} with generators U_1, \dots, U_{n-1} and defining relations

$$U_i^2 = \delta U_i$$

$$U_i U_{i\pm 1} U_i = U_i$$

$$U_i U_j = U_j U_i \quad \text{for } |i - j| > 1.$$

See figure 2.8 for a graphical example of multiplying two elements in $TL_5(\delta)$. In this example, multiplication is understood as vertical stacking and any closed loop is replaced by the distinguished scaling factor, δ .

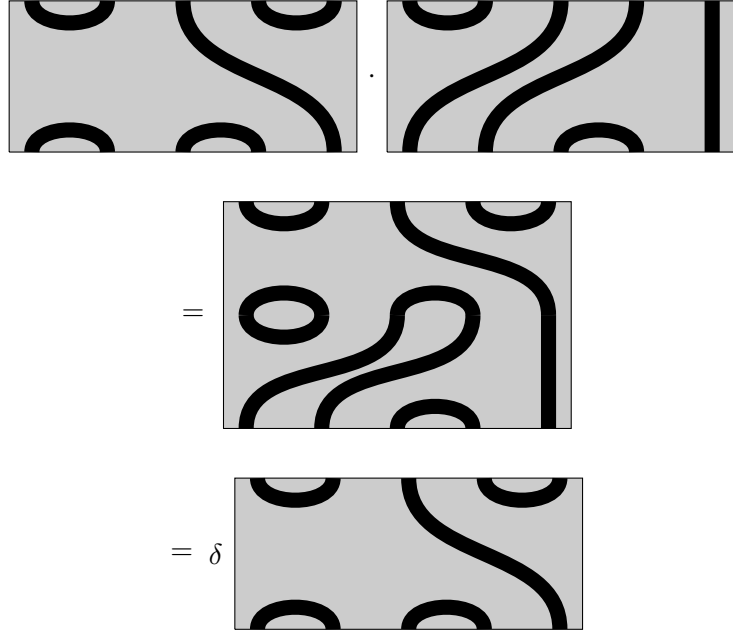


Figure 2.8: Multiplication in $TL_n(\delta)$ corresponds to vertical concatenation.

$TL_n(\delta)$ can be realized as the algebra of intertwining operators acting on the $U_q(\mathfrak{sl}_2)$ -module $L(1)^{\otimes n}$, as follows:

$$U_i \mapsto \text{id}^{\otimes(i-1)} \otimes (\text{coev} \circ \text{ev}) \otimes \text{id}^{\otimes(n-i-1)},$$

where $\text{ev} : L(1) \otimes L(1) \rightarrow L(0)$ and $\text{coev} : L(0) \rightarrow L(1) \otimes L(1)$. Notice how these maps correspond to the evaluation and coevaluation maps defined for rigid categories. Therefore, the diagrammatic interpretations of coev and ev correspond to cups and caps.

$$\text{coev} \circ \text{ev} = \text{⊙}$$

In particular, TL_n can be diagrammatically understood without any crossings and without any trivalent coupons (see figure 2.8). Moreover, the following proposition relates the Hecke algebra with a corresponding Temperley-Lieb algebra.

Proposition 2.4.29. There is a surjective algebra homomorphism

$$\mathbf{H}(S_m) \twoheadrightarrow TL_m(-q - q^{-1})$$

$$T_i \mapsto q + U_i.$$

When $m = 2$, this is an algebra isomorphism.

Proof. Call this map φ and notice that φ is a well-defined map as

$$\begin{aligned} \varphi(T_i T_i^{-1}) &= (q + U_i)(q^{-1} + U_i) \\ &= 1 + (q + q^{-1})U_i + U_i^2 \\ &= 1 \end{aligned}$$

$$\begin{aligned} \varphi(T_i T_{i+1} T_i) &= (q + U_i)(q + U_{i+1})(q + U_i) \\ &= q^3 + q^2 U_i + q^2 U_{i+1} + q U_i U_{i+1} + q U_{i+1} U_i + q^2 U_i + q U_i^2 + U_i U_{i+1} U_i \\ &= q^3 + q^2 (U_i + U_{i+1}) + q (U_i U_{i+1} + U_{i+1} U_i) \\ &= \varphi(T_{i+1} T_i T_{i+1}) \end{aligned}$$

$$\begin{aligned} \varphi(T_i T_j) &= (q + U_i)(q + U_j) \\ &= (q + U_j)(q + U_i) \\ &= \varphi(T_j T_i) \end{aligned}$$

for $|i - j| > 1$. As this is an algebra homomorphism and $\varphi(T_i - q) = U_i$ for all i , φ is surjective.

If $n = 2$, then both algebras only have one generator. Thus, the relations are greatly simplified and both algebras are two dimensional. For any $a, b \in \mathbb{C}$, if

$$0 = \varphi(aT + b) = a(q + U) + b$$

then $a = b = 0$ as $\{1, U\}$ is a basis for $TL_2(-q - q^{-1})$ and so φ is injective. This clearly fails for even just $n = 3$ by a dimension counting argument. \square

Therefore, the Hecke algebra will always surject onto the Temperley-Lieb algebra. It turns out that when working in the setting of $U_q(\mathfrak{sl}_2)$, $TL_m(-q - q^{-1})$ accounts for the entire algebra $\text{End}_{U_q(\mathfrak{sl}_2)}(L(1)^{\otimes m})$, just like the Hecke algebra. As TL_m doesn't use trivalent coupons and this completely overlaps with the action of $\mathbf{H}(S_m)$, quantum Schur-Weyl duality says $U_q(\mathfrak{sl}_2)$ -Rep doesn't need to consider them either.

Remark 2.4.30. Note that coupons are usually used when discussing skein categories or specifically A -Rep itself. When focusing on particular skein modules, many works will drop the coupons altogether and just use traditional vertices instead, a convention that we'll be following for the rest of this thesis.

Note: The previous definition that we used for the quantized universal enveloping algebra, $U_q(\mathfrak{sl}_2)$, follows the fairly standard convention found in most textbooks. However, in skein theory, mathematicians often reparameterize q to q^2 for convenience. It's important to note that for the remainder of this work, we will adopt this reparameterization as well.

$$U_q(\mathfrak{sl}_2) = \frac{\mathbb{C}[E, F, K^{\pm 1}]}{\left(\begin{array}{l} KEK^{-1} = q^4 E \\ KFK^{-1} = q^{-4} F \\ [E, F] = \frac{K - K^{-1}}{q^2 - q^{-2}} \end{array} \right)}$$

This adjustment simplifies notation, reducing the need for fractional powers of q and limiting us to using at worst $q^{1/2}$.

2.5 Kauffman Bracket Skein Algebras

When in the case of $\mathfrak{g} = \mathfrak{sl}_2$, the R -matrix (the braiding) has a sum decomposition that can be somewhat understood as a constant times the identity map and another constant times an evaluation map composed with a coevaluation map. This diagrammatically looks like the following.

$$\begin{array}{c} L(1) \otimes L(1)^* \\ \text{---} \bullet \quad \bullet \text{---} \\ \diagdown \quad \diagup \\ \diagup \quad \diagdown \\ \text{---} \bullet \quad \bullet \text{---} \\ L(1) \otimes L(1)^* \end{array} = q \begin{array}{c} L(1) \otimes L(1)^* \\ \text{---} \bullet \quad \bullet \text{---} \\ | \quad | \\ \text{---} \bullet \quad \bullet \text{---} \\ L(1) \otimes L(1)^* \end{array} + q^{-1} \begin{array}{c} L(1) \otimes L(1)^* \\ \text{---} \bullet \quad \bullet \text{---} \\ \cup \\ L(1) \otimes L(1)^* \\ \text{---} \bullet \quad \bullet \text{---} \\ \cap \\ \text{---} \bullet \quad \bullet \text{---} \\ L(1) \otimes L(1)^* \end{array}$$

Similarly, as ribbon categories are rigid categories, we can also compute $\text{eval} \circ \text{coeval}$ and find

$$\begin{array}{c} \text{---} \\ \circ \\ \text{---} \end{array} = -q^2 - q^{-2}.$$

These two relations create what are called the Kauffman bracket skein relations.

One might consider the implications of extending these relations to 3-manifolds beyond $\mathbb{R}^2 \times I$. Such extensions gives rise to skein modules, which notably, in the case of \mathfrak{sl}_2 , results in the Kauffman bracket skein module. These modules have proven to be quite important in noncommutative geometry, knot theory, and, of course, quantum representation theory.

As mentioned in section 2.4, we will always use a blackboard framing for our curves (see figure 2.6) and avoid using half-twists. Moreover, using the above relations, we can explicitly compute both framing relations:

$$\begin{aligned}
 \text{Diagram 1} &= q \text{ Diagram 2} + q^{-1} \text{ Diagram 3} \\
 &= q \text{ Diagram 4} + q^{-1}(-q^2 - q^{-2}) \text{ Diagram 5} \\
 &= -q^{-3} \text{ Diagram 6}
 \end{aligned}$$

$$\begin{aligned}
 \text{Diagram 1} &= q \text{ Diagram 2} + q^{-1} \text{ Diagram 3} \\
 &= q(-q^2 - q^{-2}) \text{ Diagram 4} + q^{-1} \text{ Diagram 5} \\
 &= -q^3 \text{ Diagram 6}
 \end{aligned}$$

Definition 2.5.31. The *Kauffman bracket skein module*, $K_q(M)$, of an oriented 3-manifold, M , is the \mathbb{C} -module generated by isotopy classes of framed unoriented links in M , modulo the following two local relations.

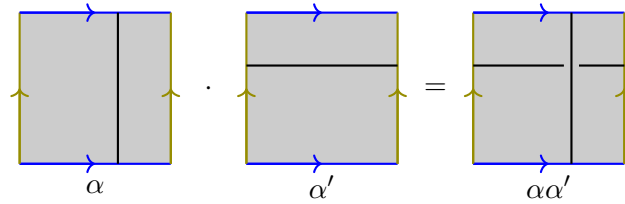
$$\text{Diagram 1} = q \text{ Diagram 2} + q^{-1} \text{ Diagram 3}$$

(R₁) Skein Relation

$$\text{Diagram 1} = (-q^2 - q^{-2}) \text{ Diagram 2}$$

(R₂) Trivial Knot Relation

If additionally $M = \Sigma \times I$, then we can define the multiplication of two diagrams, $\alpha \cdot \alpha'$, by stacking α above α' along the interval I . For example, if M is a thickened torus, multiplying the longitude and meridian together results in the following diagram.



While Kauffman bracket skein modules are technically only defined for 3-manifolds, we often use the shorthand $K_q(\Sigma)$ to refer to $K_q(\Sigma \times [0, 1])$ for a surface Σ . This notation also conveys to the reader that there is more than just the module structure—it includes the additional algebra structure defined by stacking.

One particular example that we’re interested in is the Kauffman bracket skein algebra of the torus, $K_q(T^2)$. In general, the simple curves on T^2 can be classified up to homotopy by their “slope.” More specifically, when $r, s \in \mathbb{Z}$ are relatively prime, we define (r, s) to be the unoriented simple closed curve in T^2 that is the image of the line $y = \frac{r}{s}x$ under the natural projection from \mathbb{R}^2 to T^2 .

The algebra $K_q(T^2)$ has been studied quite heavily and thus has an explicit basis. Let $T_n(x)$ be the n th Chebyshev polynomial, defined recursively where $T_0(x) = 2$, $T_1(x) = x$, and $T_{n+1} = xT_n - T_{n-1}$. Define $(r, s)_T$ to be the evaluation of T_d on the $(r/d, s/d)$ -curve where $r, s \in \mathbb{Z}$ and $d = \gcd(r, s)$.

Theorem 2.5.32 ([26]). The set $\{(r, s)_T\}_{r, s \in \mathbb{Z}} / \sim$ where $(r, s)_T \sim (-r, -s)_T$ is a basis for $K_q(T^2)$.

2.6 Stated Skein Algebras

The main restriction of Kauffman bracket skein modules is that they are only defined using links. Whenever one works with links, it's natural to ask whether the framework can be extended to tangles as well. Moreover, in the definition of $K_q(M)$, the boundary of M doesn't play any crucial part, and hence we have $K_q(M) \cong K_q(\overset{\circ}{M})$. In [38], Thang Lê reinterpreted the quantum trace maps in [8] by introducing *stated skein modules*, which addressed how to incorporate both tangles and boundary components to establish an excision property for these modules.

Definition 2.6.33. A *marked 3-manifold* is a pair (M, \mathcal{N}) where M is a compact oriented 3-manifold with (possibly empty) boundary ∂M , and $\mathcal{N} \subset \partial M$ are oriented arcs called *markings*.

Remark 2.6.34. The orientation of the marking provides the points on this arc with a natural ordering.

Definition 2.6.35. A *marked surface* is a pair (Σ, \mathcal{P}) where Σ is a compact oriented surface with (possibly empty) boundary $\partial\Sigma$, and $\mathcal{P} \subset \partial\Sigma$ is a finite set, called the set of marked points.

The associated marked 3-manifold (M, \mathcal{N}) is defined by $M = \Sigma \times I$ and its markings $\mathcal{N} = \mathcal{P} \times I$.

Definition 2.6.36. A *stated \mathcal{N} -tangle* is a pair (α, s) where α is a compact 1-dimensional unoriented submanifold with a framing such that $\partial\alpha = \alpha \cap \mathcal{N}$ and s is a map $s : \partial\alpha \rightarrow \{\pm\}$.

The decorations of these states at each endpoint correspond to our two basis vectors in the fundamental representation of $U_q(\mathfrak{sl}_2)$, $L(1)$. Once again, as $L(1)$ is self-dual, we don't have to worry about orientations of these tangles.

Definition 2.6.37. The *stated skein module* of (M, \mathcal{N}) , denoted $\mathcal{S}(M, \mathcal{N})$, is the quotient of the free module spanned by isotopy classes of stated \mathcal{N} -tangles subject to the following local relations.

(R₁) Skein Relation (R₂) Trivial Knot Relation

(R₃) Trivial Arc Relation 1 (R₄) Trivial Arc Relation 2

(R₅) State Exchange Relation

Using relations $(R_1) - (R_5)$ we can easily find the following state exchange relation, and hence get every state exchange relation.

It's also not too hard to see that for any $\nu \in \{\pm\}$, (R_5) is equivalent to the following height exchange relations.

Diagrammatic equations for Height Exchange Relation (R_6):

- Top row: A diagram with two strands labeled ν meeting at a central dot on a curved boundary, with the region above shaded. This is equal to q times another identical diagram.
- Middle row: A diagram with two strands labeled $-$ and $+$ meeting at a central dot on a curved boundary, with the region above shaded. This is equal to q^{-1} times another identical diagram.
- Bottom row: A diagram with two strands labeled $+$ and $-$ meeting at a central dot on a curved boundary, with the region above shaded. This is equal to q^{-3} times a diagram with two strands labeled $+$ and $-$ meeting at a central dot on a curved boundary, with the region above shaded, plus $q^{-3/2}(q^2 - q^{-2})$ times a diagram with a single strand forming a loop above a central dot on a curved boundary, with the region above shaded.

(R_6) Height Exchange Relation

Lastly, we can also quickly find all trivial arc relations. Below are the trivial arc relations corresponding to different states, (R_3).

Diagrammatic equations for trivial arc relations (R_3):

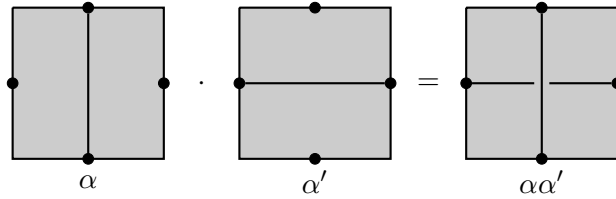
- Top diagram: A diagram with two strands labeled $+$ and $-$ meeting at a central dot on a curved boundary, with the region above shaded. A loop is formed by the strands above the dot. This is equal to $-q^{5/2}$.
- Second diagram: A diagram with two strands labeled $-$ and $+$ meeting at a central dot on a curved boundary, with the region above shaded. A loop is formed by the strands above the dot. This is equal to $q^{1/2}$.
- Third diagram: A diagram with two strands labeled $+$ and $-$ meeting at a central dot on a curved boundary, with the region above shaded. A loop is formed by the strands above the dot. This is equal to $-q^{-5/2}$.
- Bottom diagram: A diagram with two strands labeled $-$ and $+$ meeting at a central dot on a curved boundary, with the region above shaded. A loop is formed by the strands above the dot. This is equal to $q^{-1/2}$.

The first and fourth diagrams, as well as the second and third diagrams, differ by a twist, which introduces a multiplicative factor of $-q^{-3}$. For consistency and convenience, through-

out this thesis, we adopt Lê's notation from [38] for these constants. That is,

$$\begin{aligned} C_+^+ &= 0, \\ C_+^- &= -q^{-5/2}, \\ C_-^+ &= q^{-1/2}, \\ C_-^- &= 0. \end{aligned}$$

Analogous to the Kauffman bracket, if $M = \Sigma \times I$ and $\mathcal{N} = \mathcal{P} \times I$ for $\mathcal{P} \subset \partial\Sigma$, then we can define a \mathbb{C} -algebra structure on the \mathbb{C} -module $\mathcal{S}(M, \mathcal{P})$ by defining products $\alpha\alpha'$ to be stacking α above α' , subject to the same 5 relations.



The Kauffman bracket skein module is functorial in the sense that $K_q(-)$ is a co-variant functor from the category of oriented 3-manifolds with isotopy classes of embeddings as morphisms to the category of \mathbb{C} -modules. Thus, each embedding, $f : M \hookrightarrow M'$, induces a module homomorphism of Kauffman bracket skein modules, $f_* : K_q(M) \rightarrow K_q(M')$, by $f_*[\alpha] = [f(\alpha)]$ for any framed link α . Similarly, the stated skein algebra $\mathcal{S}(-)$ is also functorial. However, the domain of this functor is the category of marked 3-manifolds where our embeddings preserve marking orientations. Indeed, each embedding, $f : (M, \mathcal{N}) \hookrightarrow (M', \mathcal{N}')$, induces a similar homomorphism, $f_* : \mathcal{S}(M, \mathcal{N}) \rightarrow \mathcal{S}(M', \mathcal{N}')$, by $f_*[\alpha] = [f(\alpha)]$ for any stated tangle α .

Since framed links exist in stated skein modules due to relations (R_5) and (R_6) , we get that $K_q(M) \hookrightarrow \mathcal{S}(M, \mathcal{N})$. This is consistent with the functoriality of our skein modules

since \mathcal{N} can be empty and $\mathcal{S}(-)$ can be restricted to the same functor on the category of oriented 3-manifolds, making $K_q(-) \rightarrow \mathcal{S}(-)$ a natural transformation.

The main reason stated skein modules were created was due to the splitting theorem. This theorem allows us to analyze skein algebras through smaller (hopefully simpler) pieces, at the cost of more complexity. As important as this result is, the splitting theorem is not particularly relevant for this thesis, and so it will not be discussed here any further. You can read more details on this theorem in [19, 38, 41].

Since the stated skein modules can be thought of as generalizations of Kauffman bracket skein modules, there are important distinctions to consider that make the stated case more difficult to work with. For example, it is clear from relation (R_1) that when $q = \pm 1$, $K_q(\Sigma \times I)$ is a commutative algebra. However, due to our additional relations, in particular (R_6) , $\mathcal{S}(M, \mathcal{N})$ is *only* commutative at $q = 1$ when \mathcal{N} is nonempty. Moreover, $K_q(M) \cong K_{-q}(M)$ as algebras (see [3]). However, this clearly can't be true in the stated case due to this lack of commutativity. Furthermore, there is additional information to keep track of when working in the stated case. Specifically, we need to keep track of not only the states but also the heights of each tangle at each marking or marked point.

2.7 The Conventional Model

The definitions of stated skein algebras given above differ slightly from the more common ones found in the literature. Our approach to stated tangles is somewhat closer to the notion of *ideal arcs* described in [19, 42] (see also Definition 2.7.40). In this section, we will first introduce the conventional definitions and then demonstrate that they are

isomorphic to our definitions, showing that they can be understood in essentially the same way.

The following definitions are primarily taken from [19] and [38]. However, they have been very slightly modified to fit in our framework. In particular, given a surface, Σ , the corresponding 3-manifold is typically taken as $\Sigma \times (0, 1)$ in the literature. However, it will be important for us to consider $\Sigma \times [0, 1]$ instead as this extra information will be important for us later.

Definition 2.7.38. Let Σ' be a (possibly punctured) oriented surface with (possibly empty) boundary, and $\mathcal{P} \subset \partial\Sigma'$ be a finite nonempty set such that every connected component of $\partial\Sigma'$ has at least one point in \mathcal{P} . Then $\Sigma = \Sigma' \setminus \mathcal{P}$ is called a *punctured bordered surface*.

Remark 2.7.39. Following the notation from definition 2.7.38, Σ' is always uniquely determined by its punctured bordered surface, Σ .

Definition 2.7.40. An *ideal arc* on Σ is an immersion $\alpha : [0, 1] \rightarrow \Sigma'$ such that $\alpha(0), \alpha(1) \in \mathcal{P}$ and the restriction of α onto $(0, 1)$ is an embedding into Σ .

Definition 2.7.41. A connected component of $\partial\Sigma$ is called a *boundary edge*.

Definition 2.7.42. Let $(s, t) \in \Sigma \times [0, 1]$. The *height* of (s, t) is t and we say a vector at (s, t) is *vertical* if it is parallel to $s \times [0, 1]$.

Definition 2.7.43. Let Σ be a punctured bordered surface. A *stated $\partial\Sigma$ -tangle* is a tuple, (α, s) where $\alpha \subset \Sigma \times [0, 1]$ is an unoriented, framed, compact, properly embedded 1-dimensional submanifold such that

- at every point in $\partial\alpha = \alpha \cap (\partial\Sigma \times [0, 1])$ the framing is *vertical*,

- for every boundary edge $b \subset \Sigma$, $\partial\alpha \cap (b \times [0, 1])$ have distinct heights,

and s is a map $s : \partial\alpha \rightarrow \{\pm\}$.

Just as before, we only consider isotopy classes of these stated $\partial\Sigma$ -tangles. Therefore, isotopies of stated $\partial\Sigma$ -tangles are required to preserve the height order.

Definition 2.7.44. The stated skein algebra of a punctured bordered surface, denoted $\mathcal{S}^{pb}(\Sigma)$ or $\mathcal{S}^{pb}(\Sigma')$, is the \mathbb{C} -module freely spanned by isotopy classes of stated $\partial\Sigma$ -tangles modulo the following local relations.

(R_1^{pb}) Skein Relation

(R_2^{pb}) Trivial Knot Relation

(R_3^{pb}) Trivial Arc Relation 1

(R_4^{pb}) Trivial Arc Relation 2

(R_5^{pb}) State Exchange Relation

Definition 2.7.45. A stated $\partial\Sigma$ -tangle, α , is said to be in *generic position* if the natural projection $\pi : \Sigma \times [0, 1] \rightarrow \Sigma$ restricts to an embedding of α , except for the possibility of transverse double points in the interior of Σ .

Each stated $\partial\Sigma$ -tangle is isotopic to one in generic position. Furthermore, we can define a \mathbb{C} -algebra structure on $\mathcal{S}^{pb}(\Sigma)$ by defining products $\alpha \cdot \alpha'$ to be stacking α above α' , just as before, and isotoping the new diagram to be in generic position.

Definition 2.7.46. Let Σ be a punctured bordered surface and \mathfrak{o} be an orientation of $\partial\Sigma$, which may differ from the orientation inherited from Σ . We say a $\partial\Sigma$ -tangle diagram, D , is \mathfrak{o} -ordered if for each boundary component, the points of ∂D increase when traversing in the direction of \mathfrak{o} .

Every $\partial\Sigma$ -tangle can be presented, after an appropriate isotopy, by an \mathfrak{o} -ordered $\partial\Sigma$ -tangle diagram. Figure 2.9 shows examples of \mathfrak{o} -ordered $\partial\Sigma$ -tangle diagrams (without states) when our surface is a torus with boundary.

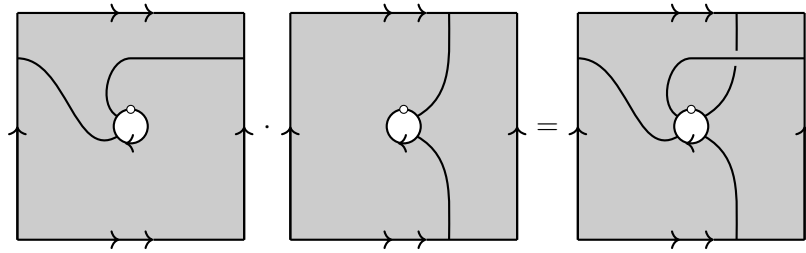


Figure 2.9: A product of \mathfrak{o} -ordered (stateless) $\partial\Sigma$ -diagram where $\Sigma' = T^2 \setminus D^2$ and \mathfrak{o} has a clockwise orientation.

Theorem 2.7.47 (Theorem 2.11 in [38]). Let Σ be a punctured bordered surface and \mathfrak{o} an orientation of $\partial\Sigma$. Define $B(\mathfrak{o}, \Sigma)$ be the set of of all isotopy classes of increasingly stated, \mathfrak{o} -ordered, simple $\partial\Sigma$ -tangle diagrams. Then $B(\mathfrak{o}, \Sigma)$ is a \mathbb{C} -basis of $\mathcal{S}^{pb}(\Sigma)$.

Definition 2.7.48. Let Σ' be a surface with boundary and $\Sigma = \Sigma' \setminus \mathcal{P}$ be the corresponding punctured bordered surface. We say a $\partial\Sigma$ -orientation, \mathfrak{o} , is *consistent* if \mathfrak{o} can be extended to $\partial\Sigma'$. That is, the direction of orientations on adjacent boundary edges agree for every boundary component.

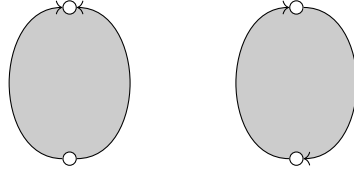


Figure 2.10: The right punctured bordered surface has a consistent orientation while the left does not.

Proposition 2.7.49. Let Σ' be a surface with boundary and $\Sigma = \Sigma' \setminus \mathcal{P}$ be the corresponding punctured bordered surface. There exists an algebra isomorphism $\phi_{\mathfrak{o}} : \mathcal{S}^{pb}(\Sigma) \xrightarrow{\sim} \mathcal{S}(\Sigma', \mathcal{P})$.

Proof. Let \mathfrak{o} be a consistent orientation on $\partial\Sigma$. By theorem 2.7.47, $B(\mathfrak{o}, \Sigma)$ is a basis for $\mathcal{S}^{pb}(\Sigma)$. Let $D \in B(\mathfrak{o}, \Sigma)$ be a fixed representative in its isotopy class.

Define $\iota : \Sigma \times [0, 1] \hookrightarrow \Sigma' \times [0, 1]$ to be the natural embedding and define

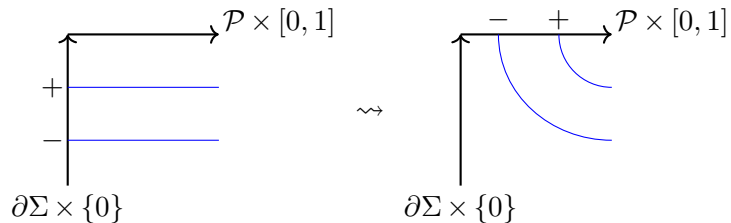
$$\overline{pr}_i : \Sigma' \times [0, 1] \rightarrow \Sigma' \times \{i\} \rightarrow \Sigma' \times [0, 1]$$

$$pr_i : \Sigma \times [0, 1] \rightarrow \Sigma \times \{i\} \rightarrow \Sigma \times [0, 1]$$

to be the natural projection maps composed with their natural embeddings for any $i \in [0, 1]$.

Notice that $(\overline{pr}_0 \circ \iota)(D)$ is simple as D was simple and in generic position.

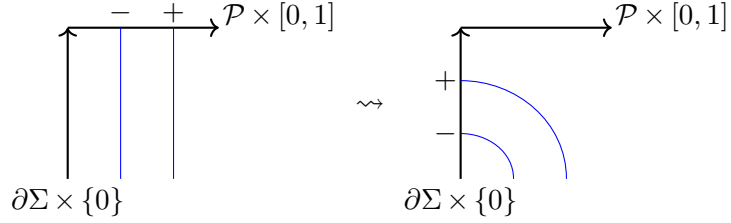
Endow $\mathcal{P} \times [0, 1]$ with its natural orientation induced by the $[0, 1]$ component. For every boundary edge, $b \subset \partial\Sigma'$, isotope the endpoints of $(\overline{pr}_0 \circ \iota)(D)$ on $b \times \{0\}$ along \mathfrak{o} and along the orientation of $\mathcal{P} \times [0, 1]$ so that all endpoints lie on $\mathcal{P}(0, 1)$. Call this new tangle diagram D' .



At this point, it is not clear if D' is still simple, now with respect to Σ' . However, we can still canonically identify D' as some element of $\mathcal{S}(\Sigma', \mathcal{P})$.

Define $\phi_{\mathfrak{o}}(D) = D'$ for each $D \in B(\mathfrak{o}, \Sigma)$ and extend linearly. Notice that $\phi_{\mathfrak{o}}$ is well-defined as D' is unique up to isotopy and $\phi_{\mathfrak{o}}$ respects the relations $(R_1^{pb}) - (R_5^{pb})$ through the corresponding relations $(R_1) - (R_5)$. Moreover, as relative heights are preserved, this is actually an algebra homomorphism as well.

Now let $\alpha' \in \mathcal{S}(\Sigma', \mathcal{P})$ be a fixed representative of its isotopy class and endow Σ with the orientation \mathfrak{o} . Isotope the endpoints of α in each summand in the reverse direction of the orientations of $\mathcal{P} \times [0, 1]$ and $\partial\Sigma \times \{0\}$ until each endpoint lies entirely on $\partial\Sigma \times \{0\}$. Since \mathfrak{o} is consistent, this is well-defined.



We can now view this new object, call it $\tilde{\alpha}'$, as living entirely on $\Sigma \times [0, 1]$. Finally, define $\alpha := pr_{1/2}(\tilde{\alpha}')$ and isotope α so that it is generic and \mathfrak{o} -ordered. Therefore, we can canonically identify α as an element in $\mathcal{S}^{pb}(\Sigma)$.

Pointwise define $\psi_{\mathfrak{o}}(\alpha') = \alpha$ for each $\alpha' \in \mathcal{S}(\Sigma', \mathcal{P})$. Clearly $(\psi_{\mathfrak{o}} \circ \phi_{\mathfrak{o}})(\alpha) = \alpha$ and $(\phi_{\mathfrak{o}} \circ \psi_{\mathfrak{o}})(\alpha') = \alpha'$ for all $\alpha \in \mathcal{S}^{pb}(\Sigma)$ and $\alpha' \in \mathcal{S}(\Sigma', \mathcal{P})$ and hence $\phi_{\mathfrak{o}}$ is bijective. \square

Definition 2.7.50. Let \mathfrak{o} be a consistent orientation on $\partial\Sigma$. We say a $D \in \mathcal{S}(\Sigma')$ is \mathfrak{o} -simple if D is simple and $\psi_{\mathfrak{o}}(D)$ is simple.

Proposition 2.7.51. Every simple diagram in $\mathcal{S}(\Sigma')$ can be written as a linear combination of increasingly stated, \mathfrak{o} -simple $\partial\Sigma'$ -tangle diagrams.

Proof. It suffices to only check for two adjacent endpoints on a single marked point. Firstly, notice that if the diagram is simple, we only need to consider two cases, depending on the orientation, σ , of the adjacent boundary.

$$\begin{array}{cc}
 \psi_\sigma \left(\begin{array}{c} \text{Diagram 1} \\ \mu \quad \nu \end{array} \right) = \begin{array}{c} \text{Diagram 2} \\ \mu \quad \nu \end{array} &
 \psi_\sigma \left(\begin{array}{c} \text{Diagram 3} \\ \mu \quad \nu \end{array} \right) = \begin{array}{c} \text{Diagram 4} \\ \mu \quad \nu \end{array} \\
 \psi_\sigma \left(\begin{array}{c} \text{Diagram 5} \\ \mu \quad \nu \end{array} \right) = \begin{array}{c} \text{Diagram 6} \\ \nu \quad \mu \end{array} &
 \psi_\sigma \left(\begin{array}{c} \text{Diagram 7} \\ \mu \quad \nu \end{array} \right) = \begin{array}{c} \text{Diagram 8} \\ \nu \quad \mu \end{array}
 \end{array}$$

When the adjacent boundary orientation is clockwise, locally we get that

$$\begin{aligned}
 \phi_\sigma \circ \psi_\sigma \left(\begin{array}{c} \text{Diagram 1} \\ \mu \quad \nu \end{array} \right) &= \phi_\sigma \left(\begin{array}{c} \text{Diagram 6} \\ \nu \quad \mu \end{array} \right) \\
 &= \phi_\sigma \left(q C_\nu^\mu \begin{array}{c} \text{Diagram 9} \\ \text{U-shape} \end{array} + q^{-1} \begin{array}{c} \text{Diagram 4} \\ \mu \quad \nu \end{array} \right) \\
 &= q C_\nu^\mu \begin{array}{c} \text{Diagram 10} \\ \text{U-shape with dot} \end{array} + q^{-1} \begin{array}{c} \text{Diagram 8} \\ \nu \quad \mu \end{array}.
 \end{aligned}$$

If the orientation is instead counterclockwise, then we get that

$$\begin{aligned}
 \phi_\sigma \circ \psi_\sigma \left(\begin{array}{c} \text{Diagram 1} \\ \mu \quad \nu \end{array} \right) &= \phi_\sigma \left(\begin{array}{c} \text{Diagram 6} \\ \nu \quad \mu \end{array} \right) \\
 &= \phi_\sigma \left(q \begin{array}{c} \text{Diagram 11} \\ \nu \quad \mu \end{array} + (q^{-1})(-q^3) C_\mu^\nu \begin{array}{c} \text{Diagram 9} \\ \text{U-shape} \end{array} \right) \\
 &= q \begin{array}{c} \text{Diagram 11} \\ \nu \quad \mu \end{array} - q^2 C_\mu^\nu \begin{array}{c} \text{Diagram 10} \\ \text{U-shape with dot} \end{array}.
 \end{aligned}$$

From here, we can use the state exchange relations, (R5), to make the diagram increasingly stated, which does not change height orders or simplicity conditions. \square

Theorem 2.7.52. The set of all isotopy classes of increasingly stated, \mathfrak{o} -simple $\partial\Sigma'$ -tangle diagrams forms a \mathbb{C} -basis for $\mathcal{S}(\Sigma', \mathcal{P})$.

Proof. This directly follows from Propositions 2.7.49 and 2.7.51. \square

Note: Unless specified otherwise, if we denote the stated skein algebra without specifying the markings or marked points (e.g., $\mathcal{S}(M)$), we assume that there is exactly one marking or marked point on its boundary. Additionally, the boundary of M should be obvious. I will always clarify beforehand if there is an exception to this convention, however, it should be clear from the context of which it's given.

2.8 Spherical Double Affine Hecke Algebra

As discussed in section 2.4, we introduced the Hecke algebra, $\mathbf{H}(S_n)$, as a deformation of $\mathbb{C}[S_n]$, the symmetric group algebra. In general, Hecke algebras can be defined over any Coxeter group. More specifically, we want to think of our Hecke algebras as deformations of a Weyl group algebra, $\mathbb{C}[W]$. Given a finite dimensional semisimple Lie algebra, \mathfrak{g} , the jump from Hecke algebra to affine Hecke algebras (AHA) and then to double affine Hecke algebras (DAHA) can be roughly understood as deformations of

$$\begin{array}{lcl} \text{Hecke} & \longleftrightarrow & W \\ \text{AHA} & \longleftrightarrow & W \ltimes P^\vee \\ \text{DAHA} & \longleftrightarrow & W \ltimes (P \oplus P^\vee) \end{array}$$

where P and P^\vee are weight and coweight lattices.

The construction of a DAHA can be done by starting with a quantum torus over $P \oplus P^\vee$, where the q -commuting coefficients are defined through a symplectic pairing, ω , between P and P^\vee . If we think of P and P^\vee as \mathbb{Z}^n , then the corresponding quantum torus is generated by $X_1^{\pm 1}, \dots, X_n^{\pm 1}, Y_1^{\pm 1}, \dots, Y_n^{\pm 1}$ with relations $X^\lambda Y^\mu = q^{\omega(\lambda, \mu)} Y^\mu X^\lambda$, where $X^\lambda := \prod_i X_i^{\lambda_i}$ and $Y^\mu := \prod_j Y_j^{\mu_j}$ for $\lambda \in P$ and $\mu \in P^\vee$. For now, we'll denote this quantum torus as \mathbb{T}_ω^{2n} . In general, the Weyl group action on P and P^\vee corresponds to permutations of the X_i and Y_i in \mathbb{T}_ω^{2n} . When $\mathfrak{g} = \mathfrak{sl}_2$, the Weyl group action corresponds to simultaneously inverting X and Y . This action gives an embedding, $W \hookrightarrow \text{Out}(\mathbb{T}_\omega^{2n}) \cong \text{SP}_{2n}(\mathbb{Z})$, which in turn determines the extension

$$0 \longrightarrow \mathbb{T}_\omega^{2n} \longrightarrow \mathcal{H}_{q,t=1} \longrightarrow \mathbb{C}[W] \longrightarrow 0.$$

As we deform $\mathcal{H}_{q,t=1}$ using the formal parameter t , we simultaneously deform the group algebra $\mathbb{C}[W]$ into its Hecke algebra, using $t \in \mathbb{C}^\times$ as the distinguished parameter now instead of q .

Let's now specialize to the case we are concerned with in this thesis. When $\mathfrak{g} = \mathfrak{sl}_2$, P and P^\vee are both isomorphic to \mathbb{Z} and $W \cong \mathbb{Z}/2\mathbb{Z} \cong S_2$. Therefore, $\mathbf{H}(W)$ has a single generator, T , and single relation, $(T - t)(T + t^{-1}) = 0$, making it a 2-dimensional algebra. Hence, the corresponding A_1 DAHA is precisely the following.

Definition 2.8.53. Define $\mathcal{H}_{q,t}$ to be the algebra generated by $X^{\pm 1}, Y^{\pm 1}$, and T , subject to the relations

$$TXT = X^{-1}, \quad TY^{-1}T = Y, \quad XY = q^2 YXT^2, \quad (T - t)(T + t^{-1}) = 0.$$

Remark 2.8.54. When $t = 1$, our last relation gives us $T^2 = 1$ and thus $XY = q^2 YX$, the same relation found in the quantum torus, \mathbb{T}_ω^2 .

Definition 2.8.55. Assume $t \neq \pm i$ and let $\mathbf{e} \in \mathcal{H}_{q,t}$ be the idempotent $(T + t^{-1})/(t + t^{-1})$. The corresponding *spherical subalgebra* of $\mathcal{H}_{q,t}$ is defined as the two-sided ideal $\mathcal{SH}_{q,t} := \mathbf{e}\mathcal{H}_{q,t}\mathbf{e}$.

Our spherical DAHA inherits its additive and multiplicative structure from $\mathcal{H}_{q,t}$. However, 1 is no longer the multiplicative identity but rather \mathbf{e} is.

Remark 2.8.56. $\mathcal{H}_{q,t}$ is not commutative, even at the limit $q = 1$. However, the spherical subalgebra $\mathcal{SH}_{q,t}$ is commutative at $q = 1$.

Remark 2.8.57. In the limit $t = 1$, $\mathcal{SH}_{q,t}$ is isomorphic to the Weyl-invariant subalgebra of \mathbb{T}_ω^2 .

Remark 2.8.58. This particular spherical DAHA specialized to $q = t = 1$ is isomorphic to the ring of functions on the moduli space of flat SL_2 -connections on a two-torus, T^2 .

Lemma 2.8.59 (Lemma 2.24 in [54]). Suppose $t^2q^{-2} - t^{-2}q^2$ is invertible. Then $\mathcal{H}_{q,t}\mathbf{e}\mathcal{H}_{q,t} = \mathcal{H}_{q,t}$ and $\mathcal{SH}_{q,t}$ is Morita equivalent to $\mathcal{H}_{q,t}$ via the functors

$$\begin{aligned} \mathcal{H}_{q,t}\text{-Mod} &\rightarrow \mathcal{SH}_{q,t}\text{-Mod} & \mathcal{SH}_{q,t}\text{-Mod} &\rightarrow \mathcal{H}_{q,t}\text{-Mod} \\ M &\mapsto \mathbf{e}M & M &\mapsto \mathcal{H}_{q,t}\mathbf{e} \otimes_{\mathcal{SH}_{q,t}} M. \end{aligned}$$

Therefore, if we want to better understand the representation theory of $\mathcal{H}_{q,t}$, it is sufficient to understand the representation theory of $\mathcal{SH}_{q,t}$. Furthermore, it was shown in [54] that $\mathcal{SH}_{q,t}$ is isomorphic to a slightly modified version of the Kauffman bracket skein algebra of the punctured torus.

Definition 2.8.60. For any surface Σ , let $K_{q,t}(\Sigma \setminus D^2)$ be the modified Kauffman bracket skein module defined as the quotient of $K_q(\Sigma \setminus D^2)$ by the relation

$$\begin{array}{c} \text{Cylinder with solid loop} \end{array} = (-q^2 t^{-2} - q^{-2} t^2) \cdot \begin{array}{c} \text{Cylinder with dashed lines} \end{array}$$

In other words, this is exactly the same as the usual Kauffman bracket skein algebra, $K_q(\Sigma \setminus D^2)$, except we have the additional relation where a loop around the boundary can be removed at the cost of the constant $-q^2 t^{-2} - q^{-2} t^2$.

Remark 2.8.61. Since the identity component of the diffeomorphism group of a surface acts transitively, choosing a different disk to remove corresponds to isomorphic algebras. Therefore, we don't need to specify where the disk we removed is located.

When $\Sigma = T^2$, the torus, notice that in the limit $t = 1$ we get $K_{q,t=1}(T^2 \setminus D^2) \cong K_q(\Sigma)$ as algebras. Therefore, setting $t = 1$ can be interpreted as filling in the disk and just considering the closed torus without the resulting boundary.

Theorem 2.8.62 (3.9 in [54]). The algebras $K_{q,t}(T^2 \setminus D^2)$ and $\mathcal{SH}_{q,t}$ are isomorphic.

Chapter 3

The Stated Skein Algebra of the Torus with Boundary

There are three main facts from the previous sections that I would like to highlight:

1. There is a natural embedding, $K_q(T^2 \setminus D^2) \hookrightarrow \mathcal{S}(T^2 \setminus D^2)$, from the Kauffman bracket skein algebra of $T^2 \setminus D^2$ to the stated skein algebra of $T^2 \setminus D^2$.
2. There is an algebra isomorphism, $\mathcal{SH}_{q,t} \xrightarrow{\sim} K_{q,t}(T^2 \setminus D^2)$, from the A_1 spherical double affine Hecke algebra to the modified Kauffman bracket skein algebra of $T^2 \setminus D^2$.
3. The A_1 double affine Hecke algebra, $\mathcal{H}_{q,t}$, is Morita equivalent to its spherical subalgebra, $\mathcal{SH}_{q,t}$.

Together, these facts give us the central idea and guiding principle of this work: modules over $\mathcal{S}(T^2 \setminus D^2)$ provide us with modules for $\mathcal{SH}_{q,t}$, and therefore for the A_1 DAHA, $\mathcal{H}_{q,t}$.

Consider the following diagram of algebras.

$$\begin{array}{ccc}
K_q(T^2 \setminus D^2) & \hookrightarrow & \mathcal{S}(T^2 \setminus D^2) \\
\downarrow & & \\
K_{q,t}(T^2 \setminus D^2) & \xrightarrow{\sim} & \mathcal{SH}_{q,t}
\end{array}$$

There is no obvious direct map between $\mathcal{S}(T^2 \setminus D^2)$ and $\mathcal{SH}_{q,t}$. However, a module over $\mathcal{S}(T^2 \setminus D^2)$ can be turned (by restricting the skein algebra) into a module over $K_q(T^2 \setminus D^2)$.

From here we can use the functor

$$K_{q,t}(T^2 \setminus D^2) \otimes_{K_q(T^2 \setminus D^2)} - : K_q(T^2 \setminus D^2)\text{-Mod} \longrightarrow K_{q,t}(T^2 \setminus D^2)\text{-Mod} \quad (3.1)$$

to create $\mathcal{SH}_{q,t}$ -modules from these $K_q(T^2 \setminus D^2)$ -modules. This is known as *extension of scalars* and is the left adjoint to the restriction functor.¹ We will explore a few different kinds of modules over $\mathcal{S}(T^2 \setminus D^2)$ in later chapters, but before we can discuss this, we should first better understand the algebra $\mathcal{S}(T^2 \setminus D^2)$.

3.1 $\mathcal{S}(T^2 \setminus D^2)$ Notation

In this section we will show that the algebra $\mathcal{S}(T^2 \setminus D^2)$ with one marking is generated by the twelve elements $B = \{X_{1,0}(\mu_1, \nu_1), X_{2,0}(\mu_2, \nu_2), X_{3,0}(\mu_3, \nu_3) \mid \mu_i, \nu_i \in \{\pm\}\}$, where

$$X_{1,0}(\mu_1, \nu_1) = \begin{array}{c} \text{---} \rightarrow \rightarrow \rightarrow \\ \square \\ \leftarrow \leftarrow \leftarrow \text{---} \\ \text{---} \end{array} \quad X_{2,0}(\mu_2, \nu_2) = \begin{array}{c} \text{---} \rightarrow \rightarrow \rightarrow \\ \square \\ \leftarrow \leftarrow \leftarrow \text{---} \\ \text{---} \end{array} \quad X_{3,0}(\mu_3, \nu_3) = \begin{array}{c} \text{---} \rightarrow \rightarrow \rightarrow \\ \square \\ \leftarrow \leftarrow \leftarrow \text{---} \\ \text{---} \end{array}$$

The second subscript will be more thoroughly explained in section 3.2.

¹Given a map of rings, $f : R \rightarrow S$, there is also a right adjoint to the corresponding restriction functor, known as *coextension of scalars*, which turns $\text{Hom}(S, M)$ in the category of $R\text{-Mod}$ into an S -module by $(s \cdot g)(s') := g(s's)$.

Definition 3.1.63. A curve is *simple* if it does not contain any self crossings. Similarly, a $\partial\mathfrak{S}$ -tangle diagram is *simple* if it does not contain any self crossings on the interior of \mathfrak{S} and has no trivial component.

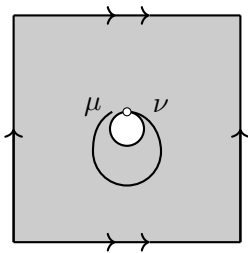
As we are working with isotopy classes of curves and isotopy classes of tangles, in general, we call α simple if there exists a representative of α that is simple.

Definition 3.1.64. A closed component of a $\partial\mathfrak{S}$ -tangle diagram is *trivial* if it bounds an open disk in \mathfrak{S} . A tangle component is *trivial* if it can be homotoped, relative to its endpoints, into a single marking.

Definition 3.1.65. A *boundary curve* is a simple closed curve that is parallel to a boundary edge.

Definition 3.1.66. A *parallel tangle* is one that can be homotoped, relative to its endpoints, to a boundary edge.

An example of a parallel tangle in $\mathcal{S}(T^2 \setminus D^2)$ with one marking is



as it can clearly be homotoped to the boundary.

Let Y_1 , Y_2 , and Y_3 be the meridian, longitude, and (1,1)-curve, respectively, and consider the stated skein algebra generated by B . Using the state-exchange relation, we

can express each Y_i in this algebra as

$$Y_i = q^{1/2}X_{i,0}(+, -) - q^{-5/2}X_{i,0}(-, +)$$

for $i \pmod 3$. Moreover, we can interchange heights using the proper height exchange relation.

Figure 3.1: Expressing Y_1 as stated $\partial(T^2 \setminus D^2)$ -tangles using the state exchange relation

As we're only considering $\mathcal{S}(T^2 \setminus D^2)$ with a single marking, there is only one simple parallel tangle and one boundary curve. The boundary curve can be expressed completely in terms of Y_i s and constants, as a quick calculation shows that

and for any $\mu, \nu \in \{\pm\}$,

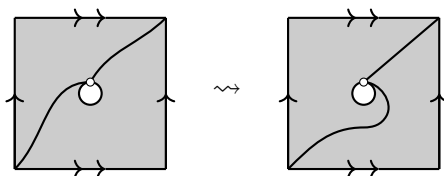
The details of this calculation can be found in A.3 of the appendix. Therefore, the rest of this section is devoted to checking that we can generate all nonparallel tangles and non-boundary curves.

There is clearly a 4-to-1 correspondence between any simple stateless $\partial(T^2 \setminus D^2)$ -tangle and simple stated $\partial(T^2 \setminus D^2)$ -tangles. Therefore, we will disregard the states in the following lemmas, as the proofs are independent of the possible states. Additionally, we will overlook relative heights along our marking, as we can readily obtain all possible heights using (R_6) alongside Y_1 , Y_2 , and Y_3 .

3.2 Half-Twists Around the Boundary

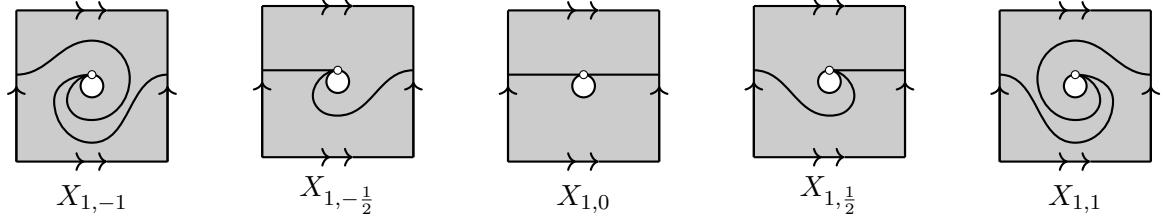
Before presenting our results, it is necessary to first explain the significance of the second index, r , in $X_{i,r}(\mu, \nu)$. While simple closed (non-boundary) curves on the torus (with boundary) are conventionally classified by their slopes, which are numbers in $\mathbb{Q} \cup \frac{1}{0}$, one might expect a similar classification for our tangles, considering that each tangle must start and end at the same marking. However, this analogy breaks down when considering tangles with what we'll call "twists" around the boundary.

For instance, if we trace along the path of $X_{3,0}$ and introduce a twist around the boundary just before reaching the marking, we get a different element back.



As these twists resemble half Dehn twists around the boundary, we distinguish these twists by indexing over $\frac{1}{2}\mathbb{Z}$ instead of \mathbb{Z} . In particular, $X_{i,r}$ is a *full* Dehn twist of $X_{i,r-1}$. The

following examples illustrate $X_{1,r}$ for various choices of $r \in \frac{1}{2}\mathbb{Z}$.



Remark 3.2.67. The distinction between two tangles with different numbers of twists becomes apparent when comparing these to fundamental groups with different base points.

Let x be a point on the boundary of $T^2 \setminus D^2$, p be a point in the interior of $T^2 \setminus D^2$, and define $\text{Sim}(T^2 \setminus D^2, z)$ as the subset of simple elements² in $\pi_1(T^2 \setminus D^2, z)$. Although there exists an isomorphism between the fundamental groups with different base points, $\varphi : \pi_1(T^2 \setminus D^2, x) \xrightarrow{\sim} \pi_1(T^2 \setminus D^2, p)$, it is not necessarily true that $\varphi(\text{Sim}(T^2 \setminus D^2, x)) = \text{Sim}(T^2 \setminus D^2, p)$. In fact, we instead observe a strict inclusion $\varphi(\text{Sim}(T^2 \setminus D^2, x)) \subsetneq \text{Sim}(T^2 \setminus D^2, p)$, as partially demonstrated in figure 3.2. The set of simple closed curves in $\pi_1(T^2 \setminus D^2)$ has already been classified in [6, 15] using cyclic reduction of words. However, this is unfortunately only under the subtle assumption that our base point is not on the boundary and so we will need to do additional work to fill in the gaps.

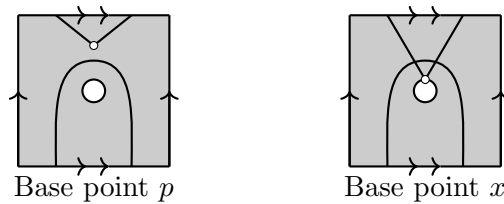


Figure 3.2: Left: a simple element with the base point off of the boundary. Right: after making a change of base point, it is no longer simple.

²An element of a fundamental group is simple if it has a representative that does not contain any self-intersections.

3.3 Generators of $\mathcal{S}(T^2 \setminus D^2)$

Given any marked surface, \mathfrak{S} , Lê shown in [38] (Theorem 2.7.47) that the set of all isotopy classes of increasingly stated, simple $\partial\mathfrak{S}$ -tangle diagrams forms a basis for $\mathcal{S}(\mathfrak{S})$. Therefore, our approach will be to first classify all possible simple (stateless) tangles in $T^2 \setminus D^2$ that start and end on $x \in \partial(T^2 \setminus D^2)$ and then demonstrate that all basis elements are contained in the subalgebra generated by $\{X_{1,0}(\mu_1, \nu_1), X_{2,0}(\mu_2, \nu_2), X_{3,0}(\mu_3, \nu_3)\}$ for all $\mu_i, \nu_j \in \{\pm\}$.

In theorem 3.3.68, we classify a large class of closed curves by their slope and number of twists. We construct this classification by covering a neighborhood of $\partial(T^2 \setminus D^2)$ with an annulus and proceed to use a Seifert-Van Kampen-style approach to calculate the slope outside the annulus as well as determine the number of twists inside the annulus.

To clean things up a bit, we'll introduce some more notation. We will denote the following set of tuples as

$$\mathcal{I} := \left\{ (p, q, r) \in \mathbb{Z} \times \mathbb{Z} \times \frac{1}{2}\mathbb{Z} \mid \gcd(p, q) = 1 \right\} / \sim$$

where $(p, q, r) \sim (-p, -q, r)$. Additionally, for any $x \in T^2 \setminus D^2$, define Ω_x to be the set of isotopy classes of simple unoriented closed non-parallel curves that begin and end on x . Any time we refer to a representative or an isotopic representative of an element in Ω_x , we are always assuming that this representative begins and ends at the point x .

Theorem 3.3.68. Let $x \in \partial(T^2 \setminus D^2)$. There exists a bijection $f_A : \mathcal{I} \longrightarrow \Omega_x$.

Proof. We will construct f_A by first constructing a map, \tilde{f}_A , from \mathcal{I} to $\tilde{\Omega}_x$, the set of simple closed unoriented non-parallel curves that begin and end on x , and then projecting onto the corresponding set of isotopy classes of curves.

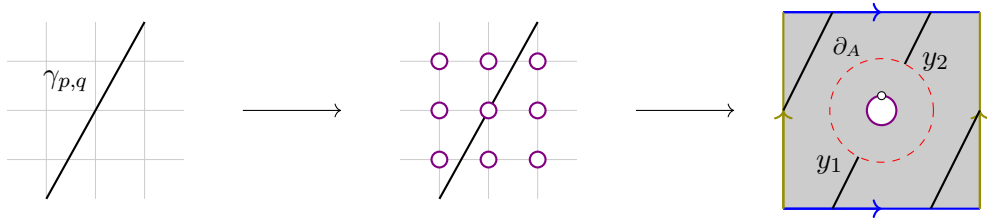
$$\begin{array}{ccc} \mathcal{I} & \xleftrightarrow{\tilde{f}_A} & \tilde{\Omega}_x \\ & \searrow f_A & \downarrow \pi_{\text{iso}} \\ & & \Omega_x \end{array}$$

We'll first introduce some definitions. Let $\varepsilon > 0$ be sufficiently small. Define $B_\varepsilon(m, n)$ to be the open ball of radius ε at point $(m, n) \in \mathbb{R}^2$, $E_\varepsilon := \mathbb{R}^2 \setminus \left(\bigcup_{(m,n) \in \mathbb{Z}^2} B_\varepsilon(m, n) \right)$, and Φ_ε to be the restriction of the identity map on \mathbb{R}^2 to E_ε , composed with the obvious covering map.

$$\Phi_\varepsilon : E_\varepsilon \longrightarrow T^2 \setminus D^2$$

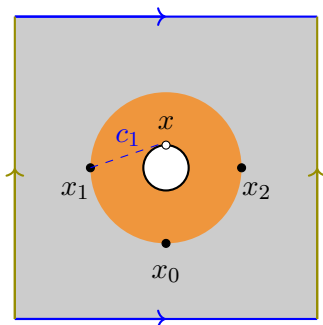
Let $A := \Phi_\varepsilon \left(\overline{E_\varepsilon \setminus E_{2\varepsilon}} \right)$ be the closed annulus and define $\partial_A := \partial A \setminus \partial(T^2 \setminus D^2)$, the “outer boundary”. ∂_A will constantly serve as a reference point throughout the rest of this proof and is the dividing bridge between the $\{p, q\}$ and $\{r\}$ in the tuple.

Choose any triple $(p, q, r) \in \mathcal{I}$. Let $\gamma_{p,q}$ be the graph of the function $y = \frac{p}{q}x$ in \mathbb{R}^2 (or $x = 0$ when $q = 0$) and consider $\gamma_0 := \Phi_\varepsilon(\gamma_{p,q}) \cap (T^2 \setminus A)$. Since $\gamma_{p,q}$ has constant slope, the two endpoints of γ_0 must lie on ∂_A as antipodal points.



Let x_0 be the unique point on ∂_A without a unique geodesic to x through A . Let

$x_1, x_2 \in \partial A$ be the midpoints between x_0 and its antipodal counterpart, labeled in clockwise order from x_0 , and let c_1 be the geodesic path from x_1 to x within A .



We'll assume y_1 and y_2 are labeled such that y_1 is closer to x_1 on ∂A . If they are both the same distance away from x_1 , then we must be in the case some $y_i = x_0$, as y_1 and y_2 are antipodal points. If this happens, label this y_i (the south pole) as y_1 and label the other (the north pole) as y_2 . Let γ_i be the geodesic paths (containing their endpoints) on ∂A from y_i to x_i . This should correspond to a clockwise path when $\frac{p}{q}$ is a positive slope or equal to $\frac{1}{0}$, and a counterclockwise path when $\frac{p}{q}$ is a negative slope.³ Define $\delta := \gamma_0 \sqcup \gamma_1 \sqcup \gamma_2$ and notice that this is simple.

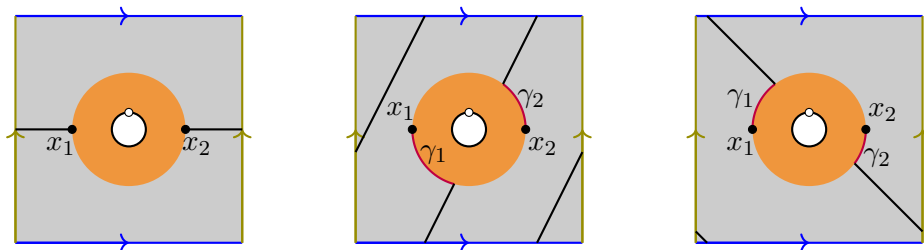
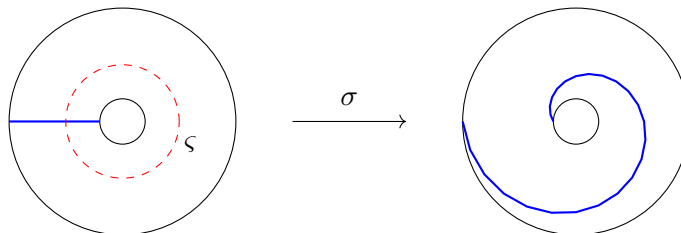


Figure 3.3: Left: When $(p, q) = (0, 1)$ we get $y_1 = x_1$ and $y_2 = x_2$ and so each γ_i is trivial. Middle: When γ_0 has a positive slope, we trace out a geodesic path clockwise from y_i to x_i . Right: When γ_0 has a negative slope we move counterclockwise instead.

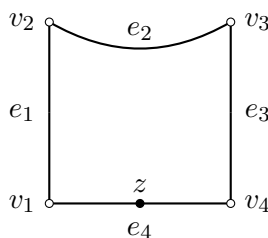
³Our choice of clockwise rotation when the slope is $\frac{1}{0}$ was made for notational convenience outside of this proof. Alternatively, one could instead use a counterclockwise rotation by swapping the labels y_1 and y_2 . The difference between these classifications results in a shift of r by $1/2$ whenever $(p, q) = (1, 0)$.

Recall that the mapping class group, $\text{Mod}(\Sigma)$, of a surface, Σ , is the group of isotopy classes of elements of $\text{Homeo}_+(\Sigma, \partial\Sigma)$, which pointwise-fix $\partial\Sigma$. Also recall that the mapping class group of the annulus is $\text{Mod}(A) = \langle \sigma \rangle$ where σ is the clockwise Dehn twist along the curve ς , parallel to the boundaries.



For $r \in \frac{1}{2}\mathbb{Z}$, notice that there is a unique decomposition, $r = \frac{r_1+r_2}{2}$, such that $r_1, r_2 \in \mathbb{Z}$ and $r_1 - r_2 \in \{0, 1\}$. Let $\alpha_1 = \sigma^{r_1}c_1$ and consider this curve in A .

Define B to be the filled-in square with corners labeled $\{v_1, v_2, v_3, v_4\}$, indexed clockwise, and edges labeled $\{e_1, e_2, e_3, e_4\}$ such that e_i has endpoints v_i and v_{i+1} for $i \pmod 4$, and let z be a point on the interior of e_4 .



Take $g_{\alpha_1} : B \rightarrow A$ to be the quotient map such that

- $g_{\alpha_1}(e_1) = g_{\alpha_1}(e_3) = \alpha_1$,
- $g_{\alpha_1}(v_2) = g_{\alpha_1}(v_3) = x$,
- $g_{\alpha_1}(v_1) = g_{\alpha_1}(v_4) = x_1$,
- $g_{\alpha_1}(z) = x_2$,

- and canonically identifies e_4 to ∂_A and e_2 to $\partial(T^2 \setminus D^2)$.

Using a pullback of the induced metric on $T^2 \setminus D^2$, if $r_2 = r_1 - 1$ define β_2 to be the geodesic path in B from z to v_2 and to be the geodesic path from z to v_3 if $r_2 = r_1$. Finally, let $\alpha_2 := g_{\alpha_1}(\beta_2)$. Then the curve $\alpha := \delta \cup \alpha_1 \cup \alpha_2$ is a simple tangle with endpoints on x . We now finally define $\tilde{f}_A(p, q, r) = \alpha$ and $f_A(p, q, r) = [\alpha]$.

The rest of this proof is primarily devoted to showing f_A is surjective.

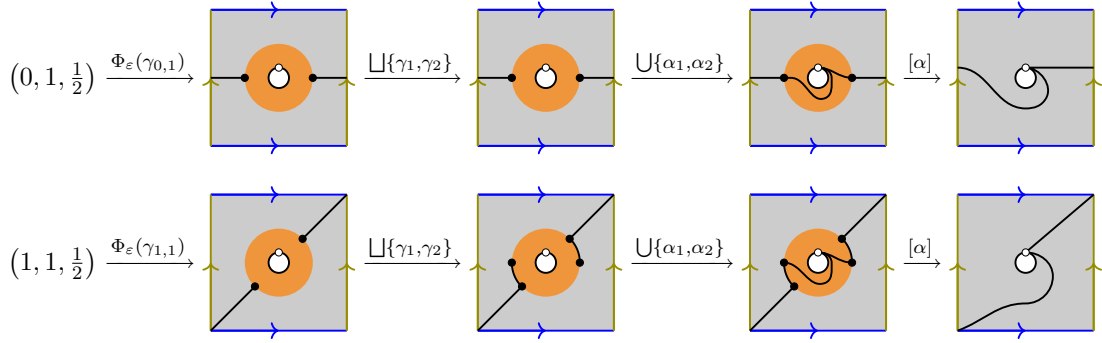


Figure 3.4: Example of $f_A(0, 1, \frac{1}{2})$ and $f_A(1, 1, \frac{1}{2})$

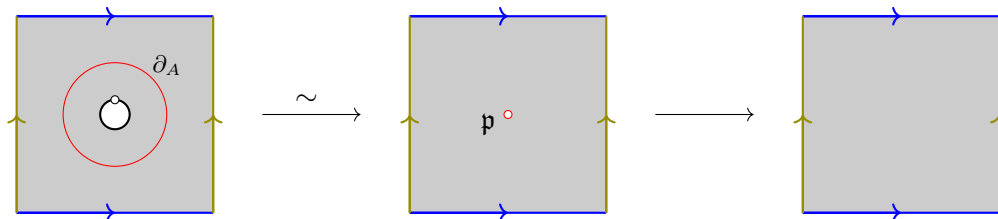
Define A , ∂_A , x_0 , x_1 , x_2 , and c_1 as before. Let η be a smooth radial vector field on a neighborhood of A , denoted $N(A)$, such that

- For all $y \in N(A) \setminus A$, $\eta(y)$ is tangent to the geodesic within $N(A)$ from y to ∂_A
- η is zero outside of $N(A)$,
- and for all $y \in \partial_A$, the vector $\eta(y)$ is normal to ∂_A and points inwards.

Define

$$\Psi : (T^2 \setminus D^2) \setminus A \xrightarrow{\sim} T^2 \setminus \{p\} \hookrightarrow T^2$$

to be the homeomorphism that flows along η , and therefore restricts to the identity on $T^2 \setminus N(A)$, followed by its canonical embedding into T^2 .



Consider any curve in Ω_x and select a simple representative, α , such that $|\alpha \cap \partial_A| = 2$ and $\Psi(\alpha \setminus (A \cap \alpha))$ has constant slope. Since we required α to be simple, if α lies entirely within A , it must either be parallel to the boundary of $T^2 \setminus D^2$ or null-homotopic, and therefore not in Ω_x . As all simple unoriented closed curves on the torus are classified as (p, q) -curves, where $(p, q) \sim (-p, -q)$ and p and q are coprime, we can uniquely associate a (p, q) pair to the closed curve $\Psi(\alpha \setminus (A \cap \alpha)) \cup \{p\}$.

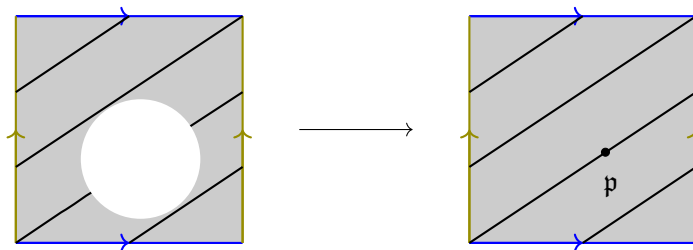


Figure 3.5: Turning the tangle, α , in the complement of A into a closed curve on the torus via Ψ . This example becomes a curve in T^2 with classification $(2, 3)$

Identify α with a map, $\alpha : [0, 1] \rightarrow T^2 \setminus D^2$, such that $\alpha(0) = \alpha(1) = x$. Label the points $\{y_1, y_2\} = \alpha \cap \partial_A$ and their preimages as $t'_i := \alpha^{-1}(y_i)$, assuming $t'_1 < t'_2$. If (p, q) is a positive slope, then let γ_i be the geodesics on ∂_A from y_i to x_i , rotating clockwise. If these geodesics intersect each other then we can swap the labels y_i by changing the orientation

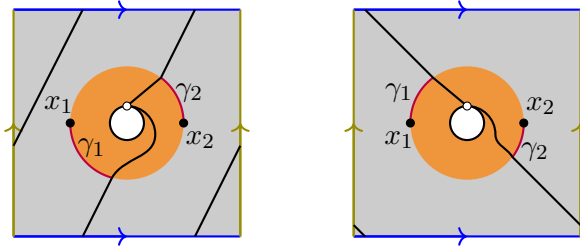
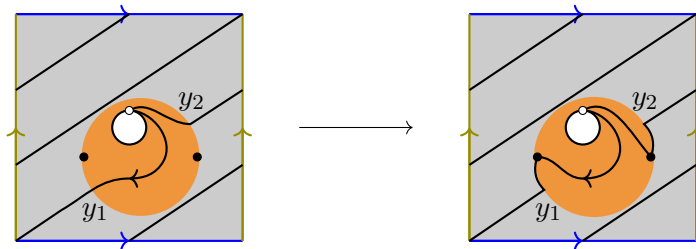


Figure 3.6: Left: Example of a curve with a positive slope. Right: Example with a negative slope.

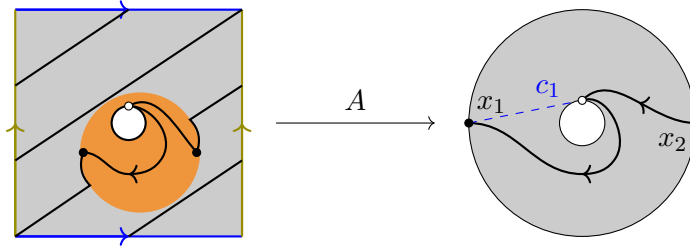
of α to avoid this. If (p, q) is a negative slope then let γ_i be the geodesics on ∂_A from y_i to x_i , rotating counterclockwise, once again changing the orientation of α if needed. If $(p, q) = (1, 0)$, the same slope as the longitude, then let γ_i be the geodesics on ∂_A from y_i to x_i , rotating clockwise. Finally, if $(p, q) = (0, 1)$ then $y_i = x_i$ and γ_i is trivial for each i .

Isotope α inside A so that for some $0 < t_1 < t'_1$ and $1 > t_2 > t'_2$, α satisfies:

- $\alpha(t_i) = x_i$,
- $\alpha([t_1, t'_1]) = \gamma_1$,
- $\alpha([t'_2, t_2]) = \gamma_2$,
- $\alpha([t'_1, t'_2] \sqcup \{0, 1\})$ remains unchanged,
- α is transverse with itself at $\alpha(0)$ and $\alpha(1)$.

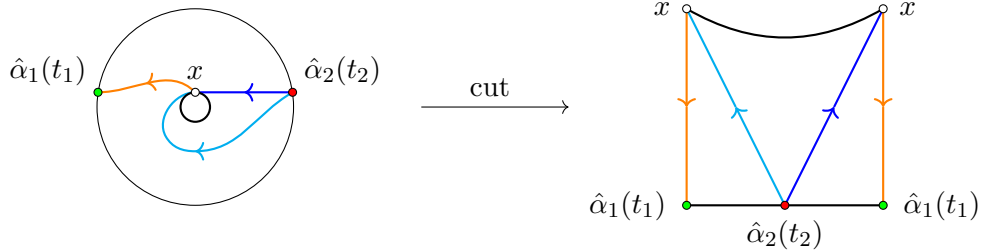


We can now focus on the region within the annulus, A , and just $\alpha([0, t_1] \sqcup [t_2, 1])$.



Consider the corresponding restriction, $\hat{\alpha} : [0, t_1] \cup [t_2, 1] \rightarrow A$, of α and further restrict this into its two components, $\hat{\alpha}_1 : [0, t_1] \rightarrow A$, and $\hat{\alpha}_2 : [t_2, 1] \rightarrow A$. Since the mapping class group of the annulus is isomorphic to \mathbb{Z} , $\hat{\alpha}_1$ must be isotopic to $\sigma^{r_{1,\alpha}} c_1$ for some $r_{1,\alpha} \in \mathbb{Z}$.

If we cut A along $\hat{\alpha}_1$, the resulting picture is a square. Since $\hat{\alpha}_2$ is a path from $\hat{\alpha}(t_2)$ to x and since $\hat{\alpha}(t_2)$ lies on ∂_A and is distinct from $\hat{\alpha}(t_1)$, there are exactly two possible ways $\hat{\alpha}$ can be simple up to isotopy.



Let $v_1 = \hat{\alpha}'_1(0)$ and $v_2 = \hat{\alpha}'_2(1)$, the corresponding tangent vectors, using the induced orientation from α 's domain.⁴ Since α is transverse with itself at $\alpha(0)$ and $\alpha(1)$, we must have that $\det(v_1 v_2) \neq 0$. Finally, define

$$r_{2,\alpha} = \begin{cases} r_{1,\alpha} & \text{if } \det(v_1 v_2) > 0 \\ r_{1,\alpha} - 1 & \text{if } \det(v_1 v_2) < 0 \end{cases} \quad (3.2)$$

⁴We may assume α is parameterized by arclength so that these vectors are never zero.

and let $r = \frac{r_{1,\alpha} + r_{2,\alpha}}{2}$ which is clearly an element of $\frac{1}{2}\mathbb{Z}$, providing us with the last entry in the tuple.⁵ Notice that this representative of α is clearly equivalent to $\tilde{f}_A(p, q, r)$ outside of A and isotopic inside of A as the decomposition of r into $r_{1,\alpha}$ and $r_{2,\alpha}$ is unique. Therefore, $(\pi_{\text{iso}} \circ \tilde{f}_A)(p, q, r) = [\alpha]$ and so this map is surjective.

Finally, suppose $f_A(p, q, r) = f_A(p', q', r') = [\alpha]$. First notice that α 's geometric intersection number with a fixed meridian and fixed longitude away from x are invariant under isotopy. As these intersection numbers correspond to p and q respectively, $p = p'$ and $q = q'$. Notice that $\tilde{f}_A(p, q, r) \cap \partial_A$ must completely agree with $\tilde{f}_A(p', q', r') \cap \partial_A$ as well as they are equivalent on $T^2 \setminus A$ and therefore $[\tilde{f}_A(p, q, r)] = [\tilde{f}_A(p', q', r')]$ on A . Because they agree up to isotopy and since $r = \frac{r_{1,\alpha} + r_{2,\alpha}}{2}$ and $r' = \frac{r'_{1,\alpha} + r'_{2,\alpha}}{2}$ have unique decompositions, $r = r'$. Thus $(p, q, r) = (p', q', r')$ and so f_A is bijective. \square

Lemma 3.3.69. If $\alpha \in \mathcal{S}(\mathfrak{S})$ is a tangle and $\gamma \in \mathcal{S}(\mathfrak{S})$ is a closed curve such that the geometric intersection number of α and γ is 1, then $\frac{1}{q^2 - q^{-2}}[\alpha, \gamma]_q$ resolves to a Dehn twist of α along γ and $\frac{-1}{q^2 - q^{-2}}[\alpha, \gamma]_{q^{-1}} = \frac{1}{q^2 - q^{-2}}[\gamma, \alpha]_q$ is the corresponding Dehn twist in the opposite direction.

Proof. Suppose α and γ intersect exactly once. Then locally, we have

$$[\alpha, \gamma]_q = q\alpha\gamma - q^{-1}\gamma\alpha$$

$$= q \begin{array}{c} \text{---} \gamma \text{---} \\ \diagup \quad \diagdown \\ \alpha \end{array} - q^{-1} \begin{array}{c} \text{---} \gamma \text{---} \\ \diagdown \quad \diagup \\ \alpha \end{array}$$

⁵If x_1 were located somewhere else on ∂_A , it might seem more natural to define $r_{2,\alpha}$ as $r_{1,\alpha} + 1$ when the determinant is positive and as $r_{1,\alpha}$ when it's negative. However, using equation (3.2) instead of this for the definition of $r_{2,\alpha}$, merely corresponds to a $\frac{1}{2}$ shift in this $\frac{1}{2}\mathbb{Z}$ -torsor and does not violate any assumptions. Furthermore, if we had chosen σ to be the counterclockwise Dehn twist instead, we would, among other things, want to define $r_{2,\alpha}$ as $r_{1,\alpha}$ when the determinant is positive and as $r_{1,\alpha} + 1$ when it's negative.

$$\begin{aligned}
&= q^2 \text{ (circle with two arcs)} + \text{ (circle with two arcs)} - \text{ (circle with two arcs)} - q^{-2} \text{ (circle with two arcs)} \\
&= (q^2 - q^{-2}) \text{ (circle with two arcs)}
\end{aligned}$$

giving us our result. Noticing that $[b, a]_q = -[a, b]_{q^{-1}}$, we get $\frac{1}{q^2 - q^{-2}}[\gamma, \alpha]_q = \frac{-1}{q^2 - q^{-2}}[\alpha, \gamma]_{q^{-1}}$ is the Dehn twist in the opposite direction. \square

Lemma 3.3.70. As an algebra, the set $\{X_{1,0}(\mu_1, \nu_1), X_{2,0}(\mu_2, \nu_2), X_{3,0}(\mu_3, \nu_3)\}$ for all $\mu_i, \nu_j \in \{\pm\}$ generates any $\{\mathbb{Q} \cup \frac{1}{0}\}$ -sloped tangle in $\mathcal{S}(T^2 \setminus D^2)$ with $0 \in \frac{1}{2}\mathbb{Z}$ twists.

Proof. Recall that $\left| \det \begin{pmatrix} a & c \\ b & d \end{pmatrix} \right| = n$ if and only if the (a, b) -curve and the (c, d) -curve (or (c, d) -tangle) have a geometric intersection number of n . Consider the (non-homomorphic) map of G -sets, $\sigma : GL_2(\mathbb{Z}) \rightarrow \mathbb{Z}^2$ defined by $A \mapsto A \cdot \begin{bmatrix} 1 \\ 1 \end{bmatrix}$. Suppose p and q are coprime. If they are not coprime then the $(p, q, 0)$ -tangle intersects itself and can be resolved into curves and $\partial(T^2 \setminus D^2)$ -tangles with $\mathbb{Q} \cup \frac{1}{0}$ slopes. We'll also assume that $0 < q < p$ (the proof is symmetric for negative slopes and when $q > p$).

By Lemma 1 in [26], we can decompose p and q into $u + w = p$ and $v + z = q$ such that $\det \begin{pmatrix} u & w \\ v & z \end{pmatrix} = \pm 1$ with $0 < w < p$, $0 < u < p - 1$, and $v, z > 0$, for $p \geq 3$. Thus for $\begin{pmatrix} p \\ q \end{pmatrix} \in \mathbb{Z}^2$, there exists an inverse, $\sigma^{-1} \begin{pmatrix} p \\ q \end{pmatrix} = \begin{pmatrix} u & w \\ v & z \end{pmatrix}$. We then find the inverse

of the second column, $\sigma^{-1} \begin{pmatrix} w \\ z \end{pmatrix}$, and repeat until we get $\begin{pmatrix} p' \\ q' \end{pmatrix}$ for $q' < p' \leq 2$. Using Lemma 3.3.69, each step in the reverse process of this algorithm corresponds to a Dehn twist, $\frac{\pm 1}{q^2 - q^{-2}} [Y_j, -]_{q^{\pm 1}}$, along some Y_j -curve corresponding to the first column.

Finally, note that the $(2, 1)$ -tangle is equal to $\frac{1}{q^2 - q^{-2}} [Y_1, X_{3,0}(\mu, \nu)]_q$. \square

Example 3.3.71. To illustrate the application of this algorithm, let's examine the $(5, 3)$ -tangle with states μ and ν , which we'll denote as $\tilde{X}(\mu, \nu)$. The matrices of interest in this example are

$$\sigma \begin{pmatrix} 0 & 1 \\ 1 & 0 \end{pmatrix} = \begin{pmatrix} 1 \\ 1 \end{pmatrix}, \quad \sigma \begin{pmatrix} 1 & 1 \\ 0 & 1 \end{pmatrix} = \begin{pmatrix} 2 \\ 1 \end{pmatrix}, \quad \sigma \begin{pmatrix} 2 & 1 \\ 1 & 1 \end{pmatrix} = \begin{pmatrix} 3 \\ 2 \end{pmatrix}, \quad \sigma \begin{pmatrix} 3 & 2 \\ 2 & 1 \end{pmatrix} = \begin{pmatrix} 5 \\ 3 \end{pmatrix}.$$

Thus, we get the following series of Dehn twists

$$\frac{-1}{(q^2 - q^{-2})^6} \left[\left[Y_3, \left[Y_1, \left[Y_2, Y_1 \right]_{q^{-1}} \right]_q \right]_{q^{-1}}, \left[Y_1, \left[Y_2, X_{1,0}(\mu, \nu) \right]_{q^{-1}} \right]_q \right] = \tilde{X}(\mu, \nu).$$

Theorem 3.3.72. B generates $\mathcal{S}(T^2 \setminus D^2)$ as an algebra.

Proof. A short calculation shows that

$$X_{i,k+1}(\mu, \nu) = \frac{1}{(q^2 - q^{-2})^3} \left[Y_{i+1}, \left[Y_i, \left[Y_{i-1}, X_{i,k}(\mu, \nu) \right]_q \right]_q \right] \quad (3.3)$$

$$X_{i,k-1}(\mu, \nu) = \frac{1}{(q^2 - q^{-2})^3} \left[\left[\left[X_{i,k}(\mu, \nu), Y_{i+1} \right]_q, Y_i \right]_q, Y_{i-1} \right]_q \quad (3.4)$$

for $i \bmod 3$ and $\mu, \nu \in \{\pm\}$. Using this result and Lemma 3.3.70, we can construct any (p, q, r) -tangle. By Theorem 2.7.52, the set of all isotopy classes of increasingly stated, \mathfrak{o} -simple $\partial(T^2 \setminus D^2)$ -tangle diagrams forms a basis for $\mathcal{S}(T^2 \setminus D^2)$. Since every simple non-parallel tangle can be expressed as a (p, q, r) -tangle, every simple $\partial(T^2 \setminus D^2)$ -tangle

diagram can be written as a linear combination of products of these (p, q, r) -tangles and powers of our single parallel tangle. Thus, the stated skein algebra generated by B spans the entire space. \square

Remark 3.3.73. Since we have the relation

$$X_{3,0}(\mu, \nu) = \frac{1}{q^2 - q^{-2}} \left[X_{1,0}(\mu, \nu), q^{1/2} X_{2,0}(+, -) - q^{-5/2} X_{2,0}(-, +) \right]_q,$$

we don't technically need to include $X_{3,0}(\mu, \nu)$ to generate $\mathcal{S}(T^2 \setminus D^2)$. We only need the eight elements $\{X_{i,0}(\mu, \nu) \mid \mu, \nu \in \{\pm\}, i \in \{1, 2\}\}$. However, as with $K_q(T^2 \setminus D^2)$, it is often more notationally convenient to include $X_{3,0}(\mu, \nu)$ as well.

3.4 Relation to Factorization Homology

Alekseev-Grosse-Schomerus moduli algebras (AGS algebras) are deformations of representation varieties of $\Sigma \setminus D^2$ for some surface Σ , via the Fock-Rosly Poisson structure. It was shown in both [22] and [36] that these AGS algebras are isomorphic as $\mathcal{O}_q(SL_2)$ -comodule algebras to $\mathcal{S}(\Sigma \setminus D^2)$, the corresponding stated skein algebra with one marking on the boundary created by removing D^2 .

Internal skein algebras (also known as internal endomorphism algebras), denoted $A_{\Sigma \setminus D^2}$, were explored in [4, 9, 30] using factorization homology and were also shown to be isomorphic to corresponding AGS algebras in [4]. It was stated in [30] and [41] and made more explicit in [40] that $A_{\Sigma \setminus D^2}$ should be isomorphic to $\mathcal{S}(\Sigma \setminus D^2)$ with one marking as $\mathcal{O}_q(SL_2)$ -comodule algebras, tying together factorization homology and stated skein theory. Using only skein theory, Haïoun proved in [31] that $\mathcal{S}(\Sigma \setminus D^2)$ (with one marking) is isomorphic to its corresponding internal skein algebra as $\mathcal{O}_q(SL_2)$ -comodule algebras.

Moving to our specific case, it was shown in [4, 9] that the algebra $A_{T^2 \setminus D^2}$, and therefore $\mathcal{S}(T^2 \setminus D^2)$, is isomorphic as an $\mathcal{O}_q(SL_2)$ -comodule algebra to the algebra of quantum differential operators, $D_q(SL_2) \cong U_q(\mathfrak{sl}_2) \rtimes \mathcal{O}_q(SL_2)$, which they called the *elliptic double* and is a subalgebra of the Heisenberg double of $U_q(\mathfrak{sl}_2)$. In [30], Gunningham, Jordan, and Safronov provided an explicit presentation for this algebra: $U_q(\mathfrak{sl}_2) \rtimes \mathcal{O}_q(SL_2)$ is generated by $a_1^1, a_2^1, a_1^2, a_2^2, b_1^1, b_2^1, b_1^2, b_2^2$, subject to the relations

$$R_{21}A_1R_{12}A_2 = A_2R_{21}A_1R_{12}$$

$$R_{21}B_1RB_2 = B_2R_{21}B_1R$$

$$R_{21}B_1RA_2 = A_2R_{21}B_1R_{21}^{-1}$$

$$1 = a_1^1 a_2^2 - q^2 a_2^1 a_1^2,$$

$$1 = b_1^1 b_2^2 - q^2 b_2^1 b_1^2,$$

where

$$A_1 = \begin{pmatrix} a_1^1 & a_2^1 \\ a_1^2 & a_2^2 \end{pmatrix} \otimes \text{Id}, \quad B_1 = \begin{pmatrix} b_1^1 & b_2^1 \\ b_1^2 & b_2^2 \end{pmatrix} \otimes \text{Id},$$

$$A_2 = \text{Id} \otimes \begin{pmatrix} a_1^1 & a_2^1 \\ a_1^2 & a_2^2 \end{pmatrix}, \quad B_2 = \text{Id} \otimes \begin{pmatrix} b_1^1 & b_2^1 \\ b_1^2 & b_2^2 \end{pmatrix},$$

and $R = R_{12}$ is the R matrix over $L(1) \otimes L(1)$. These generators correspond to the same generators just discussed.

$$\begin{array}{ll}
X_{1,0}(+, +) \mapsto a_2^2 & X_{2,0}(+, +) \mapsto b_2^2 \\
X_{1,0}(+, -) \mapsto a_2^1 & X_{2,0}(+, -) \mapsto b_2^1 \\
X_{1,0}(-, +) \mapsto a_1^2 & X_{2,0}(-, +) \mapsto b_1^2 \\
X_{1,0}(-, -) \mapsto a_1^1 & X_{2,0}(-, -) \mapsto b_1^1
\end{array}$$

However, multiplication in these two algebras are defined a bit differently and so the relations on $\mathcal{S}(T^2 \setminus D^2)$ aren't going to be the same on the nose. In particular, the product structure in $D_q(SL_2)$ is an associative braided product (called the covariantised product in [44]) which corresponds to a transmutation of $\mathcal{O}_q(SL_2)$, the Hopf dual of $U_q(\mathfrak{sl}_2)$. You can read more about transmutation in [44] and for great pictures and details on how it relates to stated skein algebras, see Lê and Sikora's preprint [40].



Figure 3.7: Very roughly speaking, the left is multiplication in $\mathcal{S}(T^2 \setminus D^2)$ and right is multiplication in the “transmuted” version.

Note that when viewing $\mathcal{S}(T^2 \setminus D^2)$ with this braided product as our multiplication, the generators $\{X_{1,0}(\mu_1, \nu_1), X_{2,0}(\mu_2, \nu_2) \mid \mu_i, \nu_i \in \{\pm\}\}$ agree with these relations under the identification above. Therefore, this is a concrete example of the relationship between factorization homology and stated skein algebras. For a more in-depth explanation of this relationship, please refer to [4, 30, 31, 40]. These details, although quite interesting, are not directly relevant to the main discussion in this work and will not be discussed here.

3.5 Towards a PBW Basis

It would be ideal and highly advantageous if we could additionally find a PBW basis for $\mathcal{S}(T^2 \setminus D^2)$. Sadly, establishing the basis for this algebra has proven to be quite challenging, primarily due to the rapid escalation of calculations. The main hurdle lies in identifying all the relations required for such a presentation, as is often the case in such endeavors.

Unfortunately, attempting to use similar techniques used in the Kauffman bracket case has not been fruitful. While we have the relation $\frac{1}{q^2 - q^{-2}}[Y_i, Y_{i+1}]_q = Y_{i+2}$ just as the Kauffman bracket case, computing an analogous relation on tangles instead yields 3.3 and 3.4, indicating the possible need to consider these half-twists when establishing a basis. Paradoxically, we also have the equality

$$Y_i = q^{1/2} X_{i,r}(+, -) - q^{-5/2} X_{i,r}(-, +) \quad (3.5)$$

for all $r \in \frac{1}{2}\mathbb{Z}$, further complicating things. Note that this also extends to all (p, q) -curves and their corresponding (p, q, r) -tangles.

For any $r \in \frac{1}{2}\mathbb{Z}$, let $\gamma_{p,q,r}$ be a simple $\partial(T^2 \setminus D^2)$ -tangle corresponding to the tuple (p, q, r) from Theorem 3.3.68. An interesting note is that for any $r, s \in \frac{1}{2}\mathbb{Z}$, resolving any crossings in the product of $\gamma_{p,q,r}\gamma_{p,q,s}$ will always result in a sum of simple tangles containing a summand element in $\gamma_{\frac{r+s}{2}}$ when $\frac{r+s}{2} \in \frac{1}{2}\mathbb{Z}$ and an element in $\gamma_{\lfloor \frac{r+s}{2} \rfloor} \gamma_{\lceil \frac{r+s}{2} \rceil}$ when $\frac{r+s}{2} \notin \frac{1}{2}\mathbb{Z}$.

Conjecture 3.5.74. The product of stateless simple tangles, $\gamma_{p,q,r}$ and $\gamma_{p,q,s}$, always resolves to a polynomial of closed (p, q) -curves, parallel tangles, parallel closed curves,

$\gamma_{p,q, \lfloor \frac{r+s}{2} \rfloor}$, and $\gamma_{p,q, \lceil \frac{r+s}{2} \rceil}$.

In particular, if $s = r \pm \frac{1}{2}$, the product can always be drawn without any crossings. Although this observation may give off the sense of a grading, the presence of this averaging formula precludes it from being classified as such. Furthermore, it, of course, could not constitute a decomposition of our algebra either, as illustrated by equation 3.5, which demonstrates the absence of linear independence among these if we tried to make them direct summands. As far as I am aware, there are no comparable examples in the existing literature of this phenomenon to serve as a reference point.

Another possible route is to employing the embedding technique described in Section 4.1 and studying the image of $\mathcal{S}(T^2 \setminus D^2)$. Although some progress has been made, extracting useful patterns from this embedding is particularly arduous. Notably, the image of seemingly simple tangle elements quickly becomes unwieldy in size as $r \in \frac{1}{2}\mathbb{Z}$ moves further away from 0 (see Appendix A.2 for an example).

For convenience and further use, I have calculated, and partially verified using a computer program (Appendix B.1), all 16 commuting relations among $X_{1,k}$ and $X_{2,k}$ for all states. Note that these calculations assume both tangles share the same number of twists with respect to our classification in Theorem 3.3.68. I have also added the full calculation for the longest calculation (in the case of 0 twists around the boundary) in Appendix A.1. Here, $\tilde{X}_{3,k}(\mu, \nu)$ corresponds to the $(1, -1)$ -tangle with k twists and \tilde{Y}_3 is the closed $(1, -1)$ -curve.

$$\begin{aligned}
X_{1,k}(+,+)X_{2,k}(+,+) &= q^2 X_{2,k}(+,+)X_{1,k}(+,+) \\
X_{1,k}(+,+)X_{2,k}(+,-) &= q^{-2} X_{2,k}(+,-)X_{1,k}(+,+) + q^{-3/2}(q^2 - q^{-2})X_{3,k}(+,+) \\
X_{1,k}(+,+)X_{2,k}(-,+) &= q^{-2} X_{2,k}(-,+)X_{1,k}(+,+) \\
X_{1,k}(+,+)X_{2,k}(-,-) &= q^{-6} X_{2,k}(-,-)X_{1,k}(+,+) + q^{-3/2}(q^2 - q^{-2})X_{3,k}(-,+) \\
X_{1,k}(+,-)X_{2,k}(+,+) &= q^6 X_{2,k}(+,+)X_{1,k}(+,-) - q^{7/2}(q^2 - q^{-2})X_{2,k}(+,+)Y_1 \\
&\quad - q^{5/2}(q^2 - q^{-2}) \left(q^2 \tilde{X}_{3,k}(+,+) + q^{-2} \tilde{X}_{3,k-\frac{1}{2}}(+,+) \right) \\
X_{1,k}(+,-)X_{2,k}(+,-) &= q^2 X_{2,k}(+,-)X_{1,k}(+,-) + (q^2 - q^{-2})\tilde{Y}_3 \\
&\quad - q^{-1/2}(q^2 - q^{-2}) \left(q \tilde{X}_{3,k}(+,-) + X_2(+,-)Y_1 - q^{-1}X_3(+,-) \right) \\
X_{1,k}(+,-)X_{2,k}(-,+) &= q^2 X_{2,k}(-,+)X_{1,k}(+,-) - q^{-1/2}(q^2 - q^{-2})\tilde{X}_{3,k-\frac{1}{2}}(-,+) \\
X_{1,k}(+,-)X_{2,k}(-,-) &= q^{-2} X_{2,k}(-,-)X_{1,k}(+,-) + q^{-3/2}(q^2 - q^{-2})X_{3,k}(-,-) \\
X_{1,k}(-,+)X_{2,k}(+,+) &= q^6 X_{2,k}(+,+)X_{1,k}(-,+) - q^{5/2}(q^2 - q^{-2})\tilde{X}_{3,k-\frac{1}{2}}(+,+) \\
X_{1,k}(-,+)X_{2,k}(+,-) &= q^2 X_{2,k}(+,-)X_{1,k}(-,+) - q^{1/2}(q^2 - q^{-2})\tilde{X}_{3,k}(-,+) \\
X_{1,k}(-,+)X_{2,k}(-,+) &= q^2 X_{2,k}(-,+)X_{1,k}(-,+) \\
X_{1,k}(-,+)X_{2,k}(-,-) &= q^{-2} X_{2,k}(-,-)X_{1,k}(-,+) \\
X_{1,k}(-,-)X_{2,k}(+,+) &= q^{10} X_{2,k}(+,+)X_{1,k}(-,-) - q^{13/2}(q^2 - q^{-2}) \left(q^4 X_{3,k}(-,+) + q^{-4} \tilde{X}_{3,k}(+,-) \right) \\
&\quad - q^{11/2}(q^2 - q^{-2}) \left(q^3 \tilde{X}_{3,k-\frac{1}{2}}(-,+) + q^{-3} \tilde{X}_{3,k-\frac{1}{2}}(+,-) \right) \\
&\quad - q^7 (q^2 - q^{-2})(q^3 + q^{-3})\tilde{Y}_{3,k} \\
X_{1,k}(-,-)X_{2,k}(+,-) &= q^6 X_{2,k}(+,-)X_{1,k}(-,-) \\
&\quad - q^{5/2}(q^2 - q^{-2}) \left(q X_{2,k}(-,-)Y_1 + (q^2 + q^{-2})\tilde{X}_{3,k}(-,-) \right) \\
X_{1,k}(-,-)X_{2,k}(-,+) &= q^6 X_{2,k}(-,+)X_{1,k}(-,-) - q^{7/2}(q^2 - q^{-2})\tilde{X}_{3,k-\frac{1}{2}}(-,-) \\
X_{1,k}(-,-)X_{2,k}(-,-) &= q^2 X_{2,k}(-,-)X_{1,k}(-,-)
\end{aligned}$$

Chapter 4

Representations from Quantum Tori

4.1 Embedding Into Quantum Tori

Definition 4.1.75. Given an anti-symmetric integral $n \times n$ matrix Q , the associated *quantum torus* is defined as

$$\mathbb{T}^n(Q) := \frac{\mathbb{C}[x_1^{\pm 1}, \dots, x_n^{\pm 1}]}{(x_i x_j = q^{Q_{ij}} x_j x_i)}$$

and the corresponding *quantum plane* is

$$\mathbb{T}_+^n(Q) := \frac{\mathbb{C}[x_1, \dots, x_n]}{(x_i x_j = q^{Q_{ij}} x_j x_i)}.$$

We will often drop the Q in $\mathbb{T}^n(Q)$ and $\mathbb{T}_+^n(Q)$ to shorten notation. Clearly, \mathbb{T}_+^n is an Ore domain and \mathbb{T}^n is an Ore localization of \mathbb{T}_+^n .

Lê and Yu proved that there exist embeddings $\mathbb{T}_+^r \xrightarrow{\psi_{\mathcal{E}}} \mathcal{S}(\mathfrak{S}) \xrightarrow{\varphi_{\mathcal{E}}} \mathbb{T}^r$, where r is the Gelfand-Kirillov dimension of $\mathcal{S}(\mathfrak{S})$ and $\psi_{\mathcal{E}}$ and $\varphi_{\mathcal{E}}$ are algebra homomorphisms. Both

of these embeddings depend on a quasitriangulation of \mathfrak{S} , denoted \mathcal{E} , and are discussed extensively in [42]. Bonahon and Wong constructed a similar map in [8] where \mathbb{T}^r would instead be rational functions in skew-commuting variables associated to the square roots of the shear coordinates of Chekhov and Fock's enhanced quantum Teichmüller space. Furthermore, Bonahon and Wong demonstrated that a change in quasitriangulation induces an algebra isomorphism between the respective Teichmüller spaces, which can also be understood as a change of shear coordinates.

Let (Σ, \mathcal{P}) be a marked surface and \mathfrak{S} the corresponding punctured bordered surface. Define $r(\Sigma, \mathcal{P}) = r(\mathfrak{S})$ to be 0 if \mathfrak{S} is the sphere with no or one ideal point, 1 if \mathfrak{S} is the sphere with two ideal points, 2 if \mathfrak{S} is the closed torus, and $3|\mathcal{P}| - 3\chi(\mathfrak{S})$ otherwise, where $\chi(\mathfrak{S})$ is the Euler characteristic of \mathfrak{S} . Lê and Yu showed in [41] that the Gelfand-Kirillov dimension of $\mathcal{S}(\mathfrak{S})$ is $r(\mathfrak{S})$. Equivalently, r can also be defined as the cardinality of the maximal collection of non-isotopic ideal arcs $\bar{\mathcal{E}} = \mathcal{E} \sqcup \hat{\mathcal{E}}_\partial = (\mathring{\mathcal{E}} \sqcup \mathcal{E}_\partial) \sqcup \hat{\mathcal{E}}_\partial$, where $\mathring{\mathcal{E}}$ are the ideal arcs not parallel to any boundary components, \mathcal{E}_∂ are the ideal arcs that are parallel to boundary components, and $\hat{\mathcal{E}}_\partial$ is a copy of \mathcal{E}_∂ . Each $e \in \bar{\mathcal{E}}$ corresponds to a generator, x_e , of \mathbb{T}_+^r . The anti-symmetric integral matrix for \mathbb{T}_+^r is defined using the anti-symmetric function

$$\begin{aligned}
 Q(a, b) &= \# \begin{array}{c} \text{Diagram 1} \\ \text{Diagram 2} \end{array} - \# \begin{array}{c} \text{Diagram 3} \\ \text{Diagram 4} \end{array} && \text{for } a, b \in \mathcal{E} \\
 Q(a, \hat{b}) &= -\# \begin{array}{c} \text{Diagram 1} \\ \text{Diagram 2} \end{array} - \# \begin{array}{c} \text{Diagram 3} \\ \text{Diagram 4} \end{array} && \text{for } a \in \mathcal{E}, b \in \mathcal{E}_\partial \\
 Q(\hat{a}, \hat{b}) &= -Q(a, b) && \text{for } a, b \in \mathcal{E}_\partial.
 \end{aligned}$$

and canonically identifying the entries of Q as $Q_{a,b} = Q(a,b)$. By $\# \begin{array}{c} \text{---} \\ \diagdown \quad \diagup \\ \circ \\ \text{---} \end{array}$ we mean the number of times a half edge of i and a half edge j meet at the same ideal point with i following j in the clockwise order.

We define $\psi_{\mathcal{E}}$ as sending each generator to the corresponding diagram (possibly scaled by some $q^{\pm 1/2}$) where the diagram has positive states if $e \in \mathcal{E}$ and is a bad arc if $e \in \hat{\mathcal{E}}_{\partial}$. For example, if both of endpoints of e end on the same ideal point, $\psi_{\mathcal{E}}$ sends e to the diagram

$$\begin{array}{c} \text{---} \\ \diagdown \quad \diagup \\ \circ \\ \text{---} \end{array} \mapsto \begin{cases} q^{-1/2} \begin{array}{c} \text{---} \\ \diagdown \quad \diagup \\ \circ \\ \text{---} \\ + \quad + \end{array} & \text{if } e \in \mathcal{E} \\ q^{1/2} \begin{array}{c} \text{---} \\ \diagdown \quad \diagup \\ \circ \\ \text{---} \\ + \quad - \end{array} & \text{if } e \in \hat{\mathcal{E}}_{\partial}. \end{cases}$$

where the $q^{\pm 1/2}$ scalar is introduced so that x_e is reflection invariant, which follows by the (R_6) relation. Therefore, in this example, we have $\begin{array}{c} \text{---} \\ \diagdown \quad \diagup \\ \circ \\ \text{---} \\ + \quad + \end{array} \mapsto q^{1/2}x_e$ and $\begin{array}{c} \text{---} \\ \diagdown \quad \diagup \\ \circ \\ \text{---} \\ + \quad - \end{array} \mapsto q^{-1/2}x_{\hat{e}}$ as $\varphi_{\mathcal{E}}$ is an algebra homomorphism.

The stated skein algebra has the property that for every $\alpha \in \mathcal{S}(\mathfrak{S})$, there is some monomial $m(x_1, \dots, x_r) \in \mathbb{T}_+^r$ such that $\psi_{\mathcal{E}}(m(x_1, \dots, x_r))\alpha \in \text{Im}(\psi_{\mathcal{E}})$. Because these are algebra homomorphisms and since $(\varphi_{\mathcal{E}} \circ \psi_{\mathcal{E}})(x_e) = x_e$, we can explicitly find where any element in our skein algebra is mapped to using the following trick

$$\varphi_{\mathcal{E}}(\alpha) = m^{-1}(x_1, \dots, x_r)m(x_1, \dots, x_r)\varphi_{\mathcal{E}}(\alpha) = m^{-1}(x_1, \dots, x_r)\varphi_{\mathcal{E}}(\psi_{\mathcal{E}}(m(x_1, \dots, x_r))\alpha),$$

where $\mathcal{S}(\mathfrak{S})$ is viewed as the canonical T_+^r -module induced by $\psi_{\mathcal{E}}$, $m \cdot \alpha := \psi_{\mathcal{E}}(m)\alpha$.

4.2 The Quantum 6-Torus

We will now perform this calculation for when $\mathfrak{S} = T^2 \setminus D^2$, with a single marked point on the boundary. Let \mathcal{E} be the quasitriangulation of $T^2 \setminus D^2$ shown in figure 4.1. Note

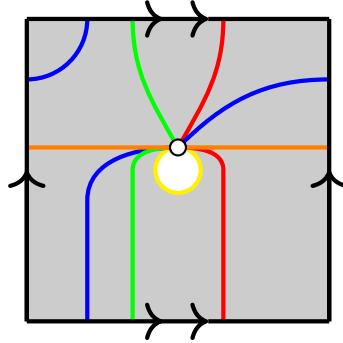
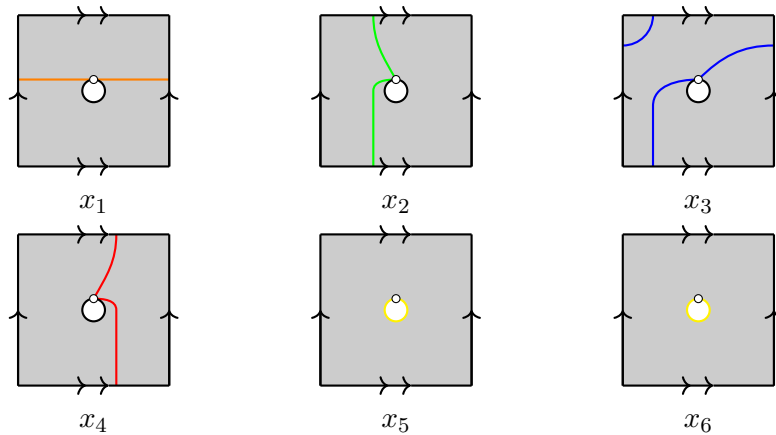


Figure 4.1: A quasitriangulation of $T^2 \setminus D^2$

that as $T^2 \setminus D^2$ does not contain any punctures, \mathcal{E} is a full triangulation of $T^2 \setminus D^2$. We will correspond our variables, x_i , to edges of \mathcal{E} in the following way.



Here x_5 corresponds to the single edge in \mathcal{E}_∂ and x_6 corresponds to our extra copy of x_5 in $\hat{\mathcal{E}}_\partial$. Using the anti-symmetric function, we find our Q to be

$$Q = \begin{pmatrix} 0 & 2 & 2 & -2 & 0 & -4 \\ -2 & 0 & -2 & -4 & 0 & -4 \\ -2 & 2 & 0 & -2 & 0 & -4 \\ 2 & 4 & 2 & 0 & 0 & -4 \\ 0 & 0 & 0 & 0 & 0 & 0 \\ 4 & 4 & 4 & 4 & 0 & 0 \end{pmatrix}.$$

Therefore, we are embedding our stated skein algebra, $\mathcal{S}(T^2 \setminus D^2)$, into a quantum 6-torus. This quantum torus is not simple as it has nontrivial center (see proposition 1.3 in [45]) when viewed as a complex twisted group algebra over the free abelian group of rank 6. However, we still need to consider the entire quantum 6-torus as $\mathcal{S}(T^2 \setminus D^2)$ has a GK-dimension of 6.

Let $y_1, y_2, y_3 \in \mathcal{S}(T^2 \setminus D^2)$ be the diagrams corresponding to the meridian, longitude, and $(1, 1)$ -curve as closed curves, respectively. Then we can use this quasitriangulation, \mathcal{E} , to find the image of y_1 in $\varphi_{\mathcal{E}}$. Note that I'm not expressing the states in these diagrams as all of the states for these calculations will be positive.

$$\psi_{\mathcal{E}}(x_2 x_4 x_3) \cdot y_1 = \left(q^{-3/2} \begin{array}{c} \begin{array}{|c|c|c|} \hline \begin{array}{c} \text{Diagram 1} \\ \text{Meridian curve} \end{array} \\ \hline \end{array} \quad \begin{array}{|c|c|} \hline \begin{array}{c} \text{Diagram 2} \\ \text{Meridian curve} \end{array} \\ \hline \end{array} \quad \begin{array}{|c|c|} \hline \begin{array}{c} \text{Diagram 3} \\ \text{Meridian curve} \end{array} \\ \hline \end{array} \end{array} \right) \begin{array}{|c|} \hline \begin{array}{c} \text{Diagram 4} \\ \text{Meridian curve} \end{array} \\ \hline \end{array}$$

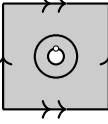
$$\begin{aligned}
&= \left(q^{-3/2} \left(\begin{array}{c} \text{Diagram 1} \\ \text{Diagram 2} \end{array} \right) \begin{array}{c} \text{Diagram 3} \end{array} \right) \\
&= \left(q^{-3/2} \left(\begin{array}{c} \text{Diagram 1} \\ \text{Diagram 2} \end{array} \right) \left(q \begin{array}{c} \text{Diagram 4} \end{array} + q^{-1} \begin{array}{c} \text{Diagram 5} \end{array} \right) \right) \\
&= \left(q^{-3/2} \begin{array}{c} \text{Diagram 1} \end{array} \right) \left(q \begin{array}{c} \text{Diagram 4} \end{array} + q^{-1} \begin{array}{c} \text{Diagram 5} \end{array} \right) \\
&= \left(q^{-3/2} \begin{array}{c} \text{Diagram 1} \end{array} \right) \left(q \begin{array}{c} \text{Diagram 4} \end{array} + \begin{array}{c} \text{Diagram 6} \end{array} + q^{-2} \begin{array}{c} \text{Diagram 7} \end{array} \right) \\
&= q^{-3/2} \left(q \begin{array}{c} \text{Diagram 4} \end{array} + \begin{array}{c} \text{Diagram 6} \end{array} + q^{-2} \begin{array}{c} \text{Diagram 7} \end{array} \right) \\
&= q^{-3/2} \left(q \begin{array}{c} \text{Diagram 4} \end{array} + \begin{array}{c} \text{Diagram 6} \end{array} + q^{-1} \begin{array}{c} \text{Diagram 8} \end{array} + q^{-3} \begin{array}{c} \text{Diagram 7} \end{array} \right) \\
&= q^{-3/2} \left(q \begin{array}{c} \text{Diagram 4} \end{array} + q \begin{array}{c} \text{Diagram 6} \end{array} + q^{-4} \begin{array}{c} \text{Diagram 8} \end{array} + q^{-3} \begin{array}{c} \text{Diagram 7} \end{array} \right)
\end{aligned}$$

where the last equality comes from the height exchange relation, (R_6) . Thus,

$$\begin{aligned}
\varphi_{\mathcal{E}}(y_1) &= (x_2x_4x_3)^{-1}(x_2x_4x_3)\varphi_{\mathcal{E}}(y_1) = (x_2x_4x_3)^{-1}\varphi_{\mathcal{E}}(\psi_{\mathcal{E}}(x_2x_4x_3)y_1) \\
&= qx_3^{-1}x_4^{-1}x_2^{-1}x_2x_4x_2 + qx_3^{-1}x_4^{-1}x_2^{-1}x_2x_1^2 + q^{-4}x_3^{-1}x_4^{-1}x_2^{-1}x_1x_3x_5 + q^{-3}x_3^{-1}x_4^{-1}x_2^{-1}x_3^2x_4 \\
&= q^{-1}x_2x_3^{-1} + q^{-1}x_2^{-1}x_3 + qx_1^2x_3^{-1}x_4^{-1} + q^2x_1x_2^{-1}x_4^{-1}x_5.
\end{aligned}$$

One can similarly calculate where y_2, y_3 , and the boundary curve get mapped to under $\varphi_{\mathcal{E}}$ (see A.2 in the appendix). Hence $\varphi_{\mathcal{E}}$ maps these diagrams as follows.

Proposition 4.2.76. Suppose $\varphi_{\mathcal{E}} : \mathcal{S}(T^2 \setminus D^2) \hookrightarrow \mathbb{T}^n$ is the algebra homomorphism defined as above. Let $y_1, y_2, y_3 \in \mathcal{S}(T^2 \setminus D^2)$ be the meridian, longitude, and $(1, 1)$ -curve

respectively and ∂ the boundary curve . Then

$$\begin{aligned}
y_1 &\mapsto q^{-1}x_2x_3^{-1} + q^{-1}x_2^{-1}x_3 + qx_1^2x_3^{-1}x_4^{-1} + q^2x_1x_2^{-1}x_4^{-1}x_5 \\
y_2 &\mapsto qx_1x_3^{-1} + qx_1^{-1}x_3 + q^{-1}x_1^{-1}x_2x_3^{-1}x_4 \\
y_3 &\mapsto q^{-1}x_1x_4^{-1} + q^{-1}x_1^{-1}x_4 + q^{-1}x_1^{-1}x_2^{-1}x_3^2 + x_2^{-1}x_3x_4^{-1}x_5 \\
\partial &\mapsto q^{-2}x_2^{-1}x_4 + q^{-2}x_2x_4^{-1} + qx_1^{-1}x_3x_4^{-1}x_5 + qx_1x_3^{-1}x_4^{-1}x_5 + q^{-3}x_1^{-1}x_3^{-1}x_4x_5 \\
&\quad + q^3x_1x_2^{-1}x_3^{-1}x_5 + q^{-1}x_1^{-1}x_2x_3^{-1}x_5 + q^{-1}x_1^{-1}x_2^{-1}x_3x_5 + q^2x_2^{-1}x_4^{-1}x_5^2
\end{aligned}$$

In particular, the images of y_i satisfy the commutation relations

$$(q^2 - q^{-2})^{-1} [\varphi_{\mathcal{E}}(y_i), \varphi_{\mathcal{E}}(y_{i+1})]_q = \varphi_{\mathcal{E}}(y_{i+2})$$

for $i \pmod 3$ and

$$\varphi_{\mathcal{E}}(\partial) = q\varphi_{\mathcal{E}}(y_1)\varphi_{\mathcal{E}}(y_2)\varphi_{\mathcal{E}}(y_3) - q^2\varphi_{\mathcal{E}}(y_1)^2 - q^{-2}\varphi_{\mathcal{E}}(y_2)^2 - q^2\varphi_{\mathcal{E}}(y_3)^2 + q^2 + q^{-2}.$$

4.3 A Module of Laurent Polynomials

Proposition 4.3.77. Let $\mathbb{T}^n(Q)$ be the quantum torus of n generators, $\frac{\mathbb{K}\langle x_1^{\pm 1}, \dots, x_n^{\pm 1} \rangle}{x_i x_j = q^{Q_{i,j}} x_j x_i}$, where Q is the corresponding skew-symmetric integral matrix. If k is the number of non-central generators of \mathbb{T}^n and $q^{\frac{Q_{i,j}}{2}} \in \mathbb{K}$ for all i, j , then the commutative ring $\mathbb{K}[y_1^{\pm 1}, \dots, y_{k-1}^{\pm 1}]$ has a well defined \mathbb{T}^n -module structure. In particular, if the first k generators, $\{x_1, \dots, x_k\}$, are our non-commutative generators, then for each $i \in \{1, \dots, k-1\}$ and $m \in \{k+1, \dots, n\}$, the operators

$$x_i \cdot f(y_1, y_2, \dots, y_{k-1}) := y_i f(q^{Q_{i,1}/2} y_1, q^{Q_{i,2}/2} y_2, \dots, q^{Q_{i,k-1}/2} y_{k-1})$$

$$x_k \cdot f(y_1, y_2, \dots, y_{k-1}) := f(q^{Q_{k,1}} y_1, q^{Q_{k,2}} y_2, \dots, q^{Q_{k,k-1}} y_{k-1})$$

$$x_m \cdot f(y_1, y_2, \dots, y_{k-1}) := f(y_1, y_2, \dots, y_{k-1}).$$

define a \mathbb{T}^n -module.

Proof. Our relations $x_i x_j = q^{Q_{i,j}} x_j x_i$ hold as for all $i, j \in \{1, \dots, k-1\}$

$$x_i x_j \cdot f(y_1, \dots, y_{k-1}) = q^{\frac{Q_{i,j}}{2}} y_i y_j f(q^{\frac{Q_{j,1}+Q_{i,1}}{2}} y_1, \dots, q^{\frac{Q_{j,k-1}+Q_{i,k-1}}{2}} y_{k-1})$$

$$= q^{Q_{i,j}} x_j x_i \cdot f(y_1, \dots, y_{k-1})$$

$$x_i x_k \cdot f(y_1, \dots, y_{k-1}) = y_i f(q^{\frac{Q_{i,1}}{2}+Q_{k,1}} y_1, \dots, q^{\frac{Q_{i,k-1}}{2}+Q_{k,k-1}} y_{k-1})$$

$$= q^{Q_{i,k}} x_k x_i \cdot f(y_1, \dots, y_{k-1}).$$

Clearly, for any $m, m' \in \{k+1, \dots, n\}$ we have $x_i x_m \cdot f(y_1, \dots, y_{k-1}) = x_m x_i \cdot f(y_1, \dots, y_{k-1})$

and $x_m x_{m'} \cdot f(y_1, \dots, y_{k-1}) = x_m x_{m'} \cdot f(y_1, \dots, y_{k-1})$. \square

By this proposition, the ring of Laurent polynomials in 4 variables is a module over our quantum 6-torus, \mathbb{T}^6 . Since $\mathcal{S}(T^2 \setminus D^2) \hookrightarrow \mathbb{T}^6$, the following actions endow

$\mathbb{C}[x^{\pm 1}, y^{\pm 1}, z^{\pm 1}, w^{\pm 1}]$ with the structure of a $\mathcal{S}(T^2 \setminus D^2)$ -module.

$$x_1 \cdot f(x, y, z, w) = xf(x, qy, qz, q^{-1}w) \quad x_2 \cdot f(x, y, z, w) = yf(q^{-1}x, y, q^{-1}z, q^{-2}w)$$

$$x_3 \cdot f(x, y, z, w) = zf(q^{-1}x, qy, z, q^{-1}w) \quad x_4 \cdot f(x, y, z, w) = wf(qx, q^2y, qz, w)$$

$$x_5 \cdot f(x, y, z, w) = f(x, y, z, w) \quad x_6 \cdot f(x, y, z, w) = f(q^4x, q^4y, q^4z, q^4w)$$

Thus, the actions of y_1, y_2, y_3 , and ∂ on this module are (and have been verified via Python as detailed in B.2)

$$\begin{aligned} y_1 \cdot f(x, y, z, w) &= yz^{-1}f(x, q^{-1}y, q^{-1}z, q^{-1}w) + y^{-1}zf(x, qy, qz, qw) \\ &\quad + x^2z^{-1}w^{-1}f(x, q^{-1}y, qz, q^{-1}w) + xy^{-1}w^{-1}f(x, q^{-1}y, qz, qw) \\ y_2 \cdot f(x, y, z, w) &= xz^{-1}f(qx, y, qz, w) + x^{-1}zf(q^{-1}x, y, q^{-1}z, w) + x^{-1}yz^{-1}wf(qx, y, q^{-1}z, w) \\ y_3 \cdot f(x, y, z, w) &= xw^{-1}f(q^{-1}x, q^{-1}y, z, q^{-1}w) + x^{-1}wf(qx, qy, z, qw) \\ &\quad + x^{-1}y^{-1}z^2f(q^{-1}x, qy, z, qw) + y^{-1}zw^{-1}f(q^{-1}x, q^{-1}y, z, qw). \\ \partial \cdot f(x, y, z, w) &= \frac{zf\left(\frac{x}{q^2}, \frac{y}{q^2}, \frac{z}{q^2}, w\right)}{xw} + \frac{zf(x, y, z, q^2w)}{xy} + \frac{wf(q^2x, q^2y, q^2z, q^2w)}{y} \\ &\quad + \frac{wf(q^2x, y, z, q^2w)}{zx} + \frac{yf\left(\frac{x}{q^2}, \frac{y}{q^2}, \frac{z}{q^2}, \frac{w}{q^2}\right)}{w} + \frac{yf\left(x, \frac{y}{q^2}, \frac{z}{q^2}, w\right)}{zx} \\ &\quad + \frac{xf\left(x, \frac{y}{q^2}, z, w\right)}{wz} + \frac{xf(q^2x, y, q^2z, q^2w)}{yz} + \frac{f\left(x, \frac{y}{q^2}, z, q^2w\right)}{yw} \end{aligned}$$

where $\partial = qy_1y_2y_3 - q^2y_1^2 - q^{-2}y_2^2 - q^2y_3^2 + q^2 + q^{-2}$ is the boundary curve.

Unfortunately, ∂ does not have any eigenvalues due to grade shifts, however, it does have an invariant subspace, $\mathbb{C}\left[\left(\frac{x}{yz}\right)^{\pm 1}, \left(\frac{y}{zx}\right)^{\pm 1}, \left(\frac{z}{xy}\right)^{\pm 1}, \left(\frac{w}{y}\right)^{\pm 1}\right]$. To condense the notation a bit, let $\kappa = k_1 + k_2 + k_3 + k_4$ and $\mathbf{k} = (k_1, k_2, k_3, k_4)$. Note that the following computation was done by hand and verified via python (once again see B.2).

$$\begin{aligned}
& \partial \cdot \sum_{\substack{\kappa=-n \\ |k_i| \leq n}}^n c_{\mathbf{k}} \left(\frac{x}{yz} \right)^{k_1} \left(\frac{y}{zx} \right)^{k_2} \left(\frac{z}{xy} \right)^{k_3} \left(\frac{w}{y} \right)^{k_4} \\
&= \sum_{\substack{\kappa=-n \\ |k_i| \leq n}}^n c_{\mathbf{k}} \left[q^{2\kappa} \left(\frac{x}{yz} \right)^{k_1} \left(\frac{y}{zx} \right)^{k_2} \left(\frac{z}{xy} \right)^{k_3+1} \left(\frac{w}{y} \right)^{k_4-1} + q^{2k_4} \left(\frac{x}{yz} \right)^{k_1} \left(\frac{y}{zx} \right)^{k_2} \left(\frac{z}{xy} \right)^{k_3+1} \left(\frac{w}{y} \right)^{k_4} \right. \\
&\quad + q^{2(\kappa-k_4)} \left(\frac{x}{yz} \right)^{k_1} \left(\frac{y}{zx} \right)^{k_2} \left(\frac{z}{xy} \right)^{k_3} \left(\frac{w}{y} \right)^{k_4-1} + q^{-2(\kappa-k_4)} \left(\frac{x}{yz} \right)^{k_1} \left(\frac{y}{zx} \right)^{k_2} \left(\frac{z}{xy} \right)^{k_3} \left(\frac{w}{y} \right)^{k_4+1} \\
&\quad + q^{2(\kappa-2k_2+k_4)} \left(\frac{x}{yz} \right)^{k_1+1} \left(\frac{y}{zx} \right)^{k_2} \left(\frac{z}{xy} \right)^{k_3+1} \left(\frac{w}{y} \right)^{k_4-1} + q^{2(\kappa-2k_2)} \left(\frac{x}{yz} \right)^{k_1+1} \left(\frac{y}{zx} \right)^{k_2} \left(\frac{z}{xy} \right)^{k_3} \left(\frac{w}{y} \right)^{k_4-1} \\
&\quad + q^{2(k_4-2k_2)} \left(\frac{x}{yz} \right)^{k_1+1} \left(\frac{y}{zx} \right)^{k_2} \left(\frac{z}{xy} \right)^{k_3} \left(\frac{w}{y} \right)^{k_4} + q^{2(2k_1+k_4)} \left(\frac{x}{yz} \right)^{k_1} \left(\frac{y}{zx} \right)^{k_2+1} \left(\frac{z}{xy} \right)^{k_3} \left(\frac{w}{y} \right)^{k_4} \\
&\quad \left. + q^{2(k_1-k_2-k_3+k_4)} \left(\frac{x}{yz} \right)^{k_1} \left(\frac{y}{zx} \right)^{k_2+1} \left(\frac{z}{xy} \right)^{k_3} \left(\frac{w}{y} \right)^{k_4+1} \right] = \sum_{\substack{\kappa=-(n+1) \\ |k_i| \leq n+1}}^{n+2} c'_{\mathbf{k}} \left(\frac{x}{yz} \right)^{k_1} \left(\frac{y}{zx} \right)^{k_2} \left(\frac{z}{xy} \right)^{k_3} \left(\frac{w}{y} \right)^{k_4}
\end{aligned}$$

Furthermore, our operators y_1 , y_2 , and y_3 also have invariant subspaces. For example, $\mathbb{C} \left[\left(\frac{x}{z} \right)^{\pm 1}, \left(\frac{yw}{xz} \right)^{\pm 1} \right]$ is an invariant subspace with respect to the action of y_2 on this module. To see this, we compute the following.

$$\begin{aligned}
& y_2 \cdot \sum_{\substack{k_1+k_2=-n \\ |k_i| \leq n}}^n c_{k_1, k_2} \left(\frac{x}{z} \right)^{k_1} \left(\frac{yw}{xz} \right)^{k_2} \\
&= \sum_{\substack{k_1+k_2=-n \\ |k_i| \leq n}}^n c_{k_1, k_2} \left[q^{2k_2} \left(\frac{x}{z} \right)^{k_1-1} \left(\frac{yw}{xz} \right)^{k_2} + q^{-2k_2} \left(\frac{x}{z} \right)^{k_1+1} \left(\frac{yw}{xz} \right)^{k_2} + q^{2k_1} \left(\frac{x}{z} \right)^{k_1} \left(\frac{yw}{xz} \right)^{k_2+1} \right] \\
&= \sum_{\substack{k_1+k_2=-(n+1) \\ |k_i| \leq n+1}}^{n+1} c'_{k_1, k_2} \left(\frac{x}{z} \right)^{k_1} \left(\frac{yw}{xz} \right)^{k_2}
\end{aligned}$$

It seems as though the algebra $\mathbb{C} [x^{\pm 1}, y^{\pm 1}, z^{\pm 1}, w^{\pm 1}]$ constitutes a minimal structure for this type of representation while still allowing for well-defined, nontrivial actions of the generators of $\mathbb{T}^6(Q)$. While it is straightforward to introduce additional variables into this algebra, it would be surprising if the number of variables could be reduced. For this reason, we give the following conjecture.

Conjecture 4.3.78. Let Q be the anti-symmetric matrix defined in section 4.2 and suppose M is a Laurent polynomial algebra with a $\mathbb{T}^6(Q)$ -module structure such that each x_i acts nontrivially. Then the Gelfend-Kirillov dimension of M is at least 4.

Chapter 5

Topologically Defined Representations

5.1 Knot Invariants

There is another, more geometric, perspective to the story of skein modules that begins by looking for knot invariants. Let M be a 3-manifold with boundary and consider the natural inclusion $\partial M \hookrightarrow M$. This inclusion induces a map on fundamental groups, denoted by $\alpha : \pi_1(\partial M) \rightarrow \pi_1(M)$, known as the *peripheral map*. In [61], Waldhausen demonstrated that the peripheral map serves as a complete invariant for a significant class of 3-manifolds, namely *sufficiently large* 3-manifolds. In particular, these kinds of manifolds include knot complements. This result was further refined by Gordon and Luecke in [28] to establish it as a knot invariant as well.

Given a knot K , the *knot complement* is defined as $M_K = S^3 \setminus N(K)$, where $N(K)$ is a tubular neighborhood of K . Since the boundary of M_K is a torus, the corresponding peripheral map is $\alpha : \pi_1(T^2) \rightarrow \pi_1(M_K)$. Notably, $\pi_1(M_K)$ alone is not a complete knot invariant, as it cannot distinguish between mirrored images of chiral knots. However, the additional information regarding how the torus embeds into the knot complement allows for this distinction.

We can study these groups by instead examining the induced maps on their representations. For any reductive group, G , the set of all G -representations, denoted $\text{Rep}(M, G) := \text{Hom}(\pi_1(M), G)$, inherits a natural variety structure from the algebraic variety structure of G . Moreover, the induced map $\text{Rep}(M, G) \rightarrow \text{Rep}(\partial M, G)$ descends to a map on G -character varieties, $\chi(M, G) \rightarrow \chi(\partial M, G)$. Here, $\chi(M, G)$ is defined as $\text{Rep}(M, G) // G$, the closed algebraic quotient of the natural conjugation action of G on the representation variety. Finally, we can instead induce the map onto the coordinate rings of these character varieties: $\mathcal{O}(\chi(\partial M, G)) \rightarrow \mathcal{O}(\chi(M, G))$. Equivalently, we can also consider $\mathcal{O}(\text{Rep}(\partial M, G))^G \rightarrow \mathcal{O}(\text{Rep}(M, G))^G$, the corresponding map between the algebras of G -invariant regular functions on $\text{Rep}(\partial M, G)$ and $\text{Rep}(M, G)$. Below is a more visual depiction of the process just described.

$$\begin{array}{ccc}
\pi_1(\partial M) & \xrightarrow{\alpha} & \pi_1(M) \\
\\
\text{Rep}(\partial M, G) & \xleftarrow{\alpha^*} & \text{Rep}(M, G) \\
\downarrow & & \downarrow \\
\chi(\partial M, G) & \xleftarrow{\hat{\alpha}} & \chi(M, G) \\
\\
\mathcal{O}(\chi(\partial M, G)) & \xrightarrow{\alpha_*} & \mathcal{O}(\chi(M, G))
\end{array}$$

So we have taken a map between not necessarily abelian groups and turned it into a map between commutative algebras, which offers several advantages. At this point, it is natural to ask whether or not we still have the same precision of knot invariants at this level. Initially the answer is no. However, it turns out that if we quantize these coordinate rings, then it is possible to extract this data.

Before we do this, let's take a moment to figure out what exactly is $\chi(\partial M, G)$. As we're only considering cases when ∂M is the two torus, $T^2 = S^1 \times S^1$, for any reductive group, G , $\chi(\partial M, G) = \text{Hom}(\mathbb{Z}^2, G) // G$. Let $\mathcal{T} \subset G$ be a maximal toral subgroup of G , and let $W = N(\mathcal{T})/\mathcal{T}$ be the corresponding Weyl group, where $N(\mathcal{T})$ is the normalizer of \mathcal{T} in G . Clearly, $\text{Rep}(T^2, \mathcal{T}) \cong \mathcal{T} \times \mathcal{T}$ since the fundamental group of the torus is \mathbb{Z}^2 . As \mathcal{T} is a subgroup of G , there is a natural inclusion of these representation varieties, $\text{Rep}(T^2, \mathcal{T}) \hookrightarrow \text{Rep}(T^2, G)$.

We can surject $\text{Rep}(T^2, G)$ onto its character variety and do the same for $\mathcal{T} \times \mathcal{T}$ by factoring it through the diagonal action of W . It's fairly straightforward to see that this induces a map, Ψ , on these character varieties.

$$\begin{array}{ccc} \text{Rep}(T^2, \mathcal{T}) & \xlongequal{\quad} & \mathcal{T} \times \mathcal{T} \hookrightarrow \text{Rep}(T^2, G) \\ & & \downarrow \quad \downarrow \\ & & \mathcal{T} \times \mathcal{T} // W \xrightarrow{\quad \Psi \quad} \chi(T^2, G) \end{array}$$

It's natural to expect and hope that Ψ is an isomorphism; however, this is not true in general. Nonetheless, a chain of results supports us in our specific situation. Thaddeus proved in [58] that when G is a connected complex reductive algebraic group, the quotient $\mathcal{T} \times \mathcal{T} // W$ is bijective with the connected component containing the trivial character, denoted $\chi_0(T^2, G)$. Moreover, Richardson's work in [53] implies that if additionally G is

simply-connected, then the character variety $\chi(T^2, G)$ is irreducible as a moduli space, and thus $\chi(T^2, G) = \chi_0(T^2, G)$. However, similar to normalization maps for cuspidal curves, the bijectivity of these spaces does not necessarily imply that they are isomorphic as varieties.

Nevertheless, combining these results, Sikora established in [57] that whenever G is a classical group, i.e. $G = GL_n(\mathbb{C})$, $SL_n(\mathbb{C})$, $SP_n(\mathbb{C})$, or $SO_n(\mathbb{C})$, Ψ is indeed an isomorphism of varieties and hence the induced map on coordinate rings,

$$\Psi_* : \mathcal{O}(\mathcal{T} \times \mathcal{T})^W \longrightarrow \mathcal{O}(\chi(T^2, G))$$

is an isomorphism of commutative algebras. As $\mathcal{O}(\mathcal{T} \times \mathcal{T})^W$ has been fairly heavily studied in representation theory, it is beneficial to instead consider the map $\alpha_* : \mathcal{O}(\mathcal{T} \times \mathcal{T})^W \rightarrow \mathcal{O}(\chi(M, G))$. Moreover, it has interesting non-commutative deformations: spherical DA-HAs.

Since we're only working with $G = SL_2(\mathbb{C})$, the above results provide us with a more concrete way of understanding the character variety $\chi(T^2, SL_2(\mathbb{C}))$. In particular, when $G = SL_2(\mathbb{C})$, a quick calculation shows the following.

$$\mathcal{T} = \left\{ \begin{pmatrix} a & 0 \\ 0 & a^{-1} \end{pmatrix} : a \in \mathbb{C}^\times \right\}$$

$$N(\mathcal{T}) = \left\{ \begin{pmatrix} a & 0 \\ 0 & a^{-1} \end{pmatrix}, \begin{pmatrix} 0 & -b \\ b & 0 \end{pmatrix} : a, b \in \mathbb{C}^\times \right\}$$

and therefore

$$W = N(\mathcal{T})/\mathcal{T} = \left\{ \begin{pmatrix} 1 & 0 \\ 0 & 1 \end{pmatrix} \mathcal{T}, \begin{pmatrix} 0 & -1 \\ 1 & 0 \end{pmatrix} \mathcal{T} \right\} \cong \mathbb{Z}/2\mathbb{Z}.$$

Since $\pi_1(T^2)$ is abelian and has two generators, we obtain the following isomorphism.

$$\mathcal{O}(\text{Rep}(T^2, SL_2(\mathbb{C}))) \cong \frac{\mathbb{C}\langle X^{\pm 1}, Y^{\pm 1} \rangle}{XY - YX}$$

There is a natural $\mathbb{Z}/2\mathbb{Z}$ -action, which corresponds to simultaneously inverting X and Y . Consequently, the ring $\mathcal{O}(\chi(T^2, SL_2(\mathbb{C})))$ is subalgebra of elements invariant under this involution.

Returning to the topic of knot invariants, we mentioned that we can recover this information through the quantization of these coordinate rings. Frohman and Gelca defined a particular quantization of $\mathcal{O}(\text{Rep}(T^2, SL_2(\mathbb{C})))$ in [26], which they call the noncommutative torus.

$$A_q := \mathbb{T}^2 \left(\begin{bmatrix} 0 & 2 \\ -2 & 0 \end{bmatrix} \right) = \frac{\mathbb{C}\langle X^{\pm 1}, Y^{\pm 1} \rangle}{XY - q^2 YX}$$

We can apply the same $\mathbb{Z}/2\mathbb{Z}$ -action on A_q and look at the corresponding invariant subalgebra, denoted $A_q^{\mathbb{Z}/2\mathbb{Z}}$. They then showed that both $K_q(T^2)$ and $A_q^{\mathbb{Z}/2\mathbb{Z}}$ are isomorphic as algebras.

Recall that by Theorem 2.5.32, $\{(r, s)_T\}_{r, s \in \mathbb{Z}} / \sim$ where $(r, s)_T \sim (-r, -s)_T$ forms a basis for $K_q(T^2)$.

Theorem 5.1.79 (Theorem 4.3 in [26]). The linear map $K_q(T^2) \rightarrow A_q^{\mathbb{Z}/2\mathbb{Z}}$ defined by $(r, s)_T \mapsto q^{-sr} (Y^{-s} X^r + Y^s X^{-r})$ is an isomorphism of algebras.

Therefore, the meridian and longitude get mapped to $X + X^{-1}$ and $Y + Y^{-1}$, respectively. This theorem tells us that $K_q(T^2)$ can be understood as a quantum deformation of the ring of $SL_2(\mathbb{C})$ -invariant regular functions over $\mathcal{O}(\text{Rep}(T^2, SL_2(\mathbb{C})))$.

Moreover, Przytycki and Sikora in [51] (as well as Bullock in [10]) showed that for any 3-manifold, the specialization of $K_{q=-1}(M)$ is isomorphic to $\mathcal{O}(\chi(M, SL_2(\mathbb{C})))$ as algebras. Therefore, $K_q(M)$ is a quantization of the commutative algebra $\mathcal{O}(\chi(M, SL_2(\mathbb{C})))$. Furthermore, when M is a surface, $K_q(M)$ is a deformation of $K_{q=-1}(M) \cong \mathcal{O}(\chi(M, SL_2(\mathbb{C})))$ in the direction of Goldman's Poisson bracket.

Recall that the induced map $\alpha_* : \mathcal{O}(\chi(\partial M, G)) \rightarrow \mathcal{O}(\chi(M, G))$ is a map between commutative algebras. Any time we have a map between algebras, we can make the codomain into a module over the domain using the map. It turns out that this module structure remains intact as we quantize both of these algebras. Furthermore, given a knot, K , the colored Jones polynomial, $J_n(K, q)$, can be extracted from the $A_q^{\mathbb{Z}/2\mathbb{Z}}$ -module structure of $K_q(M_K)$. The natural embedding $N(K) \sqcup M_K \hookrightarrow S^3$ induces the pairing

$$\langle -, - \rangle : K_q(S^1 \times D^2) \otimes_{K_q(T^2)} K_q(M_K) \rightarrow K_q(S^3) \cong \mathbb{C}.$$

It's not too hard to see that $K_q(S^1 \times D^2) \cong \mathbb{C}[u]$ as vector spaces, and a theorem of Kirby and Melvin from [35] shows

$$J_n(K, q) = \langle S_{n-1}(u), 1_K \rangle.$$

Here, 1_K denotes the empty link in M_K and S_n is the n th Chebyshev polynomials, but now with initial conditions $S_0(x) = 1$, $S_1(x) = x$, and $S_{n+1} = xS_n - S_{n-1}$.

As the $K_q(T^2)$ -module structure of $K_q(M_K)$ comes from the peripheral map, we can geometrically interpret this as isotoping any curves in $K_q(M_K)$ away from a neighborhood of ∂M_k and embedding $T^2 \times I$ into this neighborhood. These $K_q(T^2)$ -module structures, as well as their connection with DAHA representations, were examined by Gelca and Sain in [27] and more thoroughly examined by Berest and Samuelson in [5]. For example,

when K is the unknot, M_k is the solid torus and so $K_q(M_k) \cong \mathbb{C}[u]1_K$. Let Y_1 , Y_2 , and Y_3 be the meridian, longitude, and $(1, 1)$ -curve respectively. Then the action of $K_q(T^2)$ on $K_q(M_K)$ is given by

$$\begin{aligned} Y_1 \cdot f(u)1_K &= uf(u)1_K, \\ Y_2 \cdot 1_K &= (-q^2 - q^{-2})1_K, \\ Y_3 \cdot 1_K &= -q^{-3}u1_K. \end{aligned}$$

Although it is quite a bit more work, this module structure can be extended to the knot complement of any knot. In [5], Berest and Samuelson describe the natural action of the A_1 DAHA on these knot complements for the trefoil, the figure eight knot, all $(2, 2p + 1)$ -torus knots, and all 2-bridge knots (when $q = \pm 1$).

5.2 Knot Complements as $\mathcal{S}(T^2 \setminus D^2)$ -Modules

Just as $K_q(M)$ can be understood as a quantization of SL_2 -invariant regular functions on $\text{Rep}(M, SL_2)$, a similar geometric approach applies to the theory of stated skein algebra, using the conventional model where Σ is a punctured bordered surface, $\mathcal{S}^{pb}(\Sigma)$.

Let Σ be an oriented surface with boundary, and fix a Riemannian metric on Σ . Denote $U\Sigma$ as the unit tangent bundle over Σ , and let $pr : U\Sigma \rightarrow \Sigma$ be the canonical projection. The preimage of any point in Σ is a circle equipped with an orientation induced from that of Σ . For any boundary edge e , and any point $x \in e$, let $v \in T_x(\Sigma)$ be the unit tangent vector pointing in the direction of the orientation of e . Define θ_e to be the half-circle from (x, v) to $(x, -v)$ in the positive direction of its orientation.¹

¹The choice of x in e does not actually make a difference here.

Just as Kauffman bracket skein modules come from representation varieties over fundamental groups, stated skein algebras come from representation varieties over fundamental groupoids. Every immersion $\alpha : [0, 1] \rightarrow \Sigma$ canonically lifts to the path $\left(\alpha(t), \frac{\alpha(t)}{\|\alpha(t)\|}\right)$ in $U\Sigma$ and thus any boundary edge, $e \subset \partial\Sigma$, canonically lifts to $\tilde{e} \subset \partial(U\Sigma)$. If

$$\widetilde{\partial\Sigma} := \bigcup_{e \subset \partial\Sigma} \tilde{e},$$

then $\pi_1(U\Sigma; \widetilde{\partial\Sigma})$ is the fundamental groupoid corresponding to a lift of the fundamental groupoid, $\pi_1(\Sigma, \partial\Sigma)$.

Definition 5.2.80. A *flat twisted $SL_2(\mathbb{C})$ -bundle* on Σ is a morphism $\rho : \pi_1(U\Sigma; \widetilde{\partial\Sigma}) \rightarrow SL_2(\mathbb{C})$ such that $\rho(\theta_e) = \begin{pmatrix} 0 & -1 \\ 1 & 0 \end{pmatrix}$ for every boundary edge, e .

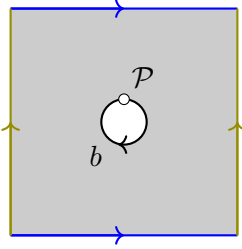
Costantino and Lê showed (Lemma 8.2 in [19]) that the set of flat twisted $SL_2(\mathbb{C})$ -bundles on Σ forms an affine algebraic variety, similar to the Kauffman bracket case. In the following theorem, they established the classical limit of stated skein algebras.

Theorem 5.2.81 (Theorem 8.12 in [19]). When $q = 1$, the stated skein algebra $\mathcal{S}(\Sigma)$ is naturally isomorphic to the coordinate ring of flat twisted $SL_2(\mathbb{C})$ -bundles on Σ .

We will now extend the action of $K_q(T^2)$ on knot complements to an action of $\mathcal{S}(T^2 \setminus D^2)$ on corresponding stated skein modules with one marking. Just as before, the action of $\mathcal{S}(T^2 \setminus D^2)$ on $\mathcal{S}(M_K)$ for some knot K should be dictated by the peripheral map, i.e. $\mathcal{S}(T^2 \setminus D^2)$ should somehow be “glued” to the boundary of M_K . In order to incorporate the data of our marking, we’ll need to add a marking to the knot complement and identify both markings in such a way that aligns with a module structure. From now on, we will

assume that M_K has a single marking in its boundary. Define $\mathcal{N}_K : [0, 1] \hookrightarrow \partial M_K$ to be this marking and consider $\mathcal{S}(M_K, \mathcal{N}_K)$.

In order to define this module structure properly, we will need to consider the “conventional model” for stated skein algebras, $\mathcal{S}^{pb}(T^2 \setminus D^2)$, where we identify $T^2 \setminus D^2$ as a punctured bordered surface (see section 2.7 for more information). Let $\mathcal{P} \in \partial(T^2 \setminus D^2)$ be our ideal point and denote $\Sigma' := (T^2 \setminus D^2) \setminus \mathcal{P}$ as the corresponding punctured bordered surface with clockwise orientation, \mathfrak{o} , on our boundary edge, $\partial\Sigma'$. Identify $\partial\Sigma'$ with the map $b : (0, 1) \rightarrow \Sigma'$ such that the induced orientation from $(0, 1)$ is compatible with \mathfrak{o} .

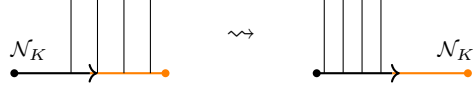


For now, we are understanding this picture as purely topological and are not yet considering the corresponding skein algebras. Glue $T^2 \times [0, 1]$ to the boundary of M_K so that $T^2 \times \{0\}$ is identified with ∂M_K via the peripheral embedding, $T^2 \times \{0\} \hookrightarrow \partial M_K$. At this point, it should be the case that $T^2 \times (0, 1] \cap M_K = \emptyset$ and \mathcal{N}_K is on the interior of $\widetilde{M}_K := M_K \cup (T^2 \times [0, 1])$. We can compose embeddings of our thickened punctured bordered surface

$$\iota_K : \Sigma' \hookrightarrow T^2 \hookrightarrow \widetilde{M}_K$$

such that $b([\epsilon, 1 - \epsilon]) \times \{0\}$ is identified with \mathcal{N}_K for some small $\epsilon > 0$. We will eventually identify $b([\epsilon, 1 - \epsilon]) \times \{1\}$ as the new marking.

Let $\alpha \in \mathcal{S}^{pb}(\Sigma')$ and $D \in \mathcal{S}(M_K)$. First isotope any closed curves in D away from the boundary and isotope the endpoints of any stated ∂M_K -tangles of D down the marking to $\mathcal{N}_K((0, \frac{1}{2}))$.



Similarly, isotope the endpoints of any stated $\partial(T^2 \setminus D^2)$ -tangles in α , remaining in generic position while doing so, up to $\mathcal{N}((\frac{1}{2}, 1 - \epsilon)) \times [0, 1]$.

We can extend any stated \mathcal{N}_K -tangles to end on $b \times \{1\}$ instead of $b \times \{0\}$. Specifically, let (m, s) be a stated \mathcal{N}_K -tangle (using definition 2.6.36) and e_1, e_2 be the endpoints of m . In addition to lying on \mathcal{N}_K in M_K , we can view e_1 and e_2 as lying in $b \times [0, 1]$ in \widetilde{M}_K . Define

$$\tilde{m} = m \bigcup_{i=1,2} (e_i \times [0, 1])$$

where $e_i \times [0, 1] \subset b \times [0, 1]$. Then (\tilde{m}, \tilde{s}) is a stated $\tilde{\mathcal{N}}_K$ -tangle where $\tilde{s}(e_i \times \{1\}) = s(e_i)$ and $\tilde{\mathcal{N}}_K := \iota_K(b([\epsilon, 1 - \epsilon]) \times \{1\})$.

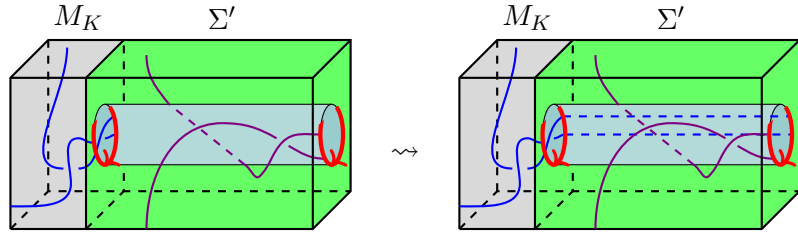


Figure 5.1: Extending the endpoints of tangles (blue) in M_K to end on the new boundary marking (blue and dashed).

In other words, we can identify the stated endpoints of m on \mathcal{N}_K as living on $b \times \{0\}$ and then “pull” these endpoints along the $[0, 1]$ component of $\partial\Sigma' \times [0, 1]$ so that the endpoints are now on $b \times \{1\}$.

Define $\alpha \cdot D$ as the stated $\tilde{\mathcal{N}}_K$ -tangle diagram in $\mathcal{S}(\tilde{M}_K, \tilde{\mathcal{N}}_K)$ consisting of the union of \tilde{m} for each stated \mathcal{N}_K -tangle m in D , along with the induced stated $\tilde{\mathcal{N}}_K$ -tangle diagram, $\iota_K^*(\alpha)$. Because α is in generic position and any of its endpoints lie on $b((\frac{1}{2}, 1 - \epsilon))$, there is no overlap in this union, ensuring that this is a well-defined element in $\mathcal{S}(\tilde{M}_K, \tilde{\mathcal{N}}_K)$.

It is clear that $\mathcal{S}(\tilde{M}_K, \tilde{\mathcal{N}}_K)$ is isomorphic to $\mathcal{S}(M_K, \mathcal{N}_K)$ as stated skein algebras. Consequently, $\alpha \cdot D$ induces a left $\mathcal{S}^{pb}(\Sigma')$ -module structure on $\mathcal{S}(M_K)$, and therefore, a left $\mathcal{S}(T^2 \setminus D^2)$ -module structure.

5.3 The Unknot Module

In this section, we will attempt to compute the $\mathcal{S}(T^2 \setminus D^2)$ -module structure for $\mathcal{S}(M_K)$ when K is the unknot. However, before we discuss this, we need to clarify a detail on how we understand $T^2 \setminus D^2$. Since we typically use the “flat” interpretation of the torus when performing calculations on $T^2 \setminus D^2$, we need to be careful how this interpretation is identified with the torus with boundary to ensure that the module action is well-defined.

Figure 5.2 provides a visual aid for this identification process.

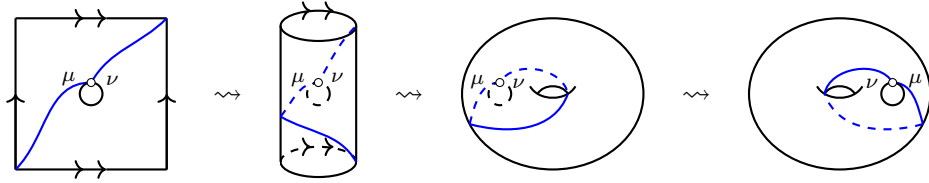


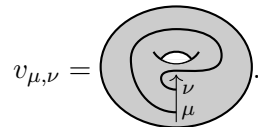
Figure 5.2: Constructing $T^2 \setminus D^2$ from a square with a disk removed.

First, identify the vertical sides and fold them towards yourself to create a cylinder (with boundary). Then, identify the top and bottom boundary circles of the cylinder to

form the torus, as shown in the third image. In figure 5.2, the boundary and marking are on the side opposite to us, so in the final step, we flip the torus over so that the boundary faces us. Note that while the marking in the first picture has an orientation pointing towards the viewer, the orientation in the final picture points away from the viewer. Specifically, the orientation points inwards, towards the inside of the torus, rather than away from the torus. This distinction is important when identifying $T^2 \setminus D^2$ with the boundary of the knot complement.

Let $K \subset S^3$ be the unknot. Then M_K is the solid torus, which is homeomorphic to the thickened annulus. Therefore, $\mathcal{S}(M_K)$ is also a \mathbb{C} -algebra and its stated skein algebra (with one marking) is isomorphic to the stated skein algebra of the once punctured monogon.

This algebra is generated by the elements $\{v_{+,+}, v_{+,-}, v_{-,+}, v_{-,-}\}$ where




There is a small subtlety in the diagram here: if the endpoints of $v_{\mu, \nu}$ were to leave the marking in opposite directions, then we would need to consider half-twists. Since we don't want to consider half-twists, we can isotope these tangles so that they always leave the marking in the same direction.

Using section 5.2, we see that

$$X_{1,0}(\mu, \nu) \cdot f = v_{\mu, \nu} f$$

$$X_{2,0}(\mu, \nu) \cdot 1_K = C_\mu^\nu 1_K$$

$$X_{3,0}(\mu, \nu) \cdot 1_K = -q^{-3} v_{\mu, \nu}$$

where 1_K is the empty link (the identity) in $\mathcal{S}(M_K)$, $f \in \mathcal{S}(M_K)$, and $C_\mu^\nu =$ .

Unlike in the Kauffman bracket case (see [5]), the action of $X_{2,0}(\mu, \nu)$ is not diagonalizable.

For example,

$$X_{2,0}(-, -) \cdot v_{+,-} = q^{-5/2}(q^2 - q^{-2})v_{-,-}$$

and so the action is more complicated.

Once again, let 1_K be the empty link diagram in $\mathcal{S}(M_K)$ and $f \in \mathcal{S}(M_K)$. Denote ∂_K as the closed curve, parallel to the boundary in M_K . Then we have

$$Y_1 \cdot f = \partial_K f$$

$$Y_2 \cdot 1_K = (-q^2 - q^{-2}) 1_K$$

$$Y_2 \cdot v_{\mu,\nu} = (-q^4 - q^{-4}) v_{\mu,\nu}$$

$$Y_3 \cdot 1_K = -q^{-3} \partial_K$$

$$\partial \cdot 1_K = (-q^2 - q^{-2}) 1_K$$

$$\partial \cdot v_{\mu,\nu} = (-q^6 - q^{-6}) v_{\mu,\nu} - (q^2 - q^{-2})^2 C_\mu^\nu \partial_K$$

It's important to note that since $\mathcal{S}(M_K)$ is only a module over $\mathcal{S}(T^2 \setminus D^2)$, this provides only a partial description of the module. Further work is needed in order to get a full description of this module structure.

5.4 A Note on the Genus Two Surface

We've discussed how skein modules of knot complements serve as modules over the torus. However, as alluded to at the beginning of this chapter, this is just a special instance of a more broader phenomenon. For any 3-manifold with boundary, M , the associated Kauffman bracket skein module, $K_q(M)$, has a natural left module structure over

the Kauffman bracket skein algebra of its boundary, $K_q(\partial M)$. This structure is induced by the homeomorphism

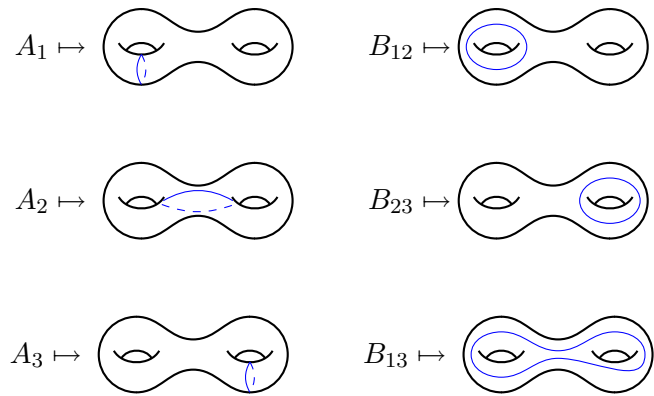
$$\partial M \times [0, 1] \bigsqcup_{\partial M \times \{0\} \sim \partial M} M \cong M.$$

When viewed as a 3-manifold, the boundary of $(T^2 \setminus D^2) \times [0, 1]$ is the genus two surface. Therefore, this suggests that $\mathcal{SH}_{q,t}$ can be made into a module over some skein module of the genus 2 surface. In [2], Arthamonov and Shakirov proposed a genus 2 generalization for the A_1 spherical DAHA, defined in terms of its action on a particular space. It turns out that the Kauffman bracket skein algebra of the genus two surface seems to correspond to this algebra.

Let $s \in \mathbb{C}^\times$ and let \mathbf{H}_2 be the genus 2 handlebody. From now on, we will denote $\Sigma_{g,n}$ as the genus g surface with n punctures and define $\Sigma_g := \Sigma_{g,0}$. Notice that $K_s(T^2 \setminus D^2) \cong K_s(\Sigma_{1,1})$ as the Kauffman bracket skein algebra is only defined with closed curves.

Definition 5.4.82. A triple, (a, b, c) , is called *admissible* if $a, b, c \geq 0$, $a + b + c$ is even, and $|a - b| \leq c \leq a + b$.

To define their algebra, Arthamonov and Shakirov use six operators, denoted $\hat{\mathcal{O}}_{B_{12}}$, $\hat{\mathcal{O}}_{B_{13}}$, $\hat{\mathcal{O}}_{B_{23}}$, $\hat{\mathcal{O}}_{A_1}$, $\hat{\mathcal{O}}_{A_2}$, and $\hat{\mathcal{O}}_{A_3}$, which correspond to the following six closed curves.



Specifically, these operators act on $\mathbb{C}[x_{12}^{\pm 1}, x_{13}^{\pm 1}, x_{23}^{\pm 1}]^{\mathbb{Z}/2\mathbb{Z}^3}$, the space of Laurent polynomials in 3 variables invariant under the $(\mathbb{Z}/2\mathbb{Z})^3$ -action that simultaneously inverts x_{12} , x_{13} , and x_{23} . Furthermore, this space has a basis given by a family of Laurent polynomials, denoted $\{\Psi_{i,j,k}\}$, where (i, j, k) are admissible triples and $\Psi_{0,0,0} = 1$.

Definition 5.4.83. Let (i, j, k) be an admissible triple and $a, b \in \{-1, 1\}$. The *Arthamonov and Shakirov coefficients* are

$$C_{a,b}(i, j, k) = ab \frac{\left[\frac{ai+bj+k}{2}, \frac{a+b+2}{2} \right]_{q,t} \left[\frac{ai+bj-k}{2}, \frac{a+b}{2} \right]_{q,t} [i-1, 2]_{q,t} [j-1, 2]_{q,t}}{\left[i, \frac{a+3}{2} \right]_{q,t} \left[i-1, \frac{a+3}{2} \right]_{q,t} \left[j, \frac{b+3}{2} \right]_{q,t} \left[j-1, \frac{b+3}{2} \right]_{q,t}}$$

where

$$[n, m]_{q,t} := \frac{q^{\frac{n}{2}} t^{\frac{m}{2}} - q^{-\frac{n}{2}} t^{-\frac{m}{2}}}{q^{\frac{1}{2}} - q^{-\frac{1}{2}}}.$$

Definition 5.4.84. The *Arthamonov-Shakirov, genus 2 spherical DAHA* is the subalgebra of the endomorphism ring of $\mathbb{C}[x_{12}^{\pm 1}, x_{13}^{\pm 1}, x_{23}^{\pm 1}]^{\mathbb{Z}/2\mathbb{Z}^3}$, generated by $\hat{\mathcal{O}}_{A_1}$, $\hat{\mathcal{O}}_{A_2}$, $\hat{\mathcal{O}}_{A_3}$, $\hat{\mathcal{O}}_{B_{12}}$, $\hat{\mathcal{O}}_{B_{13}}$, and $\hat{\mathcal{O}}_{B_{23}}$, where

$$\begin{aligned} \hat{\mathcal{O}}_{A_1} \Psi_{i,j,k} &= \left(q^{i/2} t^{1/2} + q^{-i/2} t^{-1/2} \right) \Psi_{i,j,k} \\ \hat{\mathcal{O}}_{A_2} \Psi_{i,j,k} &= \left(q^{j/2} t^{1/2} + q^{-j/2} t^{-1/2} \right) \Psi_{i,j,k} \\ \hat{\mathcal{O}}_{A_3} \Psi_{i,j,k} &= \left(q^{k/2} t^{1/2} + q^{-k/2} t^{-1/2} \right) \Psi_{i,j,k} \\ \hat{\mathcal{O}}_{B_{12}} \Psi_{i,j,k} &= \sum_{a,b \in \{-1,1\}} C_{a,b}(i, j, k) \Psi_{i+a, j+b, k} \\ \hat{\mathcal{O}}_{B_{13}} \Psi_{i,j,k} &= \sum_{a,b \in \{-1,1\}} C_{a,b}(i, k, j) \Psi_{i+a, j, k+b} \\ \hat{\mathcal{O}}_{B_{23}} \Psi_{i,j,k} &= \sum_{a,b \in \{-1,1\}} C_{a,b}(j, k, i) \Psi_{i, j+a, k+b}. \end{aligned}$$

See [2] for details.

In particular, this genus 2 spherical DAHA depends on two parameters, q and t . Using the action of $K_s(\Sigma_{1,1})$ and $K_s(\Sigma_{0,4})$ on $K_s(\mathbf{H}_2)$ and the fact that the action of the skein algebra of a closed surface on the skein module of a handlebody is faithful [Le21], Cooke and Samuelson showed the following theorem.

Theorem 5.4.85 (Corollary 5.11 in [17]). The $t = q = s^4$ specialization of the Arthamonov-Shakirov algebra is isomorphic to the skein algebra $K_s(\Sigma_2)$.

More recently, Arthamonov proved in [1] that the one-parameter deformation, the Arthamonov-Shakirov algebra, of $K_q(\Sigma_2)$ is flat.

As mentioned at the beginning of this section, there is an inclusion

$$\Sigma_2 \hookrightarrow \partial((T^2 \setminus D^2) \times [0, 1])$$

which induces a $K_q(\Sigma_2)$ -module structure for $\mathcal{SH}_{q,t} \cong K_q(T^2 \setminus D^2)$. Roughly speaking, let a be a closed curve on the genus of Σ_2 that gets glued to the boundary $(T^2 \setminus D^2) \times \{1\}$, b be a closed curve that lives on the other genus, and let α and β be the respective curves from the induced map. Then to see how these act on some $x_1x_2 \in K_q(T^2 \setminus D^2)$ we get

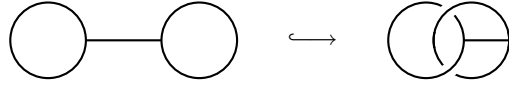
$$a \cdot (x_1x_2) = \alpha x_1x_2$$

$$b \cdot (x_1x_2) = x_1x_2\beta$$

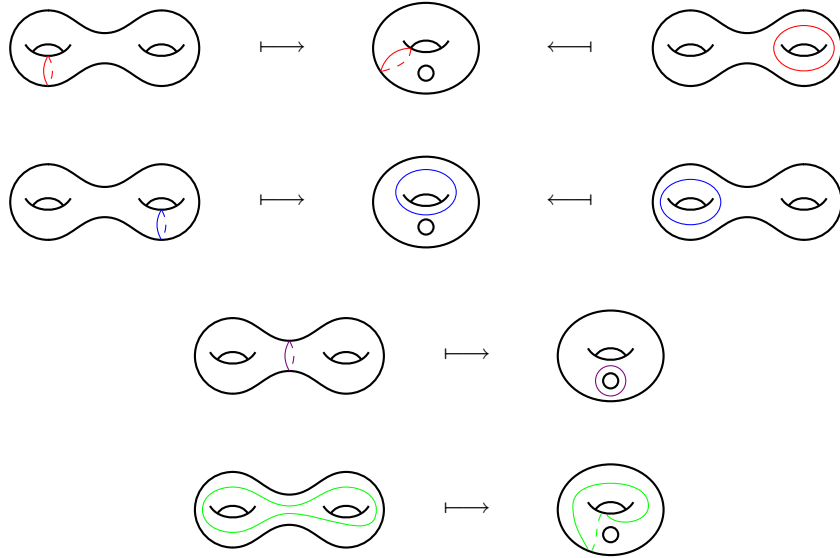
It's important to note that the algebra structure from $K_q(T^2 \setminus D^2)$ does not carry over and this is only a module. Although it respects the algebra's associativity, $a \cdot (x_1x_2) = (a \cdot x_1)x_2$, it is not true that $(a \cdot x_1)x_2 = x_1(a \cdot x_2)$.

We can construct this structure a bit more explicitly in the following way. Consider the graph defined by two loops connected by an arc and embed it into S^3 in the following

way.

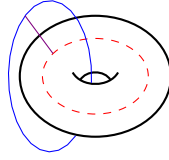


Call this embedded graph G and consider an open tubular neighborhood of G , $N(G)$. Notice that $N(G)$ is homeomorphic to the filled in genus two surface and $S^3 \setminus N(G)$ is homeomorphic to $T^2 \setminus D^2$. Therefore, the boundary of $T^2 \setminus D^2$ is Σ_2 and so $K_q(T^2 \setminus D^2)$ is a left $K_q(\Sigma_2)$ -module. However, since one of these genera corresponds to the internal boundary, $(T^2 \setminus D^2) \times \{0\}$, the action by any tangle solely living on this “inner genus” corresponds to right multiplication. This is because any curves or elements in the module $K_q(T^2 \setminus D^2)$ must lie in $(T^2 \setminus D^2) \times (0, 1)$, and therefore *above* this boundary.



You may have noticed that we have replaced B_{13} with a different curve. This change corresponds to a different set of generators, but a set of generators nonetheless.

This module structure can alternatively be understood through the following figure.



The dashed red line corresponds to the inside boundary, $(T^2 \setminus D^2) \times \{0\}$ (the “core” of our torus). The blue line will correspond to the outside boundary, $(T^2 \setminus D^2) \times \{1\}$. The purple line is the connecting arc that corresponds to the removed disk.

We can factor through the module structure as follows. Take the disjoint union of two tori with boundary and embed them into the genus two surface. Then, embed the genus two surface into the boundary of $T^2 \setminus D^2$. These embeddings induce maps on corresponding Kauffman brackets skein algebras.

$$\begin{array}{c}
 \text{Diagram: } \text{torus} \sqcup \text{torus} \hookrightarrow \text{genus 2 surface} \hookrightarrow \partial \left(\text{torus} \times I \right) \\
 \mathcal{S}(T^2 \setminus D^2) \otimes \mathcal{S}(T^2 \setminus D^2) \longrightarrow \mathcal{S}(\Sigma_2) \longrightarrow \mathcal{S}(T^2 \setminus D^2)
 \end{array}$$

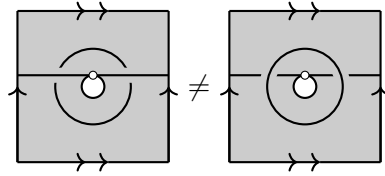
Let $\alpha, \beta, \gamma \in K_q(T^2 \setminus D^2)$. If we view α and β as each lying on a genus of Σ_2 , then we have the left action

$$(\alpha \otimes \beta) \cdot \gamma = \alpha \gamma \beta.$$

Let δ be the loop around the boundary. It is central in $K_q(T^2 \setminus D^2)$ and it’s left module action on $K_q(T^2 \setminus D^2)$ (when viewed on Σ_2) can be viewed as left or right multiplication in $K_q(T^2 \setminus D^2)$.

If we attempt to extend this action of $K_q(\Sigma_2)$ to $\mathcal{S}(T^2 \setminus D^2)$, we quickly run into a problem. By the same logic, the underlying topological structure suggests that the action

of δ should correspond to multiplication by a central element. However, this is clearly not the case as δ is no longer central in $\mathcal{S}(T^2 \setminus D^2)$.



Therefore, any module structure here would need to be extended in a different way. One possible remedy could be to introduce a boundary component to Σ_2 , and shifting our focus to $\mathcal{S}(\Sigma_2 \setminus D^2)$ instead. However, there is currently no reason to believe that this corresponds to a double affine Hecke algebra.

Bibliography

- [1] Semeon Arthamonov. Classical limit of genus two daha, 2023.
- [2] Semeon Arthamonov and Shamil Shakirov. Genus two generalization of A_1 spherical DAHA. *Selecta Math. (N.S.)*, 25(2):Paper No. 17, 29, 2019.
- [3] John W. Barrett. Skein spaces and spin structures. *Math. Proc. Cambridge Philos. Soc.*, 126(2):267–275, 1999.
- [4] David Ben-Zvi, Adrien Brochier, and David Jordan. Integrating quantum groups over surfaces. *J. Topol.*, 11(4):874–917, 2018.
- [5] Yuri Berest and Peter Samuelson. Double affine Hecke algebras and generalized Jones polynomials. *Compos. Math.*, 152(7):1333–1384, 2016.
- [6] Joan S. Birman and Caroline Series. An algorithm for simple curves on surfaces. *Journal of the London Mathematical Society*, s2-29(2):331–342, 1984.
- [7] Wade Bloomquist and Thang T. Q. Lê. The Chebyshev-Frobenius homomorphism for stated skein modules of 3-manifolds. *Math. Z.*, 301(1):1063–1105, 2022.
- [8] Francis Bonahon and Helen Wong. Quantum traces for representations of surface groups in $SL_2(\mathbb{C})$. *Geom. Topol.*, 15(3):1569–1615, 2011.
- [9] Adrien Brochier and David Jordan. Fourier transform for quantum D -modules via the punctured torus mapping class group. *Quantum Topol.*, 8(2):361–379, 2017.
- [10] Doug Bullock. Rings of $SL_2(\mathbb{C})$ -characters and the Kauffman bracket skein module. *Comment. Math. Helv.*, 72(4):521–542, 1997.
- [11] Vyjayanthi Chari and Andrew Pressley. *A guide to quantum groups*. Cambridge University Press, Cambridge, 1994.
- [12] Bang-Yen Chen. Geometry and topology of maximal antipodal sets and related topics. *Rom. J. Math. Comput. Sci.*, 13(2):6–25, 2023.
- [13] Ivan Cherednik. Double affine Hecke algebras and Macdonald’s conjectures. *Ann. of Math. (2)*, 141(1):191–216, 1995.

- [14] Ivan Cherednik. *Double affine Hecke algebras*, volume 319 of *London Mathematical Society Lecture Note Series*. Cambridge University Press, Cambridge, 2005.
- [15] Marshall Cohen, Wolfgang Metzler, and Albert Zimmermann. What does a basis of $f(a, b)$ look like? *Mathematische Annalen*, 257(4):435–445, 1981.
- [16] Juliet Cooke. Excision of skein categories and factorisation homology. *Adv. Math.*, 414:Paper No. 108848, 51, 2023.
- [17] Juliet Cooke and Peter Samuelson. On the genus two skein algebra. *J. Lond. Math. Soc. (2)*, 104(5):2260–2298, 2021.
- [18] Benjamin Cooper and Peter Samuelson. The Hall algebras of surfaces I. *J. Inst. Math. Jussieu*, 19(3):971–1028, 2020.
- [19] Francesco Costantino and Thang T. Q. Lê. Stated skein algebras of surfaces. *Journal of the European Mathematical Society*, 2022.
- [20] Freeman J. Dyson. Statistical Theory of the Energy Levels of Complex Systems. I. *Journal of Mathematical Physics*, 3(1):140–156, 01 1962.
- [21] Pavel Etingof, Shlomo Gelaki, Dmitri Nikshych, and Victor Ostrik. *Tensor categories*, volume 205 of *Mathematical Surveys and Monographs*. American Mathematical Society, Providence, RI, 2015.
- [22] Matthieu Faitg. Holonomy and (stated) skein algebras in combinatorial quantization, 2022.
- [23] Benson Farb and Dan Margalit. *A primer on mapping class groups*, volume 49 of *Princeton Mathematical Series*. Princeton University Press, Princeton, NJ, 2012.
- [24] Igor B. Frenkel and Mikhail G. Khovanov. Canonical bases in tensor products and graphical calculus for $U_q(\mathfrak{sl}_2)$. *Duke Math. J.*, 87(3):409–480, 1997.
- [25] Igor B. Frenkel and Hyun Kyu Kim. Quantum Teichmüller space from the quantum plane. *Duke Math. J.*, 161(2):305–366, 2012.
- [26] Charles Frohman and Răzvan Gelca. Skein modules and the noncommutative torus. *Trans. Amer. Math. Soc.*, 352(10):4877–4888, 2000.
- [27] Răzvan Gelca and Jeremy Sain. The noncommutative A-ideal of a $(2, 2p + 1)$ -torus knot determines its Jones polynomial. *J. Knot Theory Ramifications*, 12(2):187–201, 2003.
- [28] Cameron McA. Gordon and John Luecke. Knots are determined by their complements. *Bull. Amer. Math. Soc. (N.S.)*, 20(1):83–87, 1989.
- [29] Sergei Gukov, Peter Koroteev, Satoshi Nawata, Du Pei, and Ingmar Saberi. *Branes and DAHA representations*, volume 48 of *SpringerBriefs in Mathematical Physics*. Springer, Cham, 2023.

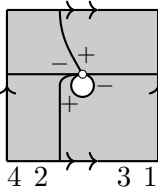
- [30] Sam Gunningham, David Jordan, and Pavel Safronov. The finiteness conjecture for skein modules. *Invent. Math.*, 232(1):301–363, 2023.
- [31] Benjamin Haioun. Relating stated skein algebras and internal skein algebras. *SIGMA Symmetry Integrability Geom. Methods Appl.*, 18:Paper No. 042, 39, 2022.
- [32] Jens Carsten Jantzen. *Lectures on quantum groups*, volume 6 of *Graduate Studies in Mathematics*. American Mathematical Society, Providence, RI, 1996.
- [33] Michio Jimbo. A q -analogue of $U(\mathfrak{gl}(N + 1))$, Hecke algebra, and the Yang-Baxter equation. *Lett. Math. Phys.*, 11(3):247–252, 1986.
- [34] Christian Kassel. *Quantum groups*, volume 155 of *Graduate Texts in Mathematics*. Springer-Verlag, New York, 1995.
- [35] Robion Kirby and Paul Melvin. The 3-manifold invariants of Witten and Reshetikhin-Turaev for $\mathfrak{sl}(2, \mathbf{C})$. *Invent. Math.*, 105(3):473–545, 1991.
- [36] Julien Korinman. Finite presentations for stated skein algebras and lattice gauge field theory. *Algebr. Geom. Topol.*, 23(3):1249–1302, 2023.
- [37] Greg Kuperberg. Spiders for rank 2 Lie algebras. *Comm. Math. Phys.*, 180(1):109–151, 1996.
- [38] Thang T. Q. Lê. Triangular decomposition of skein algebras. *Quantum Topol.*, 9(3):591–632, 2018.
- [39] Thang T. Q. Lê. Quantum Teichmüller spaces and quantum trace map. *J. Inst. Math. Jussieu*, 18(2):249–291, 2019.
- [40] Thang T. Q. Lê and Adam S. Sikora. Stated $\mathrm{SL}(n)$ -skein modules and algebras, 2024.
- [41] Thang T. Q. Lê and Tao Yu. Stated skein modules of marked 3-manifolds/surfaces, a survey. *Acta Math. Vietnam.*, 46(2):265–287, 2021.
- [42] Thang T. Q. Lê and Tao Yu. Quantum traces and embeddings of stated skein algebras into quantum tori. *Selecta Math. (N.S.)*, 28(4):Paper No. 66, 48, 2022.
- [43] Ian G. Macdonald. Some conjectures for root systems. *SIAM J. Math. Anal.*, 13(6):988–1007, 1982.
- [44] Shahn Majid. *Foundations of quantum group theory*. Cambridge University Press, Cambridge, 1995.
- [45] John C. McConnell and J. J. Pettit. Crossed products and multiplicative analogues of Weyl algebras. *J. London Math. Soc. (2)*, 38(1):47–55, 1988.
- [46] Hugh R. Morton and Peter Samuelson. DAHAs and skein theory. *Comm. Math. Phys.*, 385(3):1655–1693, 2021.

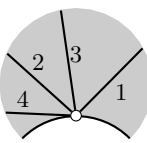
- [47] Greg Muller. Skein and cluster algebras of marked surfaces. *Quantum Topol.*, 7(3):435–503, 2016.
- [48] Alexei Oblomkov. Double affine Hecke algebras of rank 1 and affine cubic surfaces. *Int. Math. Res. Not.*, 2004(18):877–912, 2004.
- [49] Alexander T. Pokorny. *Dubrovnik Skein Theory and Power Sum Elements*. ProQuest LLC, Ann Arbor, MI, 2021. Thesis (Ph.D.)—University of California, Riverside.
- [50] Józef H. Przytycki. Skein modules of 3-manifolds. *Bull. Polish Acad. Sci. Math.*, 39(1-2):91–100, 1991.
- [51] Józef H. Przytycki and Adam S. Sikora. On skein algebras and $SL_2(\mathbb{C})$ -character varieties. *Topology*, 39(1):115–148, 2000.
- [52] Nicolai Y. Reshetikhin and Vladimir G. Turaev. Ribbon graphs and their invariants derived from quantum groups. *Comm. Math. Phys.*, 127(1):1–26, 1990.
- [53] Roger W. Richardson. Commuting varieties of semisimple Lie algebras and algebraic groups. *Compositio Math.*, 38(3):311–327, 1979.
- [54] Peter Samuelson. Iterated torus knots and double affine Hecke algebras. *Int. Math. Res. Not. IMRN*, 2019(9):2848–2893, 2017.
- [55] Ramanujan Santharoubane. Algebraic generators of the skein algebra of a surface. 2018.
- [56] Nikolai Saveliev. *Lectures on the topology of 3-manifolds*. De Gruyter Textbook. Walter de Gruyter & Co., Berlin, revised edition, 2012. An introduction to the Casson invariant.
- [57] Adam S. Sikora. Character varieties of abelian groups. *Math. Z.*, 277(1-2):241–256, 2014.
- [58] Michael Thaddeus. Mirror symmetry, Langlands duality, and commuting elements of Lie groups. *Internat. Math. Res. Notices*, 2001(22):1169–1193, 2001.
- [59] Vladimir G. Turaev. The Conway and Kauffman modules of a solid torus. *Zap. Nauchn. Sem. Leningrad. Otdel. Mat. Inst. Steklov. (LOMI)*, 167:79–89, 190, 1988.
- [60] Vladimir G. Turaev. *Quantum invariants of knots and 3-manifolds*, volume 18 of *De Gruyter Studies in Mathematics*. Walter de Gruyter & Co., Berlin, revised edition, 2010.
- [61] Friedhelm Waldhausen. On irreducible 3-manifolds which are sufficiently large. *The Annals of Mathematics*, 87(1):56, January 1968.
- [62] Zhihao Wang. Stated sl_n -skein modules, roots of unity, and tqft, 2024.

Appendix A

Diagrammatic Calculations

Throughout all of these calculation, we use positive integers placed at the bottom of the diagrams to indicate the relative height ordering of the tangle endpoints, where larger values correspond to lower heights. For each diagram, starting from the leftmost endpoint moving clockwise with respect to our marked point, we assign these integers to the endpoints. The integers are read from left to right at the bottom, corresponding to this

clockwise order. For example, $X_{1,0}(-, -)X_{2,0}(+, +) =$

 $$ where our heights cor-

respond to
 
 . We will also use our previous notation of $\tilde{X}_{3,0}(\mu, \nu)$ corresponding to the the $(1, -1)$ -tangle with 0 twists and \tilde{Y}_3 corresponding to the $(1, -1)$ -curve.

A.1 Commuting Relation for $X_{1,0}(-, -)$ and $X_{2,0}(+, +)$

$$\begin{aligned}
X_{1,0}(-, -)X_{2,0}(+, +) &= \begin{array}{c} \text{Diagram 1} \\ \text{Diagram 2} \end{array} = q \begin{array}{c} \text{Diagram 3} \\ \text{Diagram 4} \end{array} \\
&= q^4 \begin{array}{c} \text{Diagram 5} \\ \text{Diagram 6} \end{array} - q^{5/2}(q^2 - q^{-2})\tilde{X}_{3,0}(+, -) \\
&= q^7 \begin{array}{c} \text{Diagram 7} \\ \text{Diagram 8} \end{array} - q^{11/2}(q^2 - q^{-2}) \begin{array}{c} \text{Diagram 9} \\ \text{Diagram 10} \end{array} - q^{5/2}(q^2 - q^{-2})\tilde{X}_{3,0}(+, -) \\
&= q^{10}X_{2,0}(+, +)X_{1,0}(-, -) - q^{17/2}(q^2 - q^{-2}) \begin{array}{c} \text{Diagram 11} \\ \text{Diagram 12} \end{array} - q^{11/2}(q^2 - q^{-2}) \begin{array}{c} \text{Diagram 13} \\ \text{Diagram 14} \end{array} \\
&\quad - q^{5/2}(q^2 - q^{-2})\tilde{X}_{3,0}(+, -) \\
&= q^{10}X_{2,0}(+, +)X_{1,0}(-, -) - q^{17/2}(q^2 - q^{-2}) \left(q^{3/2}\tilde{Y}_{3,0} + \tilde{X}_{3,-\frac{1}{2}}(-, +) + q^2X_{3,0}(-, +) \right) \\
&\quad - q^{11/2}(q^2 - q^{-2}) \left(q^{-3}\tilde{X}_{3,-\frac{1}{2}}(+, -) + q^{-3/2}\tilde{Y}_{3,0} \right) - q^{5/2}(q^2 - q^{-2})\tilde{X}_{3,0}(+, -) \\
&= q^{10}X_{2,0}(+, +)X_{1,0}(-, -) - q^7(q^2 - q^{-2})(q^3 + q^{-3})\tilde{Y}_{3,0} - q^{5/2}(q^2 - q^{-2})\tilde{X}_{3,0}(+, -) \\
&\quad - (q^2 - q^{-2}) \left(q^{17/2}\tilde{X}_{3,-\frac{1}{2}}(-, +) + q^{21/2}X_{3,0}(-, +) + q^{5/2}\tilde{X}_{3,-\frac{1}{2}}(+, -) \right) \\
&= q^{10}X_{2,0}(+, +)X_{1,0}(-, -) - q^{21/2}(q^2 - q^{-2})X_{3,0}(-, +) - q^{5/2}(q^2 - q^{-2})\tilde{X}_{3,0}(+, -) \\
&\quad - q^{11/2}(q^2 - q^{-2}) \left(q^3\tilde{X}_{3,-\frac{1}{2}}(-, +) + q^{-3}\tilde{X}_{3,-\frac{1}{2}}(+, -) \right) - q^7(q^2 - q^{-2})(q^3 + q^{-3})\tilde{Y}_{3,0} \\
&= q^{10}X_{2,0}(+, +)X_{1,0}(-, -) - q^{13/2}(q^2 - q^{-2}) \left(q^4X_{3,0}(-, +) + q^{-4}\tilde{X}_{3,0}(+, -) \right) \\
&\quad - q^{11/2}(q^2 - q^{-2}) \left(q^3\tilde{X}_{3,-\frac{1}{2}}(-, +) + q^{-3}\tilde{X}_{3,-\frac{1}{2}}(+, -) \right) - q^7(q^2 - q^{-2})(q^3 + q^{-3})\tilde{Y}_{3,0}
\end{aligned}$$

A.2 Image of $\varphi_{\mathcal{E}}$

Following the calculations of $\varphi_{\mathcal{E}}(y_1)$, we can similarly determine the images of other tangles as well. In particular, we left-multiply each diagram, α , by the image of an appropriate monomial from \mathbb{T}_+^6 under $\psi_{\mathcal{E}}$, ensuring that the resulting product is expressed solely in terms of the images of elements from \mathbb{T}_+^6 . Since the composition of injections yields the identity map on \mathbb{T}_+^6 , we then left-multiply by the inverse monomial in T^6 to explicitly find $\varphi_{\mathcal{E}}(\alpha)$. Unless stated otherwise, every tangle is assumed to have positive states.

A.2.1 Longitude

$$\begin{aligned}
 \psi_{\mathcal{E}}(x_1 x_3) y_2 &= q^{-1} \left(\begin{array}{c} \text{Diagram 1} \\ \text{Diagram 2} \\ \text{Diagram 3} \end{array} \right) \\
 &= q^{-1} \left(\begin{array}{c} \text{Diagram 4} \\ \text{Diagram 5} \end{array} \right) \\
 &= q^{-1} \left(\begin{array}{c} \text{Diagram 6} \\ \left(q \begin{array}{c} \text{Diagram 7} \\ \text{Diagram 8} \end{array} + q^{-1} \begin{array}{c} \text{Diagram 9} \end{array} \right) \end{array} \right) \\
 &= q^{-1} \left(\begin{array}{c} q \begin{array}{c} \text{Diagram 10} \\ \text{Diagram 11} \end{array} + q^{-1} \begin{array}{c} \text{Diagram 12} \end{array} \end{array} \right)
 \end{aligned}$$

The diagrams are tangles with four strands and a central circle. The strands are labeled with numbers 1, 2, 3, 4 at the bottom. Diagram 1: Strands 1, 2, 3, 4 from left to right. Diagram 2: Strands 1, 2, 3, 4 from left to right. Diagram 3: Strands 1, 2, 3, 4 from left to right. Diagram 4: Strands 1, 2, 3, 4 from left to right. Diagram 5: Strands 1, 2, 3, 4 from left to right. Diagram 6: Strands 1, 2, 3, 4 from left to right. Diagram 7: Strands 1, 2, 3, 4 from left to right. Diagram 8: Strands 1, 2, 3, 4 from left to right. Diagram 9: Strands 1, 2, 3, 4 from left to right. Diagram 10: Strands 1, 2, 3, 4 from left to right. Diagram 11: Strands 1, 2, 3, 4 from left to right. Diagram 12: Strands 1, 2, 3, 4 from left to right.

$$\begin{aligned}
&= q^{-1} \left(\begin{array}{c} \text{Diagram 1} \\ \text{Diagram 2} \\ \text{Diagram 3} \end{array} \right) \\
&= q^{-1} \left(\begin{array}{c} \text{Diagram 1} \\ \text{Diagram 2} \\ \text{Diagram 3} \end{array} \right) \\
&\Rightarrow \varphi_{\mathcal{E}}(y_2) = (x_1 x_3)^{-1} (x_1 x_3) \varphi_{\mathcal{E}}(y_2) = (x_1 x_3)^{-1} \varphi_{\mathcal{E}}(\psi_{\mathcal{E}}(x_1 x_3) y_2) \\
&= q^3 x_3^{-1} x_1^{-1} x_3^2 + q^{-1} x_3^{-1} x_1^{-1} x_4 x_2 + q^{-1} x_3^{-1} x_1^{-1} x_1^2 \\
&= q x_1 x_3^{-1} + q x_1^{-1} x_3 + q^{-1} x_1^{-1} x_2 x_3^{-1} x_4.
\end{aligned}$$

A.2.2 (1, 1)-Curve

$$\begin{aligned}
\psi_{\mathcal{E}}(x_4 x_2 x_1) y_3 &= \left(\begin{array}{c} \text{Diagram 1} \\ \text{Diagram 2} \\ \text{Diagram 3} \end{array} \right) \text{Diagram 4} \\
&= \left(\begin{array}{c} \text{Diagram 1} \\ \text{Diagram 2} \end{array} \right) \text{Diagram 3}
\end{aligned}$$

$$\begin{aligned}
&= \left(\begin{array}{c} \text{Diagram 1} \\ \text{Diagram 2} \end{array} \right) \left(\begin{array}{c} \text{Diagram 3} + \text{Diagram 4} \\ \text{Diagram 5} \end{array} \right) \\
&= \left(\begin{array}{c} \text{Diagram 6} \\ \text{Diagram 7} \end{array} \right) \left(\begin{array}{c} \text{Diagram 8} + \text{Diagram 9} \\ \text{Diagram 10} \end{array} \right) \\
&= \left(\begin{array}{c} \text{Diagram 11} \\ \text{Diagram 12} \end{array} \right) \left(\begin{array}{c} \text{Diagram 13} + \text{Diagram 14} + \text{Diagram 15} \\ \text{Diagram 16} \end{array} \right) \\
&= q^{-3/2} \left(\begin{array}{c} \text{Diagram 17} + \text{Diagram 18} + \text{Diagram 19} \\ \text{Diagram 20} \end{array} \right) \\
&= q^{-3/2} \left(\begin{array}{c} \text{Diagram 21} + \text{Diagram 22} + \text{Diagram 23} + \text{Diagram 24} \\ \text{Diagram 25} \end{array} \right) \\
&= q^{-3/2} \left(\begin{array}{c} \text{Diagram 26} + \text{Diagram 27} + \text{Diagram 28} + \text{Diagram 29} \\ \text{Diagram 30} \end{array} \right)
\end{aligned}$$

$$\Rightarrow \varphi_{\mathcal{E}}(y_3) = (x_4 x_2 x_1)^{-1} (x_4 x_2 x_1) \varphi_{\mathcal{E}}(y_3) = (x_4 x_2 x_1)^{-1} \varphi_{\mathcal{E}}(\psi_{\mathcal{E}}(x_4 x_2 x_1) y_3)$$

$$= q^7 x_1^{-1} x_2^{-1} x_4^{-1} x_2 x_1^2 + q^2 x_1^{-1} x_2^{-1} x_4^{-1} x_5 x_1 x_3 + q^{-1} x_1^{-1} x_2^{-1} x_3^2 + q^{-1} x_1^{-1} x_4$$

$$= q^{-1} x_1 x_4^{-1} + q^{-1} x_1^{-1} x_4 + q^{-1} x_1^{-1} x_2^{-1} x_3^2 + x_2^{-1} x_3 x_4^{-1} x_5.$$

A.2.3 $(1, -1)$ -Tangle

$$\begin{aligned}
 \psi_{\mathcal{E}}(x_3) &= q^{-1/2} \left(\text{Diagram 1} \right) \\
 &= q^{1/2} \left(\text{Diagram 2} \right) + q^{-3/2} \left(\text{Diagram 3} \right) \\
 &= q^{3/2} \left(\text{Diagram 4} \right) + q^{-5/2} \left(\text{Diagram 5} \right)
 \end{aligned}$$

$$\begin{aligned}
 \Rightarrow \varphi_{\mathcal{E}}(\alpha) &= x_3^{-1} x_3 \varphi_{\mathcal{E}}(\alpha) = x_3^{-1} \varphi_{\mathcal{E}}(\psi_{\mathcal{E}}(x_3)\alpha) \\
 &= q^{5/2} x_3^{-1} x_2 x_4 + q^{-3/2} x_3^{-1} x_1^2 \\
 &= q^{1/2} x_2 x_3^{-1} x_4 + q^{5/2} x_1^2 x_3^{-1}
 \end{aligned}$$

A.2.4 $X_{1, \frac{1}{2}}(+, +)$

$$\begin{aligned}
 \psi_{\mathcal{E}}(x_2 x_3) &= q^{-1} \left(\text{Diagram 1} \right) \left(\text{Diagram 2} \right) \left(\text{Diagram 3} \right) \\
 &= q^{-1} \left(\text{Diagram 4} \right) \left(\text{Diagram 5} \right)
 \end{aligned}$$

$$\begin{aligned}
&= q^{-1} \left(\begin{array}{c} \text{Diagram 1} \\ 2 \ 1 \end{array} \right) \left(\begin{array}{c} \text{Diagram 2} \\ 2 \ 1 \ 4 \ 3 \end{array} + q^{-1} \begin{array}{c} \text{Diagram 3} \\ 2 \ 1 \ 4 \ 3 \end{array} \right) \\
&= \begin{array}{c} \text{Diagram 4} \\ 4 \ 2 \ 1 \ 3 \ 6 \ 5 \end{array} + q^{-2} \begin{array}{c} \text{Diagram 5} \\ 2 \ 4 \ 1 \ 3 \ 6 \ 5 \end{array} \\
&= \begin{array}{c} \text{Diagram 6} \\ 4 \ 2 \ 1 \ 3 \ 6 \ 5 \end{array} + q^{-1} \begin{array}{c} \text{Diagram 7} \\ 2 \ 4 \ 1 \ 3 \ 6 \ 5 \end{array} + q^{-3} \begin{array}{c} \text{Diagram 8} \\ 2 \ 4 \ 1 \ 3 \ 6 \ 5 \end{array} \\
&= q^{-2} \begin{array}{c} \text{Diagram 9} \\ 6 \ 2 \ 1 \ 4 \ 3 \ 5 \end{array} + q^{-6} \begin{array}{c} \text{Diagram 10} \\ 6 \ 4 \ 2 \ 1 \ 3 \ 5 \end{array} + q^{-7} \begin{array}{c} \text{Diagram 11} \\ 4 \ 2 \ 6 \ 3 \ 1 \ 5 \end{array}
\end{aligned}$$

$$\begin{aligned}
\Rightarrow \varphi_{\mathcal{E}}(X_{1, \frac{1}{2}}) &= (x_2 x_3)^{-1} (x_2 x_3) \varphi_{\mathcal{E}} \left(X_{1, \frac{1}{2}} \right) \\
&= (x_2 x_3)^{-1} \varphi_{\mathcal{E}} \left(\psi_{\mathcal{E}}(x_2 x_3) X_{1, \frac{1}{2}} \right) \\
&= x_3^{-1} x_2^{-1} \varphi_{\mathcal{E}} \left(q^{-2} x_2 x_4 x_5 + q^{-6} x_1^2 x_5 + q^{-7} x_1 x_3 x_4 \right) \\
&= q^{-1/2} x_3^{-1} x_4 x_5 + q^{11/2} x_1^2 x_2^{-1} x_3^{-1} x_5 + q^{1/2} x_1 x_2^{-1} x_4.
\end{aligned}$$

A.2.5 $X_{3, \frac{1}{2}}(+, +)$

$$\begin{aligned}
 \psi_{\mathcal{E}}(x_2) &= q^{-1/2} \left(\text{Diagram 1} + \text{Diagram 2} \right) \\
 &= q^{1/2} \left(\text{Diagram 3} \right) + q^{-3/2} \left(\text{Diagram 4} \right) \\
 &= q^{-3/2} \left(\text{Diagram 5} \right) + q^{-5/2} \left(\text{Diagram 6} \right)
 \end{aligned}$$

$$\begin{aligned}
 \Rightarrow x_2^{-1} x_2 \varphi_{\mathcal{E}} \left(X_{3, \frac{1}{2}} \right) &= x_2^{-1} \varphi_{\mathcal{E}} \left(\psi_{\mathcal{E}}(x_2) X_{3, \frac{1}{2}} \right) \\
 &= x_2^{-1} \varphi_{\mathcal{E}} \left(q^{-3/2} x_1 x_5 + q^{-5/2} x_3 x_4 \right) \\
 &= x_2^{-1} \left(q^{-1/2} x_1 x_5 + q^{-3/2} x_3 x_4 \right) \\
 &= q^{3/2} x_1 x_2^{-1} x_5 + q^{-3/2} x_2^{-1} x_3 x_4.
 \end{aligned}$$

A.2.6 $X_{1,1}(+, +)$

$$\begin{aligned}
 \psi_{\mathcal{E}}(x_1x_4) &= q^{-1} \left(\begin{array}{c} \text{Diagram 1} \\ \text{Diagram 2} \end{array} \right) \\
 &= q^{-1} \left(\begin{array}{c} \text{Diagram 3} \\ \left(q \begin{array}{c} \text{Diagram 4} \\ \text{Diagram 5} \end{array} + q^{-1} \begin{array}{c} \text{Diagram 6} \\ \text{Diagram 7} \end{array} \right) \end{array} \right) \\
 &= \begin{array}{c} \text{Diagram 8} \\ \text{Diagram 9} \end{array} + q^{-2} \begin{array}{c} \text{Diagram 10} \\ \text{Diagram 11} \end{array} \\
 &= q \begin{array}{c} \text{Diagram 12} \\ \text{Diagram 13} \end{array} + q^{-1} \begin{array}{c} \text{Diagram 14} \\ \text{Diagram 15} \end{array} + q^{-1} \begin{array}{c} \text{Diagram 16} \\ \text{Diagram 17} \end{array} + q^{-3} \begin{array}{c} \text{Diagram 18} \\ \text{Diagram 19} \end{array} \\
 &= q^{-3} \begin{array}{c} \text{Diagram 20} \\ \text{Diagram 21} \end{array} + q^{-6} \begin{array}{c} \text{Diagram 22} \\ \text{Diagram 23} \end{array} + q^{-8} \begin{array}{c} \text{Diagram 24} \\ \text{Diagram 25} \end{array} + q^{-7} \begin{array}{c} \text{Diagram 26} \\ \text{Diagram 27} \end{array}
 \end{aligned}$$

$$\Rightarrow \varphi_{\mathcal{E}}(X_{1,1}(+, +)) = x_4^{-1}x_1^{-1}\varphi_{\mathcal{E}}(\psi_{\mathcal{E}}(x_1x_4)X_{1,1})$$

$$= q^{-3/2}x_4^{-1}x_1^{-1}x_4x_5^2 + q^{-11/2}x_4^{-1}x_1^{-1}x_5\varphi_{\mathcal{E}} \left(\begin{array}{c} \text{Diagram 28} \\ \text{Diagram 29} \end{array} \right) \varphi_{\mathcal{E}} \left(\begin{array}{c} \text{Diagram 30} \\ \text{Diagram 31} \end{array} \right)$$

$$\begin{aligned}
& + q^{-15/2} x_4^{-1} x_1^{-1} x_5 \varphi \mathcal{E} \left(\begin{array}{c} \text{Diagram 1} \\ \left(\begin{array}{c} \text{Square with boundary arrows} \\ \text{Internal paths and a circle} \\ \text{Labels } 2 \text{ and } 1 \text{ at bottom} \end{array} \right) \end{array} \right) \varphi \mathcal{E} \left(\begin{array}{c} \text{Diagram 2} \\ \left(\begin{array}{c} \text{Square with boundary arrows} \\ \text{Internal paths and a circle} \\ \text{Labels } 2 \text{ and } 1 \text{ at bottom} \end{array} \right) \end{array} \right) \\
& + q^{-13/2} x_4^{-1} x_1^{-1} x_4 \varphi \mathcal{E} \left(\begin{array}{c} \text{Diagram 3} \\ \left(\begin{array}{c} \text{Square with boundary arrows} \\ \text{Internal paths and a circle} \\ \text{Labels } 2 \text{ and } 1 \text{ at bottom} \end{array} \right) \end{array} \right)^2
\end{aligned}$$

$$= q^{1/2} x_1^{-1} x_5^2$$

$$+ q^{-7/2} x_1^{-1} x_4^{-1} x_5 (q^{-1/2} x_3^{-1} x_4 x_5 + q^{11/2} x_1^2 x_2^{-1} x_3^{-1} x_5 + q^{1/2} x_1 x_2^{-1} x_4) (q^{1/2} x_2 x_3^{-1} x_4 + q^{5/2} x_1^2 x_3^{-1})$$

$$+ q^{-11/2} x_1^{-1} x_4^{-1} x_5 (q^{-1/2} x_3^{-1} x_4 x_5 + q^{11/2} x_1^2 x_2^{-1} x_3^{-1} x_5 + q^{1/2} x_1 x_2^{-1} x_4) (q^{3/2} x_1 x_2^{-1} x_5 + q^{-3/2} x_2^{-1} x_3 x_4)$$

$$+ q^{-9/2} x_1^{-1} (q^{-1/2} x_3^{-1} x_4 x_5 + q^{11/2} x_1^2 x_2^{-1} x_3^{-1} x_5 + q^{1/2} x_1 x_2^{-1} x_4)^2$$

$$= q^{1/2} x_1^{-1} x_5^2 + q^{-7/2} x_1^{-1} x_4^{-1} x_5 (x_2 x_3^{-2} x_4^2 x_5 + q^8 x_1^2 x_3^{-2} x_4 x_5 + q^4 x_1^2 x_3^{-2} x_4 x_5 + q^{16}$$

$$x_1^4 x_2^{-1} x_3^{-2} x_5 + q^3 x_1 x_3^{-1} x_4^2 + q^9 x_1^3 x_2^{-1} x_3^{-1} x_4) + q^{-11/2} x_1^{-1} x_4^{-1} x_5 (q^3 x_1 x_2^{-1} x_3^{-1} x_4 x_5^2 + q^{-2} x_2^{-1} x_4^2 x_5$$

$$+ q^{13} x_1^3 x_2^{-2} x_3^{-1} x_5^2 + q^6 x_1^2 x_2^{-2} x_4 x_5 + q^2 x_1^2 x_2^{-2} x_4 x_5 + q^{-3} x_1 x_2^{-2} x_3 x_4^2)$$

$$+ q^{-9/2} x_1^{-1} (q^{-3} x_3^{-2} x_4^2 x_5^2 + q^9 x_1^2 x_2^{-1} x_3^{-2} x_4 x_5^2 + q^2 x_1 x_2^{-1} x_3^{-1} x_4^2 x_5 + q^5 x_1^2 x_2^{-1} x_3^{-2} x_4 x_5^2$$

$$+ q^{21} x_1^4 x_2^{-2} x_3^{-2} x_5^2 + q^{12} x_1^3 x_2^{-2} x_3^{-1} x_4 x_5 + q^{-2} x_1 x_2^{-1} x_3^{-1} x_4^2 x_5 + q^8 x_1^3 x_2^{-2} x_3^{-1} x_4 x_5 + q x_1^2 x_2^{-2} x_4^2)$$

$$\begin{aligned}
&= q^{1/2}x_1^{-1}x_5^2 + q^{-7/2}x_1^{-1}x_2x_3^{-2}x_4x_5^2 + (q^{9/2} + q^{1/2})x_1x_3^{-2}x_5^2 + q^{25/2}x_1^3x_2^{-1}x_3^{-2}x_4^{-1}x_5^2 \\
&+ q^{-1/2}x_3^{-1}x_4x_5 + q^{11/2}x_1^2x_2^{-1}x_3^{-1}x_5 + q^{3/2}x_2^{-1}x_3^{-1}x_5^3 + q^{-7/2}x_1^{-1}x_2^{-1}x_4x_5^2 + q^{23/2}x_1^2x_2^{-2}x_3^{-1}x_4^{-1}x_5^3 \\
&+ (q^{1/2} + q^{-7/2})x_1x_2^{-2}x_5^2 + q^{-9/2}x_2^{-2}x_3x_4x_5 + q^{-15/2}x_1^{-1}x_3^{-2}x_4^2x_5^2 + (q^{9/2} + q^{1/2})x_1x_2^{-1}x_3^{-2}x_4x_5^2 \\
&+ (q^{-5/2} + q^{-13/2})x_2^{-1}x_3^{-1}x_4^2x_5 + q^{33/2}x_1^3x_2^{-2}x_3^{-2}x_5^2 + (q^{15/2} + q^{7/2})x_1^2x_2^{-2}x_3^{-1}x_4x_5 + q^{-3/2}x_1x_2^{-2}x_4^2.
\end{aligned}$$

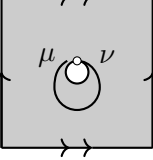
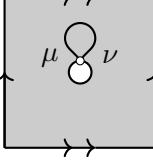
A.2.7 $X_{1,-\frac{1}{2}}$

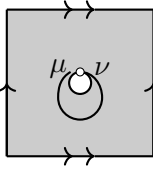
$$\begin{aligned}
\psi_{\mathcal{E}}(x_4) \cdot \begin{array}{c} \text{Diagram 1} \\ \hline 2 \quad 1 \end{array} &= q^{-1/2} \begin{array}{c} \text{Diagram 2} \\ \hline 2 \quad 1 \end{array} \\
&= q^{1/2} \begin{array}{c} \text{Diagram 3} \\ \hline 4 \quad 3 \quad 2 \quad 1 \end{array} + q^{-3/2} \begin{array}{c} \text{Diagram 4} \\ \hline 4 \quad 3 \quad 2 \quad 1 \end{array} \\
&= q^{3/2} \begin{array}{c} \text{Diagram 5} \\ \hline 4 \quad 2 \quad 3 \quad 1 \end{array} + q^{1/2} \begin{array}{c} \text{Diagram 6} \\ \hline 4 \quad 2 \quad 1 \quad 3 \end{array} \\
\Rightarrow \varphi_{\mathcal{E}}(X_{1,-\frac{1}{2}}(+, +)) &= x_4^{-1} \left(q^{5/2}x_1x_2 + q^{3/2}x_3x_5 \right) \\
&= q^{-7/2}x_1x_2x_4^{-1} + q^{-1/2}x_3x_4^{-1}x_5
\end{aligned}$$

$$\begin{aligned}
Y_1 X_{2,0}(\mu, \nu) Y_3 &= \text{Diagram 1} \\
&= q \text{Diagram 2} + q^{-1} \text{Diagram 3} \\
&= q^2 \text{Diagram 4} + \text{Diagram 5} - q^3 \text{Diagram 6} + q^{-2} \text{Diagram 7} \\
&= q \text{Diagram 8} + q \text{Diagram 9} + q^{-1} \text{Diagram 10} \\
&\quad + q^{-1} \text{Diagram 11} + q^{-3} \text{Diagram 12} \\
\Rightarrow \text{Diagram 13} &= q Y_1 X_{2,0}(\mu, \nu) Y_3 - q^2 X_{1, -\frac{1}{2}}(\mu, \nu) Y_1 - q^{-2} X_{2,0}(\mu, \nu) Y_2 - q^2 X_{3,0}(\mu, \nu) Y_3 - C_\mu^\nu
\end{aligned}$$

$$\begin{aligned}
Y_1 Y_2 X_{3,0}(\mu, \nu) &= \text{Diagram 1} \\
&= q \text{Diagram 2} + q^{-1} \text{Diagram 3} \\
&= q \text{Diagram 4} + q \text{Diagram 5} + q^{-2} \text{Diagram 6} \\
&= q \text{Diagram 7} + q \text{Diagram 8} + q^{-1} \text{Diagram 9} \\
&\quad + q^{-1} \text{Diagram 10} + q^{-3} \text{Diagram 11}
\end{aligned}$$

$$\Rightarrow \text{Diagram 12} = q Y_1 Y_2 X_{3,0}(\mu, \nu) - q^2 X_{1,0}(\mu, \nu) Y_1 - q^{-2} X_{2,0}(\mu, \nu) Y_2 - q^2 X_{3,0}(\mu, \nu) Y_3 - C'_\mu$$

When resolving crossings in these calculations, the process is conducted locally and away from the boundary. As a result, it is possible to initiate the calculation with $Y_1 Y_2 X_{3,k}(\mu, \nu)$ (likewise $X_{1,k}(\mu, \nu) Y_2 Y_3$ or $Y_1 X_{2,k}(\mu, \nu) Y_3$) for any $k \in \frac{1}{2}\mathbb{Z}$ and substitute each stated tangle in the diagrams with k twists (or their relative twists) around the boundary. Since  and $C_\mu^\nu =$  correspond to half twists of each other in either direction, and their coefficients are identical, interchanging their diagrams during the calculations does not affect the equations. Therefore, we get slightly more general formulas for our parallel tangle.

Measuring a half twist by using the different equations for $X_5(\mu, \nu) =$ .

$$\begin{aligned}
X_5(\mu, \nu) &= qX_{1,k}(\mu, \nu)Y_2Y_3 - q^2X_{1,k}(\mu, \nu)Y_1 - q^{-2}X_{2,k+\frac{1}{2}}(\mu, \nu)Y_2 - q^2X_{3,k}(\mu, \nu)Y_3 - C_\mu^\nu \\
&= qY_1X_{2,k}(\mu, \nu)Y_3 - q^2X_{1,k-\frac{1}{2}}(\mu, \nu)Y_1 - q^{-2}X_{2,k}(\mu, \nu)Y_2 - q^2X_{3,k}(\mu, \nu)Y_3 - C_\mu^\nu \\
&= qY_1Y_2X_{3,k}(\mu, \nu) - q^2X_{1,k}(\mu, \nu)Y_1 - q^{-2}X_{2,k}(\mu, \nu)Y_2 - q^2X_{3,k}(\mu, \nu)Y_3 - C_\mu^\nu \\
&\Rightarrow qY_1(X_{2,k}Y_3 - Y_2X_{3,k}) = q^2Y_1(X_{1,k-\frac{1}{2}} - X_{1,k}) - q^{-2}Y_2(X_{2,k} - X_{2,k+\frac{1}{2}})
\end{aligned}$$

$$(X_{1,k} - X_{1,k-\frac{1}{2}})Y_1 = q^{-1}(Y_1Y_2X_{3,k} - Y_1X_{2,k}Y_3)$$

$$(X_{2,k+\frac{1}{2}} - X_{2,k})Y_2 = q^3(Y_1Y_2X_{3,k} - X_{1,k}Y_2Y_3)$$

Appendix B

Python Code

B.1 Quantum Commuting Relations

```
1 '''
2 ~~~~~
3 ~~~~~ Program Outline & Limitations ~~~~~
4 ~~~~~
5 I created this program to help calculate many relations pertaining to my
6   dissertation. You can find more information about general stated skein
7   modules/algebras in "Stated Skein Modules of Marked 3-Manifolds/Surfaces,
8   A Survey" by Thang Le and Tao Yu. This survey paper is available on arxiv
9   and on Dr. Le's website: https://letu.math.gatech.edu/Papers/Survey.pdf
10
11 The purpose of this program is to help calculate the q-commuting relations of
12   nontrivial stated tangles on the once marked torus. This program doesn't
13   support calculations done with more than one marking and major adjustments
14   will need to be made if one would like to do this. It is, however,
15   theoretically quite doable to use this program on any other surface with a
16   single marking with minimal coding adjustments.
17
18 https://letu.math.gatech.edu/Papers/Survey.pdf
19 The logic of this program goes as follows:
20 - Create a list of all possible state combinations
21 - For each state combination we run through the below algorithm using height
22   exchange relations and keep track of the commuting costs
23 - Using sympy variables, each time we perform a height exchange we
24   substitute the exchange cost into that variable
25 - Finally, tell the user what the equality comes out to
26 We keep track of all the necessary information throughout the process using
27   object-oriented programming by using the endpoints as dictionary-type
28   attributes.
29
30 Note that this is not a complete calculation as there are several different
31   variables that can appear (in particular from exchange relations from bad
32   arc states) that are difficult for a computer to program without
33   implementing an excessive number of edge cases and specificity, of our
34   manifold. We instead insert new variables to replace these pictures and
35   allow the user to figure them out by hand. Assuming that the user wants to
36   use this program in the first place more than likely implies that there
37   are enough calculations that need to be found to where this program will
```

```

still save significant time for the user. By replacing these edge cases
with new variables, we're able to incorporate more generality into this
program so that it can be used in other cases. This means that the program
is merely an aid to finding these relations and does not completely
compute the commuting relations.
-----
17 '''
18
19
20 import itertools
21 from sympy import *
22
23 '''
24 ----- Program Variables -----
25 ----- Edit The Following Parameters If Needed -----
26 This order list tells us the order of which we perform our height exchange
relations
27 The order of each pairing helps us identify the relative positions of
endpoints. For example, # [2,3] tells us that in the picture, the third
endpoint (the one in front) is locally to the right of the second where as
[3,2] would tell us the third endpoint is locally to the left. # Here
when I say local I mean local and canonical.
28
29      [2,3]  ->
30              \  /
31              2 3
32
33 The only parameters you should need to edit here are the the orders of the
elements within the inner-most lists (NOT the order of the lists
themselves).
34
35 Example: We want to see how a 'boundary-parallel' tangle and a 'meridian'
tangle commute. Then the height swaps should correspond to a middle-left-
right-middle swap:
36
37      1 2 3 4  ->  1 3 2 4  ->  3 1 2 4  ->  3 1 4 2  ->  3 4 1 2
38      (32)      (21)      (34)      (23)
39      (left position, right position)
40 A possible calculation order list could be:
41      calculationOrderList = [[3, 2], [2, 1], [3, 4], [2, 3]]
42
43 Below is a more visual interpretation of what's happening in this
example. The horizontal dashed line corresponds to the marking and we're
looking at it from a side perspective. The vertical lines correspond to
the ends of the tangles and the numbered labelings at the bottom keeps
track of them as they move past each other throughout the algorithm. Above
the first vertical line are the labels correspond to the local
relationships of each endpoint to each other (as explained above). The
labels LL, L, R, RR correspond to leftmost, middle left, middle right, and
rightmost respectively.
44
45      L   R   LL  RR
46      |   |   |   |
47      |   |   |   |
48      |   |   |   |
49      |   |   |   |
50      |   |   |   |
51      |   |   |   |
52      |   |   |   |
53      |   |   |   |
54      |   |   |   |
55      |   |   |   |
56      |   |   |   |
57      |   |   |   |
58      |   |   |   |
59      |   |   |   |
60      |   |   |   |
61      |   |   |   |
62      |   |   |   |
63      |   |   |   |
64      |   |   |   |
65      |   |   |   |
66      |   |   |   |
67      |   |   |   |
68      |   |   |   |
69      |   |   |   |
70      |   |   |   |
71      |   |   |   |
72      |   |   |   |
73      |   |   |   |
74      |   |   |   |
75      |   |   |   |
76      |   |   |   |
77      |   |   |   |
78      |   |   |   |
79      |   |   |   |
80      |   |   |   |
81      |   |   |   |
82      |   |   |   |
83      |   |   |   |
84      |   |   |   |
85      |   |   |   |
86      |   |   |   |
87      |   |   |   |
88      |   |   |   |
89      |   |   |   |
90      |   |   |   |
91      |   |   |   |
92      |   |   |   |
93      |   |   |   |
94      |   |   |   |
95      |   |   |   |
96      |   |   |   |
97      |   |   |   |
98      |   |   |   |
99      |   |   |   |
100     |   |   |   |
101     |   |   |   |
102     |   |   |   |
103     |   |   |   |
104     |   |   |   |
105     |   |   |   |
106     |   |   |   |
107     |   |   |   |
108     |   |   |   |
109     |   |   |   |
110     |   |   |   |
111     |   |   |   |
112     |   |   |   |
113     |   |   |   |
114     |   |   |   |
115     |   |   |   |
116     |   |   |   |
117     |   |   |   |
118     |   |   |   |
119     |   |   |   |
120     |   |   |   |
121     |   |   |   |
122     |   |   |   |
123     |   |   |   |
124     |   |   |   |
125     |   |   |   |
126     |   |   |   |
127     |   |   |   |
128     |   |   |   |
129     |   |   |   |
130     |   |   |   |
131     |   |   |   |
132     |   |   |   |
133     |   |   |   |
134     |   |   |   |
135     |   |   |   |
136     |   |   |   |
137     |   |   |   |
138     |   |   |   |
139     |   |   |   |
140     |   |   |   |
141     |   |   |   |
142     |   |   |   |
143     |   |   |   |
144     |   |   |   |
145     |   |   |   |
146     |   |   |   |
147     |   |   |   |
148     |   |   |   |
149     |   |   |   |
150     |   |   |   |
151     |   |   |   |
152     |   |   |   |
153     |   |   |   |
154     |   |   |   |
155     |   |   |   |
156     |   |   |   |
157     |   |   |   |
158     |   |   |   |
159     |   |   |   |
160     |   |   |   |
161     |   |   |   |
162     |   |   |   |
163     |   |   |   |
164     |   |   |   |
165     |   |   |   |
166     |   |   |   |
167     |   |   |   |
168     |   |   |   |
169     |   |   |   |
170     |   |   |   |
171     |   |   |   |
172     |   |   |   |
173     |   |   |   |
174     |   |   |   |
175     |   |   |   |
176     |   |   |   |
177     |   |   |   |
178     |   |   |   |
179     |   |   |   |
180     |   |   |   |
181     |   |   |   |
182     |   |   |   |
183     |   |   |   |
184     |   |   |   |
185     |   |   |   |
186     |   |   |   |
187     |   |   |   |
188     |   |   |   |
189     |   |   |   |
190     |   |   |   |
191     |   |   |   |
192     |   |   |   |
193     |   |   |   |
194     |   |   |   |
195     |   |   |   |
196     |   |   |   |
197     |   |   |   |
198     |   |   |   |
199     |   |   |   |
200     |   |   |   |
201     |   |   |   |
202     |   |   |   |
203     |   |   |   |
204     |   |   |   |
205     |   |   |   |
206     |   |   |   |
207     |   |   |   |
208     |   |   |   |
209     |   |   |   |
210     |   |   |   |
211     |   |   |   |
212     |   |   |   |
213     |   |   |   |
214     |   |   |   |
215     |   |   |   |
216     |   |   |   |
217     |   |   |   |
218     |   |   |   |
219     |   |   |   |
220     |   |   |   |
221     |   |   |   |
222     |   |   |   |
223     |   |   |   |
224     |   |   |   |
225     |   |   |   |
226     |   |   |   |
227     |   |   |   |
228     |   |   |   |
229     |   |   |   |
230     |   |   |   |
231     |   |   |   |
232     |   |   |   |
233     |   |   |   |
234     |   |   |   |
235     |   |   |   |
236     |   |   |   |
237     |   |   |   |
238     |   |   |   |
239     |   |   |   |
240     |   |   |   |
241     |   |   |   |
242     |   |   |   |
243     |   |   |   |
244     |   |   |   |
245     |   |   |   |
246     |   |   |   |
247     |   |   |   |
248     |   |   |   |
249     |   |   |   |
250     |   |   |   |
251     |   |   |   |
252     |   |   |   |
253     |   |   |   |
254     |   |   |   |
255     |   |   |   |
256     |   |   |   |
257     |   |   |   |
258     |   |   |   |
259     |   |   |   |
260     |   |   |   |
261     |   |   |   |
262     |   |   |   |
263     |   |   |   |
264     |   |   |   |
265     |   |   |   |
266     |   |   |   |
267     |   |   |   |
268     |   |   |   |
269     |   |   |   |
270     |   |   |   |
271     |   |   |   |
272     |   |   |   |
273     |   |   |   |
274     |   |   |   |
275     |   |   |   |
276     |   |   |   |
277     |   |   |   |
278     |   |   |   |
279     |   |   |   |
280     |   |   |   |
281     |   |   |   |
282     |   |   |   |
283     |   |   |   |
284     |   |   |   |
285     |   |   |   |
286     |   |   |   |
287     |   |   |   |
288     |   |   |   |
289     |   |   |   |
290     |   |   |   |
291     |   |   |   |
292     |   |   |   |
293     |   |   |   |
294     |   |   |   |
295     |   |   |   |
296     |   |   |   |
297     |   |   |   |
298     |   |   |   |
299     |   |   |   |
300     |   |   |   |
301     |   |   |   |
302     |   |   |   |
303     |   |   |   |
304     |   |   |   |
305     |   |   |   |
306     |   |   |   |
307     |   |   |   |
308     |   |   |   |
309     |   |   |   |
310     |   |   |   |
311     |   |   |   |
312     |   |   |   |
313     |   |   |   |
314     |   |   |   |
315     |   |   |   |
316     |   |   |   |
317     |   |   |   |
318     |   |   |   |
319     |   |   |   |
320     |   |   |   |
321     |   |   |   |
322     |   |   |   |
323     |   |   |   |
324     |   |   |   |
325     |   |   |   |
326     |   |   |   |
327     |   |   |   |
328     |   |   |   |
329     |   |   |   |
330     |   |   |   |
331     |   |   |   |
332     |   |   |   |
333     |   |   |   |
334     |   |   |   |
335     |   |   |   |
336     |   |   |   |
337     |   |   |   |
338     |   |   |   |
339     |   |   |   |
340     |   |   |   |
341     |   |   |   |
342     |   |   |   |
343     |   |   |   |
344     |   |   |   |
345     |   |   |   |
346     |   |   |   |
347     |   |   |   |
348     |   |   |   |
349     |   |   |   |
350     |   |   |   |
351     |   |   |   |
352     |   |   |   |
353     |   |   |   |
354     |   |   |   |
355     |   |   |   |
356     |   |   |   |
357     |   |   |   |
358     |   |   |   |
359     |   |   |   |
360     |   |   |   |
361     |   |   |   |
362     |   |   |   |
363     |   |   |   |
364     |   |   |   |
365     |   |   |   |
366     |   |   |   |
367     |   |   |   |
368     |   |   |   |
369     |   |   |   |
370     |   |   |   |
371     |   |   |   |
372     |   |   |   |
373     |   |   |   |
374     |   |   |   |
375     |   |   |   |
376     |   |   |   |
377     |   |   |   |
378     |   |   |   |
379     |   |   |   |
380     |   |   |   |
381     |   |   |   |
382     |   |   |   |
383     |   |   |   |
384     |   |   |   |
385     |   |   |   |
386     |   |   |   |
387     |   |   |   |
388     |   |   |   |
389     |   |   |   |
390     |   |   |   |
391     |   |   |   |
392     |   |   |   |
393     |   |   |   |
394     |   |   |   |
395     |   |   |   |
396     |   |   |   |
397     |   |   |   |
398     |   |   |   |
399     |   |   |   |
400     |   |   |   |
401     |   |   |   |
402     |   |   |   |
403     |   |   |   |
404     |   |   |   |
405     |   |   |   |
406     |   |   |   |
407     |   |   |   |
408     |   |   |   |
409     |   |   |   |
410     |   |   |   |
411     |   |   |   |
412     |   |   |   |
413     |   |   |   |
414     |   |   |   |
415     |   |   |   |
416     |   |   |   |
417     |   |   |   |
418     |   |   |   |
419     |   |   |   |
420     |   |   |   |
421     |   |   |   |
422     |   |   |   |
423     |   |   |   |
424     |   |   |   |
425     |   |   |   |
426     |   |   |   |
427     |   |   |   |
428     |   |   |   |
429     |   |   |   |
430     |   |   |   |
431     |   |   |   |
432     |   |   |   |
433     |   |   |   |
434     |   |   |   |
435     |   |   |   |
436     |   |   |   |
437     |   |   |   |
438     |   |   |   |
439     |   |   |   |
440     |   |   |   |
441     |   |   |   |
442     |   |   |   |
443     |   |   |   |
444     |   |   |   |
445     |   |   |   |
446     |   |   |   |
447     |   |   |   |
448     |   |   |   |
449     |   |   |   |
450     |   |   |   |
451     |   |   |   |
452     |   |   |   |
453     |   |   |   |
454     |   |   |   |
455     |   |   |   |
456     |   |   |   |
457     |   |   |   |
458     |   |   |   |
459     |   |   |   |
460     |   |   |   |
461     |   |   |   |
462     |   |   |   |
463     |   |   |   |
464     |   |   |   |
465     |   |   |   |
466     |   |   |   |
467     |   |   |   |
468     |   |   |   |
469     |   |   |   |
470     |   |   |   |
471     |   |   |   |
472     |   |   |   |
473     |   |   |   |
474     |   |   |   |
475     |   |   |   |
476     |   |   |   |
477     |   |   |   |
478     |   |   |   |
479     |   |   |   |
480     |   |   |   |
481     |   |   |   |
482     |   |   |   |
483     |   |   |   |
484     |   |   |   |
485     |   |   |   |
486     |   |   |   |
487     |   |   |   |
488     |   |   |   |
489     |   |   |   |
490     |   |   |   |
491     |   |   |   |
492     |   |   |   |
493     |   |   |   |
494     |   |   |   |
495     |   |   |   |
496     |   |   |   |
497     |   |   |   |
498     |   |   |   |
499     |   |   |   |
500     |   |   |   |
501     |   |   |   |
502     |   |   |   |
503     |   |   |   |
504     |   |   |   |
505     |   |   |   |
506     |   |   |   |
507     |   |   |   |
508     |   |   |   |
509     |   |   |   |
510     |   |   |   |
511     |   |   |   |
512     |   |   |   |
513     |   |   |   |
514     |   |   |   |
515     |   |   |   |
516     |   |   |   |
517     |   |   |   |
518     |   |   |   |
519     |   |   |   |
520     |   |   |   |
521     |   |   |   |
522     |   |   |   |
523     |   |   |   |
524     |   |   |   |
525     |   |   |   |
526     |   |   |   |
527     |   |   |   |
528     |   |   |   |
529     |   |   |   |
530     |   |   |   |
531     |   |   |   |
532     |   |   |   |
533     |   |   |   |
534     |   |   |   |
535     |   |   |   |
536     |   |   |   |
537     |   |   |   |
538     |   |   |   |
539     |   |   |   |
540     |   |   |   |
541     |   |   |   |
542     |   |   |   |
543     |   |   |   |
544     |   |   |   |
545     |   |   |   |
546     |   |   |   |
547     |   |   |   |
548     |   |   |   |
549     |   |   |   |
550     |   |   |   |
551     |   |   |   |
552     |   |   |   |
553     |   |   |   |
554     |   |   |   |
555     |   |   |   |
556     |   |   |   |
557     |   |   |   |
558     |   |   |   |
559     |   |   |   |
560     |   |   |   |
561     |   |   |   |
562     |   |   |   |
563     |   |   |   |
564     |   |   |   |
565     |   |   |   |
566     |   |   |   |
567     |   |   |   |
568     |   |   |   |
569     |   |   |   |
570     |   |   |   |
571     |   |   |   |
572     |   |   |   |
573     |   |   |   |
574     |   |   |   |
575     |   |   |   |
576     |   |   |   |
577     |   |   |   |
578     |   |   |   |
579     |   |   |   |
580     |   |   |   |
581     |   |   |   |
582     |   |   |   |
583     |   |   |   |
584     |   |   |   |
585     |   |   |   |
586     |   |   |   |
587     |   |   |   |
588     |   |   |   |
589     |   |   |   |
590     |   |   |   |
591     |   |   |   |
592     |   |   |   |
593     |   |   |   |
594     |   |   |   |
595     |   |   |   |
596     |   |   |   |
597     |   |   |   |
598     |   |   |   |
599     |   |   |   |
600     |   |   |   |
601     |   |   |   |
602     |   |   |   |
603     |   |   |   |
604     |   |   |   |
605     |   |   |   |
606     |   |   |   |
607     |   |   |   |
608     |   |   |   |
609     |   |   |   |
610     |   |   |   |
611     |   |   |   |
612     |   |   |   |
613     |   |   |   |
614     |   |   |   |
615     |   |   |   |
616     |   |   |   |
617     |   |   |   |
618     |   |   |   |
619     |   |   |   |
620     |   |   |   |
621     |   |   |   |
622     |   |   |   |
623     |   |   |   |
624     |   |   |   |
625     |   |   |   |
626     |   |   |   |
627     |   |   |   |
628     |   |   |   |
629     |   |   |   |
630     |   |   |   |
631     |   |   |   |
632     |   |   |   |
633     |   |   |   |
634     |   |   |   |
635     |   |   |   |
636     |   |   |   |
637     |   |   |   |
638     |   |   |   |
639     |   |   |   |
640     |   |   |   |
641     |   |   |   |
642     |   |   |   |
643     |   |   |   |
644     |   |   |   |
645     |   |   |   |
646     |   |   |   |
647     |   |   |   |
648     |   |   |   |
649     |   |   |   |
650     |   |   |   |
651     |   |   |   |
652     |   |   |   |
653     |   |   |   |
654     |   |   |   |
655     |   |   |   |
656     |   |   |   |
657     |   |   |   |
658     |   |   |   |
659     |   |   |   |
660     |   |   |   |
661     |   |   |   |
662     |   |   |   |
663     |   |   |   |
664     |   |   |   |
665     |   |   |   |
666     |   |   |   |
667     |   |   |   |
668     |   |   |   |
669     |   |   |   |
670     |   |   |   |
671     |   |   |   |
672     |   |   |   |
673     |   |   |   |
674     |   |   |   |
675     |   |   |   |
676     |   |   |   |
677     |   |   |   |
678     |   |   |   |
679     |   |   |   |
680     |   |   |   |
681     |   |   |   |
682     |   |   |   |
683     |   |   |   |
684     |   |   |   |
685     |   |   |   |
686     |   |   |   |
687     |   |   |   |
688     |   |   |   |
689     |   |   |   |
690     |   |   |   |
691     |   |   |   |
692     |   |   |   |
693     |   |   |   |
694     |   |   |   |
695     |   |   |   |
696     |   |   |   |
697     |   |   |   |
698     |   |   |   |
699     |   |   |   |
700     |   |   |   |
701     |   |   |   |
702     |   |   |   |
703     |   |   |   |
704     |   |   |   |
705     |   |   |   |
706     |   |   |   |
707     |   |   |   |
708     |   |   |   |
709     |   |   |   |
710     |   |   |   |
711     |   |   |   |
712     |   |   |   |
713     |   |   |   |
714     |   |   |   |
715     |   |   |   |
716     |   |   |   |
717     |   |   |   |
718     |   |   |   |
719     |   |   |   |
720     |   |   |   |
721     |   |   |   |
722     |   |   |   |
723     |   |   |   |
724     |   |   |   |
725     |   |   |   |
726     |   |   |   |
727     |   |   |   |
728     |   |   |   |
729     |   |   |   |
730     |   |   |   |
731     |   |   |   |
732     |   |   |   |
733     |   |   |   |
734     |   |   |   |
735     |   |   |   |
736     |   |   |   |
737     |   |   |   |
738     |   |   |   |
739     |   |   |   |
740     |   |   |   |
741     |   |   |   |
742     |   |   |   |
743     |   |   |   |
744     |   |   |   |
745     |   |   |   |
746     |   |   |   |
747     |   |   |   |
748     |   |   |   |
749     |   |   |   |
750     |   |   |   |
751     |   |   |   |
752     |   |   |   |
753     |   |   |   |
754     |   |   |   |
755     |   |   |   |
756     |   |   |   |
757     |   |   |   |
758     |   |   |   |
759     |   |   |   |
760     |   |   |   |
761     |   |   |   |
762     |   |   |   |
763     |   |   |   |
764     |   |   |   |
765     |   |   |   |
766     |   |   |   |
767     |   |   |   |
768     |   |   |   |
769     |   |   |   |
770     |   |   |   |
771     |   |   |   |
772     |   |   |   |
773     |   |   |   |
774     |   |   |   |
775     |   |   |   |
776     |   |   |   |
777     |   |   |   |
778     |   |   |   |
779     |   |   |   |
780     |   |   |   |
781     |   |   |   |
782     |   |   |   |
783     |   |   |   |
784     |   |   |   |
785     |   |   |   |
786     |   |   |   |
787     |   |   |   |
788     |   |   |   |
789     |   |   |   |
790     |   |   |   |
791     |   |   |   |
792     |   |   |   |
793     |   |   |   |
794     |   |   |   |
795     |   |   |   |
796     |   |   |   |
797     |   |   |   |
798     |   |   |   |
799     |   |   |   |
800     |   |   |   |
801     |   |   |   |
802     |   |   |   |
803     |   |   |   |
804     |   |   |   |
805     |   |   |   |
806     |   |   |   |
807     |   |   |   |
808     |   |   |   |
809     |   |   |   |
810     |   |   |   |
811     |   |   |   |
812     |   |   |   |
813     |   |   |   |
814     |   |   |   |
815     |   |   |   |
816     |   |   |   |
817     |   |   |   |
818     |   |   |   |
819     |   |   |   |
820     |   |   |   |
821     |   |   |   |
822     |   |   |   |
823     |   |   |   |
824     |   |   |   |
825     |   |   |   |
826     |   |   |   |
827     |   |   |   |
828     |   |   |   |
829     |   |   |   |
830     |   |   |   |
831     |   |   |   |
832     |   |   |   |
833     |   |   |   |
834     |   |   |   |
835     |   |   |   |
836     |   |   |   |
837     |   |   |   |
838     |   |   |   |
839     |   |   |   |
840     |   |   |   |
841     |   |   |   |
842     |   |   |   |
843     |   |   |   |
844     |   |   |   |
845     |   |   |   |
846     |   |   |   |
847     |   |   |   |
848     |   |   |   |
849     |   |   |   |
850     |   |   |   |
851     |   |   |   |
852     |   |   |   |
853     |   |   |   |
854     |   |   |   |
855     |   |   |   |
856     |   |   |   |
857     |   |   |   |
858     |   |   |   |
859     |   |   |   |
860     |   |   |   |
861     |   |   |   |
862     |   |   |   |
863     |   |   |   |
864     |   |   |   |
865     |   |   |   |
866     |   |   |   |
867     |   |   |   |
868     |   |   |   |
869     |   |   |   |
870     |   |   |   |
871     |   |   |   |
872     |   |   |   |
873     |   |   |   |
874     |   |   |   |
875     |   |   |   |
876     |   |   |   |
877     |   |   |   |
878     |   |   |   |
879     |   |   |   |
880     |   |   |   |
881     |   |   |   |
882     |   |   |   |
883     |   |   |   |
884     |   |   |   |
885     |   |   |   |
886     |   |   |   |
887     |   |   |   |
888     |   |   |   |
889     |   |   |   |
890     |   |   |   |
891     |   |   |   |
892     |   |   |   |
893     |   |   |   |
894     |   |   |   |
895     |   |   |   |
896     |   |   |   |
897     |   |   |   |
898     |   |   |   |
899     |   |   |   |
900     |   |   |   |
901     |   |   |   |
902     |   |   |   |
903     |   |   |   |
904     |   |   |   |
905     |   |   |   |
906     |   |   |   |
907     |   |   |   |
908     |   |   |   |
909     |   |   |   |
910     |   |   |   |
911     |   |   |   |
912     |   |   |   |
913     |   |   |   |
914     |   |   |   |
915     |   |   |   |
916     |   |   |   |
917     |   |   |   |
918     |   |   |   |
919     |   |   |   |
920     |   |   |   |
921     |   |   |   |
922     |   |   |   |
923     |   |   |   |
924     |   |   |   |
925     |   |   |   |
926     |   |   |   |
927     |   |   |   |
928     |   |   |   |
929     |   |   |   |
930     |   |   |   |
931     |   |   |   |
932     |   |   |   |
933     |   |   |   |
934     |   |   |   |
935     |   |   |   |
936     |   |   |   |
937     |   |   |   |
938     |   |   |   |
939     |   |   |   |
940     |   |   |   |
941     |   |   |   |
942     |   |   |   |
943     |   |   |   |
944     |   |   |   |
945     |   |   |   |
946     |   |   |   |
947     |   |   |   |
948     |   |   |   |
949     |   |   |   |
950     |   |   |   |
951     |   |   |   |
952     |   |   |   |
953     |   |   |   |
954     |   |   |   |
955     |   |   |   |
956     |   |   |   |
957     |   |   |   |
958     |   |   |   |
959     |   |   |   |
960     |   |   |   |
961     |   |   |   |
962     |   |   |   |
963     |   |   |   |
964     |   |   |   |
965     |   |   |   |
966     |   |   |   |
967     |   |   |   |
968     |   |   |   |
969     |   |   |   |
970     |   |   |   |
971     |   |   |   |
972     |   |   |   |
973     |   |   |   |
974     |   |   |   |
975     |   |   |   |
976     |   |   |   |
977     |   |   |   |
978     |   |   |   |
979     |   |   |   |
980     |   |   |   |
981     |   |   |   |
982     |   |   |   |
983     |   |   |   |
984     |   |   |   |
985     |   |   |   |
986     |   |   |   |
987     |   |   |   |
988     |   |   |   |
989     |   |   |   |
990     |   |   |   |
991     |   |   |   |
992     |   |   |   |
993     |   |   |   |
994     |   |   |   |
995     |   |   |   |
996     |   |   |   |
997     |   |   |   |
998     |   |   |   |
999     |   |   |   |
1000    |   |   |   |

```

```

56 global q
57 q = Symbol('q', commutative=True)
58 x = Symbol('x', commutative=False) # x will be our picture
59 ',,'
60 a,b,c,d are additional symbols representing occasionally arising pictures with
    only two states, which appear in bad arc state exchange relations.
    Depending where the states we're looking at are located, we can have up to
    6 different variations and so the two numbers appended onto these
    variable names help us distinguish which variation we're dealing with.
61
62 Assuming we're dealing with the MLRM order list, should only need x12, x34,
    x14. Note that since this algorithm swaps the middle twice, x14 has two
    different variations that can appear. Feel free to add an additional
    variable to distinguish between the two if you'd like. I did not really
    need it so I didn't add one. Luckily, we only need half of them using this
    algorithm.
63 ',,'
64 # a -> states == (+, +)
65 a12_l = Symbol('a12_l', commutative=False) # (*, *, -, -)
66 a14_l = Symbol('a14_l', commutative=False) # (*, -, -, *)
67 a34_l = Symbol('a34_l', commutative=False) # (-, -, *, *)
68 a12_r = Symbol('a12_r', commutative=False) # (*, *, -, -)
69 a14_r = Symbol('a14_r', commutative=False) # (*, -, -, *)
70 a14_r = Symbol('a14_r', commutative=False) # (*, -, -, *)
71 a34_r = Symbol('a34_r', commutative=False) # (-, -, *, *)
72 # b -> states == (+, -)
73 b12_l = Symbol('b12_l', commutative=False) # (*, *, -, -)
74 b14_l = Symbol('b14_l', commutative=False) # (*, -, -, *)
75 b34_l = Symbol('b34_l', commutative=False) # (-, -, *, *)
76 b12_r = Symbol('b12_r', commutative=False) # (*, *, -, -)
77 b14_r = Symbol('b14_r', commutative=False) # (*, -, -, *)
78 b14_r = Symbol('b14_r', commutative=False) # (*, -, -, *)
79 b34_r = Symbol('b34_r', commutative=False) # (-, -, *, *)
80 # c -> states == (-, +)
81 c12_l = Symbol('c12_l', commutative=False) # (*, *, -, -)
82 c14_l = Symbol('c14_l', commutative=False) # (*, -, -, *)
83 c34_l = Symbol('c34_l', commutative=False) # (-, -, *, *)
84 c12_r = Symbol('c12_r', commutative=False) # (*, *, -, -)
85 c14_r = Symbol('c14_r', commutative=False) # (*, -, -, *)
86 c14_r = Symbol('c14_r', commutative=False) # (*, -, -, *)
87 c34_r = Symbol('c34_r', commutative=False) # (-, -, *, *)
88 # d -> states == (-, -)
89 d12_l = Symbol('d12_l', commutative=False) # (*, *, -, -)
90 d14_l = Symbol('d14_l', commutative=False) # (*, -, -, *)
91 d34_l = Symbol('d34_l', commutative=False) # (-, -, *, *)
92 d12_r = Symbol('d12_r', commutative=False) # (*, *, -, -)
93 d14_r = Symbol('d14_r', commutative=False) # (*, -, -, *)
94 d14_r = Symbol('d14_r', commutative=False) # (*, -, -, *)
95 d34_r = Symbol('d34_r', commutative=False) # (-, -, *, *)
96
97 # This dictionary is used only in the 'findRepSym' function
98 additionalSymbolDictLeftFront = {
99     (('+', '+'), 1, 2) : a12_l,
100    (('+', '+'), 1, 4) : a14_l,
101    (('+', '+'), 3, 4) : a34_l,
102    (('+', '-'), 1, 2) : b12_l,
103    (('+', '-'), 1, 4) : b14_l,
104    (('+', '-'), 3, 4) : b34_l,
105    (('-', '+'), 1, 2) : c12_l,
106    (('-', '+'), 1, 4) : c14_l,
107    (('-', '+'), 3, 4) : c34_l,
108    (('-', '-'), 1, 2) : d12_l,
109    (('-', '-'), 1, 4) : d14_l,
110    (('-', '-'), 3, 4) : d34_l,
111 }

```

```

112 |
113 | additionalSymbolDietRightFront = {
114 |     (('+', '+'), 1, 2) : a12_r,
115 |     (('+', '+'), 1, 4) : a14_r,
116 |     (('+', '+'), 3, 4) : a34_r,
117 |     (('+', '-'), 1, 2) : b12_r,
118 |     (('+', '-'), 1, 4) : b14_r,
119 |     (('+', '-'), 3, 4) : b34_r,
120 |     (('-', '+'), 1, 2) : c12_r,
121 |     (('-', '+'), 1, 4) : c14_r,
122 |     (('-', '+'), 3, 4) : c34_r,
123 |     (('-', '-'), 1, 2) : d12_r,
124 |     (('-', '-'), 1, 4) : d14_r,
125 |     (('-', '-'), 3, 4) : d34_r,
126 | }
127 |
128 |
129 |
130 | class statedEndpoint(object):
131 |     def __init__(self, initialData):
132 |         # Create keys for our statedEndpoint dictionaries to make calling their
133 |         # values easier
134 |         for key in initialData:
135 |             setattr(self, key, initialData[key])
136 |
137 | class statedProduct(object):
138 |     """
139 |     Each endpoint of each factor in our product has a tag identifying its
140 |     starting position and a value corresponding to its state. The current
141 |     position of each endpoint will be changed throughout the program by
142 |     swapping its corresponding attribute data. This data structure has been
143 |     configured this way to help with dynamic access throughout the algorithm.
144 |
145 |     It is possible to instead create another attribute corresponding to its
146 |     position as that's debatably cleaner organization, however, access to the
147 |     position seems to get a bit more complicated due to how dynamic we need
148 |     its current position to be. Using the 'swapAttr' function when needed
149 |     instead seemed like the easiest workaround.
150 |     """
151 |     def __init__(self, startStates):
152 |         # SEP == stated endpoint
153 |         self.SEP1 = statedEndpoint({"identifier": "Factor 1 Left", "state":
154 |             startStates[0][0]})
155 |         self.SEP2 = statedEndpoint({"identifier": "Factor 1 Right", "state":
156 |             startStates[0][1]})
157 |         self.SEP3 = statedEndpoint({"identifier": "Factor 2 Left", "state":
158 |             startStates[1][0]})
159 |         self.SEP4 = statedEndpoint({"identifier": "Factor 2 Right", "state":
160 |             startStates[1][1]})
161 |         self.expr = x
162 |
163 |     def findSEPAttr(self, num):
164 |         """
165 |         Use this function when you want to dynamically use one of the SEP
166 |         attributes. This functions takes in an integer, n in {1,2,3,4}, and
167 |         returns that corresponding self.SEPn' attribute/object using a dictionary
168 |         in a switch-case manner.
169 |         """
170 |         switcher = {
171 |             1: self.SEP1,
172 |             2: self.SEP2,
173 |             3: self.SEP3,
174 |             4: self.SEP4
175 |         }
176 |         return switcher.get(num)

```

```

162 def printCurrentStatus(self):
163     # This function prints the current attribute/endpoint information/status
    to the user
164     print("Position 1 \tID: " + self.SEP1.identifier + "\tState: " + self.SEP1
    .state)
165     print("Position 2 \tID: " + self.SEP2.identifier + "\tState: " + self.SEP2
    .state)
166     print("Position 3 \tID: " + self.SEP3.identifier + "\tState: " + self.SEP3
    .state)
167     print("Position 4 \tID: " + self.SEP4.identifier + "\tState: " + self.SEP4
    .state + "\n")
168
169 def swapAttr(self, pos1, pos2):
    # This function swaps two of the SEP attributes/objects
170     tempAttr = getattr(self, 'SEP%d' % pos1)
171     setattr(self, 'SEP%d' % pos1, getattr(self, 'SEP%d' % pos2))
172     setattr(self, 'SEP%d' % pos2, tempAttr)
173     del tempAttr
174     # Returns the complement endpoints that weren't swapped for possible bad
    arc relations
175     return list(set([1, 2, 3, 4]) - set([pos1, pos2]))
176
177
178 def findRepSym(self, complementStates, leftFrontBool):
179     ',,'
180     When we must swap heights of endpoints with bad arc states, an additional
    term appears, which pictorially has the two endpoints connected together
    rather than lying on themarking. The function identifies which new term
    must be added based on the leftover state values and where these states
    are located, 'complementStates', with respect to our picture variable 'x'.
    Although this additional term can only have 4 possible states, there are
    6 = (4 choose 2) variants per combination of states along with an
    additional variation depending on which endpoint is locally in front (x2)
    => up to 48 possible variations. Rather than having a bunch of messy
    nested if statements, we instead use the two dictionaries '
    additionalSymbolDictLeftFront' and 'additionalSymbolDictRightFront', which
    is located outside of any loops and functions for memory efficiency.
    ',,'
181
182     if leftFrontBool:
183         return additionalSymbolDictLeftFront.get(((self.findSEPAAttr(
    complementStates[0]).state, self.findSEPAAttr(complementStates[1]).state),
    complementStates[0], complementStates[1]))
184         return additionalSymbolDictRightFront.get(((self.findSEPAAttr(
    complementStates[0]).state, self.findSEPAAttr(complementStates[1]).state),
    complementStates[0], complementStates[1]))
185
186 def swapHeights(self, endpointLeft, endpointRight):
187     leftEndpoint = self.findSEPAAttr(endpointLeft)
188     rightEndpoint = self.findSEPAAttr(endpointRight)
189     # Is the left endpoint in front of the right endpoint?
190     leftFrontBool = False if endpointLeft < endpointRight else True
191     # Find the q-coefficient cost of swapping and whether or not this is a bad
    arc state
192     qConst, badArc = self.stateExchangeCoeff(leftEndpoint.state, rightEndpoint
    .state, leftFrontBool)
193     # Swap the endpoint attributes and return complement endpoints for
    possible bad arc state
194     complementStates = self.swapAttr(endpointLeft, endpointRight)
195     # If a bad arc state is found then we need to add a summand to our
    expression
196     if badArc:
197         summand = q**(-3/2)*(q**2 - q**-2)*self.findRepSym(complementStates,
    leftFrontBool) if qConst == q**-3 else -q**(3/2)*(q**2 - q**-2)*self.
    findRepSym(complementStates, leftFrontBool)
198     else:
199         summand = 0
200     # Substitute updated height and costs into our expression

```

```

201     self.expr = self.expr.subs(x, qConst*x + summand)
202
203 def stateExchangeCoeff(self, stateLeft, stateRight, leftFrontBool):
204     # Does this state pair correlate to a bad arc? (+,-)
205     badArc = True if (stateLeft == "+" and stateRight == "-") else False
206     # Find the q-coefficient based on the states
207     if stateLeft == stateRight:
208         qConst = q**-1 if leftFrontBool else q
209         elif (stateLeft, stateRight) == ('-', '+'):
210             qConst = q if leftFrontBool else q**-1
211         elif (stateLeft, stateRight) == ('+', '-'):
212             qConst = q**-3 if leftFrontBool else q**3
213         else:
214             print("Error: Unknown state arguments in function 'stateExchangeCoeff'."
215                   ,
216                   "Arguments received: stateLeft = '" + str(stateLeft) + "', stateRight
217                   = '" + str(stateRight) + "'."
218                   )
219             print("Please use known states only!")
220             quit()
221         return qConst, badArc
222
223 def calcCommutingRelation(self, orderList):
224     for myList in orderList:
225         self.swapHeights(myList[0], myList[1])
226     return self.expr
227
228
229 # Creates a nested tuple, 'productStateTuple', of all 16 possible states
230 possibleStates = ["+", "-"]
231 stateTuple = list(itertools.product(possibleStates, possibleStates))
232 productStateTuple = list(itertools.product(stateTuple, stateTuple))
233
234
235 for statesTuple in productStateTuple:
236     myProd = statedProduct(statesTuple)
237     myProd.calcCommutingRelation(calculationOrderList)
238     print("x1(" + str(statesTuple[1][0]) + "," + str(statesTuple[1][1]) + ")x2(
239           " + str(statesTuple[0][0]) + "," + str(statesTuple[0][1]) + ") = " + str(
240           sympify(expand(myProd.expr)))
241
242     """
243     Since a*b is defined as a on top of b and states area read from left to right
244     (right on top), we swap a and b at the end print statement and keep things
245     aligned throughout the calculations.
246     — a[0] — a[1] — b[0] — b[1] —>
247     """

```

code/qCommRel_DissVer.py

B.2 Quantum 6-Torus Operators

```

1 from sympy import *
2
3 def qBracket(a, b, normalized=False, operatorInput=None):
4     """
5     This function takes in 'sympy' elements, 'a' and 'b', and returns their
6     corresponding quantum bracket: qab - q^(-1)ba. If 'a' and 'b' are

```

```

6     operators acting on 'f', then we require an input for the operator as well
7     , 'operatorInput', and need to treat the arguments as functions to allow
8     for the operators to act in the proper order. We also allow for bracket
9     normalization, i.e. divide by  $q^2 - q^{-2}$ , if desired.
10    Example of calling this function:
11    ,,
12    expression = lambda f: qBracket(y1, y2, normalized=True, operatorInput=f)
13    ,,
14    myExpr = q * a(b(operatorInput)) - q**(-1) * b(a(operatorInput)) if
15    operatorInput else q*a*b - q**(-1)*b*a
16    if normalized:
17        myExpr = myExpr*(q**2 - q**(-2))**(-1)
18    return myExpr
19
20 # Define variables
21 x, y, z, w, q = symbols('x y z w q')
22
23 # Define a commutative multivariable polynomial
24 f = Function('f')(x, y, z, w)
25
26 # Define quantum operators
27 x1 = lambda f: x * f.subs({x: x, y: q * y, z: q * z, w: q**(-1) * w})
28 x2 = lambda f: y * f.subs({x: q**(-1) * x, y: y, z: q**(-1) * z, w: q**(-2) * w})
29 x3 = lambda f: z * f.subs({x: q**(-1) * x, y: q * y, z: z, w: q**(-1) * w})
30 x4 = lambda f: w * f.subs({x: q * x, y: q**2 * y, z: q * z, w: w})
31 x5 = lambda f: f
32 x6 = lambda f: f.subs({x: q**4 * x, y: q**4 * y, z: q**4 * z, w: q**4 * w})
33 x1inv = lambda f: x**(-1) * f.subs({x: x, y: q**(-1) * y, z: q**(-1) * z, w: q * w})
34 x2inv = lambda f: y**(-1) * f.subs({x: q * x, y: y, z: q * z, w: q**2 * w})
35 x3inv = lambda f: z**(-1) * f.subs({x: q * x, y: q**(-1) * y, z: z, w: q * w})
36 x4inv = lambda f: w**(-1) * f.subs({x: q**(-1) * x, y: q**(-2) * y, z: q**(-1) * z, w:
37     w})
38 x5inv = lambda f: f
39 x6inv = lambda f: f.subs({x: q**(-4) * x, y: q**(-4) * y, z: q**(-4) * z, w: q**(-4) *
40     w})
41
42 # Meridian, Longitude, and (1,1)-Curve
43 y1 = lambda f: y*z**(-1)*f.subs({x: x, y: q**(-1)*y, z: q**(-1)*z, w: q**(-1)*w}) + y
44     **(-1)*z*f.subs({x: x, y: q*y, z: q*z, w: q*w}) + x**2*z**(-1)*w**(-1)*f.subs({x
45     : x, y: q**(-1)*y, z: q*z, w: q**(-1)*w}) + x*y**(-1)*w**(-1)*f.subs({x: x, y: q
46     **(-1)*y, z: q*z, w: q*w})
47 y2 = lambda f: x*z**(-1)*f.subs({x: q*x, y: y, z: q*z, w: w}) + x**(-1)*z*f.subs({
48     x: q**(-1)*x, y: y, z: q**(-1)*z, w: w}) + x**(-1)*y*z**(-1)*w*f.subs({x: q*x, y:
49     y, z: q**(-1)*z, w: w})
50 y3 = lambda f: x*w**(-1)*f.subs({x: q**(-1)*x, y: q**(-1)*y, z: z, w: q**(-1)*w}) + x
51     **(-1)*w*f.subs({x: q*x, y: q*y, z: z, w: q*w}) + x**(-1)*y**(-1)*z**2*f.subs({x
52     : q**(-1)*x, y: q*y, z: z, w: q*w}) + y**(-1)*z*w**(-1)*f.subs({x: q**(-1)*x, y: q
53     **(-1)*y, z: z, w: q*w})
54
55 # Central \partial = q^2*y1*y2*y3 - q^2*y1^2 - q^-2*y2^2 - q^2*y3^2 + q^2 + q
56     ^(-2)
57 dee = lambda f: q*y1(y2(y3(f))) - q**2*y1(y1(f)) - q**(-2)*y2(y2(f)) - q**2*y3(
58     y3(f)) + q**2*f + q**(-2)*f

```

code/T6Operators_DissVer.py